Université de Montréal

The Graptolite *Rhabdopleura recondita* Tube Composition, Development and Morphological Invariance (Hemichordata, Pterobranchia)

Par

Elena Beli

Département de sciences biologiques, Université de Montréal, Faculté des arts et des sciences

Thèse présentée en vue de l'obtention du grade de *Philosophiae Doctor* (Ph. D.) en sciences biologiques

Juillet 2020

Université de Montréal

Département de sciences biologiques, Université de Montréal

Ce mémoire intitulé

The Graptolite *Rhabdopleura recondita* Tube Composition, Development and Morphological Invariance (Hemichordata, Pterobranchia)

Présenté par

Elena Beli

A été évalué par un jury composé des personnes suivantes

Jean-François Pflieger

Président-rapporteur

Christopher B. Cameron

Directeur de recherche

Stefano Piraino

Codirecteur

Sandra Binning

Membre du jury

Charles Mitchell

Examinateur externe

The Graptolite *Rhabdopleura recondita* Tube Composition, Development and Morphological Invariance (Hemichordata, Pterobranchia)

Doctor of Philosophy
Département de sciences biologiques
Université de Montréal

RÉSUMÉ

Le phylum Hemichordata est composé exclusivement d'organismes marins et, avec les embranchement Echinodermata et chordata, il forme le groupe des Deutérostomes sur l'arbre de la vie des animaux. Dans les chapitres d'introduction et le deuxième, je donne un aperçu des hémichordés, y compris les enteropneustes solitaires et les pterobranches coloniaux et je les défini dans un contexte évolutif ou phylogénétique. Les enteropneustes sont souvent considérés comme le meilleur proxy vivant de l'ancêtre des deutérostomes. Les ptérobranches comprennent les Cephalodiscida et les Graptolithina. Les graptolites (graptos = écrit, lithos = roche) sont principalement représentés par des espèces fossiles remontant à la Période Cambrienne, il y a plus de 500 millions d'années. Ces «écritures dans la roche» sont largement connues et étudiées par les paléontologues et sont si abondantes qu'elles sont utilisées comme fossiles indicateurs pour identifier les couches sédimentaires. Les graptolites sont éteints sauf pour cinq espèces benthiques appartenant au genre *Rhabdopleura*, membres de la famille Rhabdopleuridae, que j'examine en détail dans le chapitre trois. *Rhabdopleura recondita* de la mer Méditerranée fait l'objet de cette thèse. Il est courant le long des côtes sud de l'Italie d'où je l'ai échantillonné en plongée sous-marine. Il est inhabituel que des colonies résident cachées à l'intérieur de la zoaria des bryozoaires morts. Seuls les tubes érigés font saillie à partir de la matrice de l'hôte.

Les chapitres quatre et cinq sont les contributions les plus significatives de cette thèse, avec un accent sur les tubes de *R. recondita*. Le chapitre quatre fournit des observations de la construction de tubes par *R. recondita* gardé en captivité. J'ai observé la capacité des larves, des zooïdes et des colonies à sécréter de nouveaux tubes en présence et en l'absence du matériel hôte du zoarium bryozoaire.

Nous avons découvert que la colonisation larvaire et la sécrétion du dôme peuvent se produire sans l'hôte bryozoaire, mais la croissance continue de la colonie nécessite le substrat de l'hôte. Les zooïdes adultes ne peuvent reformer de nouveaux tubes que s'ils sont capables de s'abriter à l'intérieur du matériel hôte. Un résultat surprenant des observations des zooïdes a été la sécrétion d'un opercule et d'un tube évasé. Les colonies qui avaient des tubes érigés enlevés ont pu fabriquer de nouveaux tubes, mais à un faible nombre. Une étude parallèle a été réalisée sur des colonies dont les tubes avaient été retirés, puis cultivées dans des canaux à quatre vitesses d'écoulement. Cette expérience a été conçue pour induire une réponse plastique phénotypique à l'écoulement. Au lieu de cela, je n'ai trouvé aucune différence significative dans la longueur du tube ou le nombre de tubes en réponse à quatre vitesses d'écoulement. Ce résultat suggère que le développement du tube de *R. recondita* peut être canalisé ou fixé. Il est significatif car il suggère que de petites différences qui distinguent les espèces primitives de graptolites encroûtantes sont bonnes.

Le chapitre cinq porte sur la composition des tubes de *R. recondita*. Plusieurs hypothèses et de nombreuses analyses ont été faites sur ce sujet, mais aucune n'a été concluante. J'utilise ici la génomique et la bioinformatique, l'immunochimie et la spectroscopie et rejette les hypothèses selon lesquelles les tubes sont de la kératine ou de la cellulose. Au lieu de cela, j'ai trouvé huit gènes de chitine synthase dans le génome et le trascriptome, un complexe composé d'un polysaccharide semblable à la chitine, d'une protéine, d'un acide gras et de composants élémentaires inattendus. Cette étude est significative car elle ferme la porte sur une ancienne hypothèse de composition de tube de graptolite et révèle qu'il s'agit d'une structure complexe comprenant de la chitine. Le chapitre de conclusion est un bref résumé des résultats et une réflexion sur les aveenues potentiellement fructueuse pour des recherches futures.

Mots-clés: *Rhabdopleura*, Graptolithina, *PhyloCode*, immunochimie, plasticité phénotypique, bioinformatique

ABSTRACT

The phylum Hemichordata is comprised of exclusively marine organisms, and together with the Echinodermata and Chordata forms the Deuterostomia branch on the animal tree of life. In the introductory and second chapters I provide a background on Hemichordata including the solitary Enteropneusta and the colonial Pterobranchia and define them in an evolutionary or phylogenetic context. The enteropneusts are often regarded as the best living proxy of the deuterostome ancestor. Pterobranchs, include the Cephalodiscida and Graptolithina. Graptolites (graptos=written, lithos=rock) are mostly represented by fossil species dating back to the Cambrian Period, more than 500 million years ago. These "writings in the rock" are widely known and studied by paleontologists and are so abundant that they are used as index fossils to identify sedimentary layers. Graptolites are extinct but for five benthic species belonging to the genus *Rhabdopleura*, members of the Rhabdopleurida, which I extensively review in chapter three. *Rhabdopleura recondita* from the Mediterranean Sea is the subject of this thesis. It is common along the south coasts of Italy from where I sample it by SCUBA diving. It is unusual in that colonies reside hidden inside of the zoaria of dead bryozoans. Only erect tubes project from the host matrix.

Chapters four and five are the most significant contributions of this thesis, with a focus on *R. recondita* tubes. Chapter four provides observations of tube building by *R. recondita* kept in captivity. I observed larvae, zooids and colonies abilities to secrete new tubes in the presence and absence of the bryozoan zoarium host material. We discovered that larval settlement and dome secretion can occur without the bryozoan host, but the continued growth of the colony requires the host substrate. Adult zooids can reform new tubes only if they are able to shelter inside of host material. A surprising result from the zooid observations was the secretion of an operculum and a flared tube. Colonies that had erect tubes removed were able to make new tubes, but fewer in number. A parallel study was done on colonies that had tubes removed and then were cultured in channels at four flow velocities. This experiment was designed to induce a phenotypic plastic response to flow. Instead, I found no significant difference in tube length or tube number in response to four flow velocities. This result suggests that the tube development of *R. recondita* may be canalized, or fixed. It is significant because it suggests that small differences that distinguish primitive, encrusting graptolite species, are good.

Chapter five is on the composition of *R. recondita* tubes. Several hypotheses and numerous analysis have been done on this topic, but none were conclusive. Here I use genomics and bioinformatics,

immunochemistry and spectroscopy and reject the hypotheses that the tubes contain keratin or cellulose. Instead I found eight chitin synthase genes in the genome and transcriptome, a complex made of a chitin-like polysaccharide, protein, fatty acid and unexpected elemental components. This study is significant because it closes the door on old hypothesis of graptolite tube composition and reveals that it is a complex structure including chitin. The conclusion chapter is a brief summary of the results and a reflection on fruitful avenues of future research.

Keywords: *Rhabdopleura*, Graptolithina, *PhyloCode*, immunochemistry, phenotypic plasticity, bioinformatics

Table of Contents

RÉSUMÉ *3*

ABSTRACT *5*

List of Tables **9**

Chapter 4 9

Chapter 5 9

List of Figures **10**

Chapter 3 10

Chapter 4 11

Chapter 5 14

ACKNOWLEDGEMENTS **17**

Chapter 1 ..... *19*

Introduction *19*

References 26

Chapter 2 ..... *32*

Cameron, C. B. and Beli, E. 2020 contributions: **32**

Hemichordata W. Bateson 1885 [C. B. Cameron and E. Beli], converted clade name **33**

References 35

Chapter 3 ..... *37*

Maletz, J. and Beli, E. 2018 contributions: **37**

Part V, Second Revision, Chapter 15: Subclass Graptolithina and *Incertae Sedis* Family Rhabdopleuridae: Introduction and Systematic Descriptions **38**

Subclass Graptolithina Bronn 1849 38

Graptolithina? *Incertae Sedis* 38

Graptolithina Families *Incertae Sedis* 39

***Incertae Sedis* Family Rhabdopleuridae Harmer 1905** 39

Morphology 40

Evolution 44

Possible Rhabdopleurid Stolons 48

References 51
Figures 60

Chapter 4 ..... ***68***

Beli, E., De Castro Mendonça, L. M., Piraino, S. and Cameron, C. B. contributions: **68**

On the development and morphological invariability of the graptolite *Rhabdopleura recondita* tubes in response to water flow velocity **69**

Abstract 69
Introduction 69
Materials and Methods 71
Results 74
Discussion 77
References 82
Figures 88
Tables 99

Chapter 5 ..... ***101***

Beli, E., Giotta, L., Guascito, M. R., Natsidis, P., Pagliara, P., Schiffer, P., Telford, J. M., Piraino, S. and Cameron, C. B. contributions: **101**

The complex chemical composition of the tubes in the graptolite *Rhabdopleura recondita* **102**

Abstract 102
Introduction 102
Materials and Methods 105
Results 109
Discussion 115
References 119
Figures 126
Tables 138

Chapter 6 ..... ***140***

Conclusions ***140***

References **145**

Supplementary materials ***146***

List of Tables

Chapter 4

Table 1. Number of new tubes reformed for each colony and flux treatment…….……99

Table 2. Mean tube length for each colony, before and after the flow-induced response…..……100

Chapter 5

Table 1. Dataset of genomes and transcriptomes used for OrthoFinder analysis. GT= genome or transcriptome. ……...138

List of Figures

Chapter 3

Fig. 1. Graptolithina? *incertae sedis* (p. 1–2)……...60

Fig. 2. *Rhabdopleura normani* Allman in Norman, 1869, monopodial growth and stolon system with diaphragm complexes. 1, Growing end of colony showing monopodial growth with permanent terminal zooid (adapted from Ridewood 1907, fig. 7). 2, Branching point; ts, transverse septum (adapted from Lankester 1884)……..61

Fig. 3. Branching of tubarium. 1, Main stem with branching, see stolon and transverse septum (ts); 2, Part of erect thecal tube with regeneration. 3, Erect tube with unusual lateral branching. (adapted from Kozłowski, 1949, fig. 14). 4, *Rhabdopleura recondita* Beli & others, 2018 finds shelter inside the dead branches of bryozoan hosts, erect tubes project from the pores (new; photo courtesy of Stefano Piraino). …….62

Fig. 4. The stolon system. 1, Stolon and inner lining (cone) of thecal tubes. 2, Diaphragm complex and connection to the fusellar tube (adapted from Urbanek & Dilly 2000)..……...63

Fig. 5. Rhabdopleuridae (p. 7)…….64

Fig. 6. Rhabdopleuridae (p. 7–10)……...65

Fig. 7. Rhabdopleuridae (p. 8–10)……...66

Fig. 8. Rhabdopleurid stolons (p. 10–11)…….....67

Chapter 4

Fig. 1. A transversal section of the bryozoan *Myriapora truncata* colonized by *Rhabdopleura recondita*. Erect semi-transparent tubes of *R. recondita* project from bryozoan host. Scale bar 2 mm.……...…….……88

Fig. 2. Colony deprived of tubes. A few individuals are visible (arrows). Scale bar 1 mm…...…88

Fig. 3. a, A drawing and b, Photograph of the experimental aquarium with flow channels. One channel was used for control, with 0 cm/s flow, and three channels were maintained at flow velocities of 1.6 cm/s, 2 cm/s, and 3.3 cm/s. In figure a, arrows indicate the direction of flow, and velocities in cm/s are reported on each channel…….……..……...…89

Fig. 4. Photos of the 16 experimental colonies, maintained in place by Plexiglas weights. Velocities were: 1-4 at 1.6 cm/s; 5-8 at 2 cm/s; 9-12 at 3.3 cm/s; 13-16 at 0 cm/s. Scale bar 3 cm.…….90

Fig. 5. *Rhabdopleura recondita* metamorphosing larvae. a, A metamorphosing larva shows the dome (arrow), arms (arrowheads) and cephalic shield (cs). b, A larva started the secretion of the dome (arrow). c, A furrow between the trunk and the cephalic shield (arrow) is a sign of metamorphosis. Larvae in b and c can still swim. Scale bar 100 µm.……...91

Fig. 6. *Rhabdopleura recondita* larval development on a bryozoan fragmented matrix. a, The larva stopped with the anterior part upward. b, The larva started secreting the dome. c, After 29 days from settlement the metamorphosis begun, the buds of naked arms are visible beyond the dome. d, The zooid is tripartite, lack developed tentacles and pierce the dome to form creeping tube after 37 days from settlement. Arrows show the dome, arrowheads the naked arms. Scale bars 100 µm for a, b, d, 150 µm for c..……....…….91

Fig. 7. a, A developing zooid survived eight days with no further development. b, One of the two naked zooids with a creeping tube, and stolon embedded in a bryozoan fragment. Scale bars 200 µm for a, 300 µm for b….……..……....92

Fig. 8ab. Two zooids united by a common stolon and exposed following fracturing of the bryozoan matrix. a, The zooid able to descend into the host matrix built a normal erect tube. b, The zooid more exposed built an unusual flared tube. Scale bar 300 µm..……..……92

Fig. 9. a, *Rhabdopleura recondita* zooids perched from the bryozoan zoarium apertures after tube removal. b, A new tube rebuilt, arrow indicate the rim of the old tube. Scale bars 500 µm for a, 300 µm for b……..……..…….93

Fig. 10. a, A brooding chamber made of a smooth and spiralised creeping tube. Female zooid (arrow) and larvae (arrowheads). b, Female zooid with ovary (arrow) and reduced tentacles (arrowheads). cs: cephalic shield. Scale bars 400 µm for a, 200 µm for b..……..93

Fig. 11. Two new tubes are indicated by arrows. Scale bar: 1 mm.……...…….94

Fig. 12. A plot for each treatment. On the abscissa the days, on the ordinate the mean number of new tubes rebuilt with error bar.……..……..……..95

Fig. 13. a, The number of tubes re-built in function of the flow velocity. b, The length of tubes rebuilt in function of flow velocity.
Each box delimits the distance between the first and third quartile, the median is the horizontal bar in the box and the "x" is the mean value. The whiskers reach the lowest and largest data point excluding the outliers (dot).……...……..……..……..……...96

Fig 14. Number of new tubes built per day grouped by speed treatment, plotted together for comparison. Trend lines used the method of least squares to find the regression line…….…….97

Fig. 15. Differences in tube length between the original tubes (blue) and the new tubes (orange) for each treatment. Each box delimits the distance between the first and third quartile, the median is the horizontal bar in the box and the "x" is the mean value. The whiskers reach the lowest and largest data point excluding the outliers (dots)……..……..97

Fig. 16. Some of the removed erect tubes were closed with a lid secreted by the zooids (arrowheads). The lid on the left is broken. Arrow indicates the naked arm tips of a zooid. Scale bar 100 μm……..98

Chapter 5

Fig. 1. OG0000859. Complete dataset. In red ambulacrarians. In the fuchsia box pterobranchs. Chordates (blue), arthropods and nematodes sequences (green). In black are the hydromedusae *Clytia hemisphaerica* and the sponge *Amphimedon queenslandica*. See the text for comments…126

Fig. 2. OG0004142. Complete dataset. Coherent clustering of protostome (green), ambulacrarians (red) and chordates (blue). See the text for comments……..127

Fig. 3. OG0006824. Ambulacrarian dataset. Enteropneusts (green), pterobranchs (red) and echinoderms (blue). See the text for comments…….128

Fig. 4. OG0012451. Ambulacrarian dataset. Enteropneusts (green), pterobranchs (red) and echinoderms (blue). See the text for comments…….129

Fig. 5. OG0012607. Ambulacrarian dataset. Enteropneusts (green), pterobranchs (red) and echinoderms (blue). See the text for comments…….130

Fig. 6. GO0023337. Ambulacrarian dataset. Enteropneusts (green), pterobranchs (red) and echinoderms (blue). See the text for comments…….131

Fig. 7. OG0040366. Ambulacrarian dataset. Pterobranchs (red) and echinoderms (blue). See the text for comments…….....132

Fig. 8. ATR-FTIR spectra. Purple line, chitosan standard compound; blue line, chitin standard compound; green line, squid pen as a biological refence for β-chitin; red line, bee leg as a biological reference for α-chitin; black line, *R. recondita* tubes sample. See text for comments……133

Fig. 9. Magnification signal of *R. recondita* spectrum from Fig. 8, in the range of absorbance of an acetamide moieties, indicating chitin……134

Fig. 10. Survey XPS spectra for samples of *R. recondita* tubes. Inset: XPS high-resolution region acquired between 55 eV and 175 eV. All peaks attributions refers to the NIST standard. reference database [NIST, X., Ray Photoelectron Spectroscopy Database: https://srdata. nist. gov/xps/Default. aspx.]……..135

Fig. 11. *R. recondita* tube sections. a, before any treatment; b, Control; c, Experiment. The brownish tint observed both in control and experimental samples suggests that the labelling is not specific in the latter. Scale bars 50 μm for a, 100 μm form b,c.…….136

Fig. 12. *R. recondita* stolon sections. a, before any treatment; b, Control; c, Experiment. It was not possible to detect DAB reaction for the natural brownish colour of the stolon. Scale bar 100 μm.....136

Fig. 13. Shrimp chitin. a, Control; b, Experiment. Contrarily to what has been observed for tube sections, the controls do not show a brownish tint suggesting a specific staining of chitin in b. Scale bar 0.5 mm.....……..……...137

To my big family

To the grandmothers

To Giada

ACKNOWLEDGEMENTS

I have to thank prof. Christopher B. Cameron who from the first day asked to be called Chris and not “professor”... Thank you Chris!

Almost seven years ago, during the Master Science internship, together with Chris I sampled and I saw my first *Rhabdopleura* under a stereo microscope, I never thought how mysterious it was and the discoveries I would have made on a millimetre-sized animal! I was told that most biologists don't study lions, well I am among the very few in Italy to study *Rhabdopleura* and the many to work with the tremendous, incredibly diversified, graptolites world.

Five years ago I made an unexpected leap: “Elena, they accepted your PhD application at the University of Montreal!”

It’s wonderful to look back and think about the opportunities I had: from sampling by SCUBA on a rough Adriatic Sea and look for *Rhabdopleura,* to splash around in the mud of a tidal zone in Maine, between *Saccoglossus* and *Limulus* (peculiar experience for a person used to the Mediterranean coasts), the night of the most red and suggestive Moon that the Darling Marine Center could give; to the experience in London where I was able to study more in details bioinformatics and met wonderful people. Not to mention the ten months I spent in Montreal in which I left part of my soul that I hope to visit every now and then.

Chris was able to give professional and, above all, human support from the beginning, when he barely knew me and left me his house to give me a place to sleep the night of my arrival in Montreal. He is an extremely prepared, humble, honest and visionary person, he supported and guided me in every job choice. I know he will keep on giving, because he lives to share science and knowledge with his students.

I thank prof Stefano Piraino, without his curiosity, *Rhabdopleura* would have stayed in alcohol locked in the cabinet with the other samples. Seven years ago for my Master, Stefano proposed me to work with a world expert of hemichordates who came no less than from Canada! He supported my application for the PhD and in the last five years he was there with his skills and patience to make me work in the laboratories of the University of Salento, we sampled *Rhabdopleura* several times, he allowed me to give my scientific contribution to the Unione Zoologica Italiana congresses as well as to be in the organization staff of the congress... with Stefano dinners and funny moments didn’t miss!

I met many people along this PhD path, and many of them I should thank for the practical and moral support I received. The co-authors of the chapters published in this thesis are among the people who made me a *Rhabdopleura* fan or to whom I hope I transferred the passion for graptolites, people who believed in my skills and desire to work: Jörg Maletz, one of the people who made me discover the world of paleontology and fossil graptolites, Luana Marina De Castro Mendonça, the beautiful mind who listened and solved statistical problems and more. Patrizia Pagliara who really guided me and was interested in my topic like few others in this adventure. Thanks to Livia Giotta and Rachele Guascito that from their chemistry laboratories worked on *Rhabdopleura* tubes with a special know-how. Thanks to Max J. Telford who accepted me in his lab at University College London and left me to his welcoming team: Paschalis Natsidis that with incredible dedication and ability, taught me what I needed about bioinformatics, Philipp Schiffer who was a super competent and passionate guide, he made me work in the laboratories of the Natural History Museum in London, an indescribable emotion! It's not easy to remember the whole team that welcomed me in London, but I owe a further thank to Paola Oliveri for her very useful scientific ideas, to Laura Piovani and Paschalia Kapli for making me feel at home.

Thanks to my friend Noura Jabr, humanly the most beautiful discovery in Montreal and to Greta Ramirez Guerrero, Charles Larouche-Bilodeau, Francis Letendre and Xavier G. Mayers with whom I shared work and playful moments.
Furthermore, I have to thank Francesco De Nuccio for making his profound knowledge of laboratory techniques available, Mario Congedo and Christian Vaglio for their fundamental help during sampling.

They owed me nothing, nevertheless they were there for me. Many other people were by my side professionally and in friendship and helped me during this adventure, in alphabetical order: Giuseppe Alfonso, Lorena Basso, Mario Ciotti, Silvia Fraissinet, Gianmarco Ingrosso, Marta Mammone, Francesco De Leo, Loredana Papa and Lucia Rizzo.

Chapter 1

Introduction

The phyla Hemichordata, Echinodermata and Chordata (our phylum) form the deuterostome clade, here are grouped animals with a common development, in which the first opening of the embryo – the blastopore – will become the anus and the second opening the mouth (Cameron 2005). Hemichordata Bateson 1885 (from Greek *hemi*, half + Latin *chorda*, chord) is a small phylum of marine benthic bilaterians that together with Echinodermata form the clade Ambulacraria. Hemichordates share a three-part body plan including an anterior prosoma, mesosoma and posterior metasoma. Included in the phylum there are two major classes, the Enteropneusta and the Pterobranchia. The Enteropneusta, or acorn worms (with about 120 species), are solitary, benthic, mobile worms living in mud or sand or on the surface. It includes four families: Harrimaniidae, Spengelidae, Torquaratoridae and Ptychoderidae. The enteropneust fossil record consists of eight species (Nanglu et al. 2015; Cameron 2016), the oldest dating back 505 million years (Caron et al. 2013).

The Pterobranchia (including the clade Graptolithina) are colonial, tube dwelling zooids, characterized by ciliated arms and tentacles, and are sister taxon to enteropneusts (Cameron 2005; Cannon et al. 2014). The group encompasses twenty-six living species, belonging to three genera: *Atubaria*, *Cephalodiscus* and *Rhabdopleura* (Barnes 1977; Dilly and Ryland 1985; Lester 1985). Most are known from deep polar seas, though some shallow temperate species are known (Jullien 1890, Jullien and Calvet 1903; Burdon-Jones 1954; Barnes 1977; Dilly and Ryland 1985). Compared with the more common acorn worms like *Balanoglossus* and *Saccoglossus*, the small tube-dwelling Pterobranchia have been encountered by relatively few zoologists (Barnes 1977). Pterobranchs are usually found in cold deep waters, so that their study was hard until the collection of *R. compacta* and *R. normani* was performed in shallow waters, about 50 years ago (Sato et al. 2008b). *Rhabdopleura* was named by Allman, and means “rod walled”, for the resemblance to a rod-like cord standing inside the tube (Allman 1869). They are sessile pseudocolonial (*Cephalodiscus*) or colonial (*Rhabdopleura*). Cephalodiscids are pseudocolonial because they are free to move throughout the tubarium. *Rhabdopleura* is colonial because each zooid is confined to one erect tube, within the larger tubarium. The zooids are from 0.5. to 15 mm long (Argano et al.

2007), and the colonies (tubaria) from a few mm to 10 cm or larger in diameter. They may reproduce via a short-lived planula larva or by asexually budding (Mitchell et al. 2013). When they reproduce by budding, colonies develop from a solitary sexually generated zooid. Two or more tentaculate feeding arms used for filter feeding characterize pterobranchs. To feed, zooids hold the rim of the tube and extend the arms and tentacles into the seawater where they can capture particles. The food particles are then conveyed to the mouth by the mean of a ciliary system covering arms and tentacles. The zooids hold onto the edge of the tube using the cephalic shield, and it is the shield that secretes the tube (Dilly 1976).

Graptolithina or graptolites (graptos= written, lithos= rock) are largely part of the fossil record, there they represent index fossils – fossils species characteristic of a certain span of geologic time. Until few years ago graptolites were regarded as completely extinct and a separate phylum to hemichordates though some speculated that they may have had some affinity to pterobranchs (Bulman 1970; Rickards and Durman 2006). Mitchell and others (2013), after a phylogenetic analysis based on morphological data, moved the graptolite inside pterobranchs and rhabdopleurids inside the graptolites. This study demonstrated that graptolites are alive and include 5 living species of *Rhabdopleura* (family Rhabdopleuridae), the fifth described two years ago from the Mediterranean Sea (Beli et al. 2018). The finding that the family Rhabdopleuridae are graptolites is of the same order of significance as the finding that birds are living dinosaurs, or that the coelacanth is a living animal.

Shared characters of graptolites include a larval dome or prosiculum, a sclerotized stolon that connects zooids, and ring-shaped annulations of the tubes called fuselli. *Rhabdopleura* is regarded as a basal, benthic, encrusting form of graptolite (Mitchell et al. 2013). The graptolite fossil record is extensive and begins as benthic encrusting forms in the mid-Cambrian, including rhabdopleurids. Graptolites dominated the world oceans throughout the Paleozoic, particularly after they enter and exploit the planktonic environment through the Ordovician and Silurian periods (ca. 500 Ma to 390 Ma) (Sato et al. 2008a). Planktic graptolites went extinct by the Lower Devonian (about 400 million years), whereas some benthic graptolites survived until the Upper Serpukhovian (Carboniferous – about 325 million years) before going extinct with the exception of *Rhabdopleura* (Maletz et al. 2020). *Cephalodiscus* is sister taxon to the graptolites and also has a fossil record dating back to

about 530 Ma in the early Middle Cambrian (Sato et al. 2008a), making *Rhabdopleura* and *Cephalodiscus* two of the longest living animal genera in the history of the planet.

Graptolites are known almost exclusively for the fossilized tubaria. Fossil zooids are rare because they are in the 1 to 2 mm size range, soft bodied and decompose quickly (Beli et al. 2017). Four poorly fossilized zooids have been found at different stages of development (Bjerreskov 1991; Chapman et al. 1995; Durman and Sennikov 1993; Loydell et al. 2004; Rickards and Durman 2006). The vast majority of pterobranch fossils, including tens of thousands of fossils, are only know from their organic tubes (Maletz et al. 2005).

The subject of this thesis are the tubes of the living graptolite *Rhabdopleura recondita* Beli, Cameron and Piraino 2018. Its colonies live along the Salento coasts among the coralligenous rocky substrate (SE Adriatic Sea and Ionian Sea), in depth range of 2 to 70 meters depth (Beli et al. 2018). Zooids occupy the dead skeleton of some bryozoan species like *Myriapora truncata, Schizoretepora serratimargo* and, more rarely, the encrusting bryozoans *Celleporina caminata* and *Reptadeonella violacea*. *Rhabdopleura recondita* has the peculiarity of living inside other hosts, for this reason their creeping tubes line the cavities of the bryozoan hosts with a thin smooth layer, and fuselli are absent. The erect tubes project perpendicularly from the bryozoan matrix and are typically graptolite-like, with fuselli. The zooid anatomy reflects the hemichordate body plan subdivision into i) a prosome, or cephalic shield, responsible for the secretion of the tube; ii) a mesosome, or collar that includes two arms with tentacles used to filter feed. The apical tips of the arms are particularly long and lack tentacles, a unique feature of the species; iii) a metasome, or trunk that includes the gonad, a U-shaped gut, and a contractile stalk that connects to the colony stolon. The stolon (pectocaulus) is not enveloped inside of a secreted tube but is free inside of the highly unusual creeping tube. Zooids are about 0.7 mm in length, and the colony size reaches a few millimeters.

There is a vast literature on graptolites, especially the fossil species. The word “graptolite” appears in the title of about 15,400 scientific publications. Of the five *Rhabdopleura* species, only two have been extensively studied: *R. normani* (Lester 1988ab; Halanich 1993) and *R. compacta* (Stebbing 1970ab; Dilly 1971, 1972, 1973, 1975, 1976; Sato 2008). The other species are *R. annulata* for which zooids were recently described (Ramírez-Guerrero et al. 2020), *R. striata* sampled just once

in Sri Lanka by Schepotieff (1909) and the protagonist of this thesis, *R. recondita*, for which taphonomy, taxonomy, zoogeography and the nervous system were studied (Beli et al. 2017, 2018; Strano et al. 2019).

Hemichordates have a key role in our understanding the evolutionary relationships among deuterostomes and the origin of chordates. *Rhabdopleura* was firstly discovered for the Mediterranean Sea by Laubier (1964) on the French coast. Except for this finding, pterobranchs have been easily overlooked because of their minute size (Maletz and Cameron 2016). Their distribution in the Mediterranean Sea – and probably around the world – is largely unknown and dependent on the lack of systematic search rather than on a real rarity (Beli et al. 2018). Their occurence in marine environment may be much more abundant than previously thought (Strano et al. 2019), and the Mediterranean source of *Rhabdopleura*, is a new and valuable hemichordate sampling basin. Studying *Rhabdopleura* in all its life aspects including morphology, physiology, genetics, and its tubes among others, helps understand the evolution of the deuterostomes and the success of an animal genus that has remained unchanged for over a half billion years.

This thesis is organized in six chapters, including this introductory chapter that provides some background and context for the research chapters. The chapter two is a contemporary classification of the phylum Hemichordata, written for *Phylonyms*, a companion to *PhyloCode*, *the International Code of Phylogenetic Nomenclature*. *Phylonyms* classification is founded on phylogenetics, rather than classical Linnaean taxonomy. The development of the *PhyloCode* arose from the awareness that the current rank-based nomenclatural systems (e.g., genus, family, etc.) do not fully satisfy the clade naming. This code uses clades - the groups of organisms including an ancestor and all of their descendants - whereas the species names are still governed by the classical code. The naming of clades is defined in terms of phylogenetic relationships rather than by taxonomic rank, as a consequence clade names do not change as happens under the rank-based code, after a change in rank. *PhyloCode* is not meant to substitute the existing names but to give an alternative system for governing the application of existing and new names. We believe this code has a high potential, and that it will be widely adopted in the future.

The third chapter is a comprehensive review of the Subclass Graptolithina, *incertae sedis* Family Rhabdopleuridae, fossil and living species. This is the chapter 15 in the Part V of the second edition

of the iconic *Treatise of Invertebrate Paleontology*. The need for an up-to-date guide for paleontologists and biologists of all invertebrate groups, is leading to the review of the entire Treatise. This is one of the many contributions to its volumes.

The fourth chapter is about tube secretion and form, or development of *R. recondita* kept in captivity. *Rhabdopleura recondita* is a living graptolite so any observations on tube formation by newly settled larvae, isolated zooids, or colonies is a valuable contribution to graptolite paleontology. In this context we made observations on larva settlement and settlement cues, metamorphosis, the secretion of the dome, and zooids tube building behavior. Addiontally, we characterized tube building by colonies that were cultured in four different flow velocities. The purpose of this experiment was to induce a phenotypic response to flow. In the aquatic world, flow velocity is among the most important selective forces and can shape the species that are exposed to it (Graus et al. 1977; Palumbi 1986; Marchinko 2003). *Phenotypic plasticity* is a universal property of phenotypes, and marks a change in an organism's behavior, physiology or morphology in response to a new environment (West-Eberhard 2003). Genetically identical organisms can respond to environmental changes in different ways. Simply, we can plot the relationship between the phenotype and the environment by placing an environmental parameter on the abscissa and a phenotype trait on the ordinates. At this point, if we consider an *average phenotypic value* of that genotype across the environment (y=constant), a line that will intersect or overlap the *average phenotypic value*, represents the function that relates the environment to which a genotype is exposed to the phenotype that can be produced by that genotype, this line is called the *reaction norm*. If the function is flat (and overlap to the average phenotypic value), it means that there is no variation in the phenotype in response to the environmental stimulus (*canalization*). On the other hand, if the function is not flat, there is *phenotypic plasticity*, quantified by the degree of the function slope (Pigliucci 2001).

Examples of *phenotypic plasticity* include the production of melanin, enhanced by low temperature in the Himalayan mouse, Himalayan rabbit and Siamese cat (Silvers 1979 and references therein), the origin of workers or queen bee from larvae fed with different nourishments (West-Eberhard 2003), the exhibition of a longer, stronger tail and colour pattern in the presence of a predator for frog tadpoles (Kraft et al. 2006), the defense helmet of a *Daphnia* in response to a predator (Pigliucci 2001), or the changes to the length and form of barnacle legs in individuals exposed to

different flow velocities (Arsenault et al. 2001). Sessile filter feeding animals that are encrusted to a surface, and reside in variable flow, where they are susceptible to damage from biomechanical drag, or variations in the availability of food, including sponges, barnacles, bryozoans and colonial tunicates, exhibit *phenotypic plasticity* (Arsenault et al. 2001; Marchinko 2003). Benthic encrusting graptolites then, may also be expected to change the tube and tubarium form in response to flow, and exhibit high variation.

Most graptolite species are fossils and in some cases, including the earliest Cambrian *Rhabdopleura*-like forms, the species definitions are based on differences in tube morphology. Fossils provide no evidence of reproductive isolation that is frequently used by biologists to define a living species (Allmon and Yacobucci 2016) and in the absence of genetic data, it is not possible to determine heritable characteristics including variation from non-heritable ones. The definition of a species may rely on minor characters, adding to this challenge the morphological *phenotypic plasticity* in response to a new environment (West-Eberhard 2003). Are these small differences in form indicative of a different species, or the variation in form of a single species? In this fourth chapter our objective was to study the response of *R. recondita* to different flow velocities. The experimental treatment was to remove the standing tubes projecting from the bryozoan matrix and then expose the colonies to four velocity treatments. Our hypothesis was that in low flow the zooids would remake longer tubes with lower density, whereas in high flow the tubes would be shorter with higher density.

Chapter five determines the composition of *Rhabdopleura recondita* tubes. The chemical composition of graptolite tubes and fossils in general is unknown because they have been subject to diagenetic changes – chemical-physical changes following death and sedimentary burial, compression and heat. *Rhabdopleura*'s tubarium is an organic matrix with foreign particles aggregated on the surface after secretion. It is shaped in half-rings adorning creeping tubes and full rings piled one upon the other on erect tubes, secreted by the zooids' cephalic shield. At the ultrastructural level the tubarium is characterized of a matrix containing fibres. Four long-standing hypotheses for the tube composition include collagen (Armstrong et al. 1984), scattered fibers that may be keratin (Dilly 1971, 1976), chitin (Kraft 1926), or a type of cellulose called tunicin that characterizes the tunic of tunicates (Sewera 2011). Here we hypothesize that *R. recondita* tubes are similar in composition to the tubaria of extinct graptolites, and we use an integrated approach of

bioinformatics, chemical and immunohistochemical methods to investigate the composition of this extracellular matrix.

Beli E. contributions to the thesis chapters:

Chapter 2: Hemichordata W. Bateson 1885 [C. B. Cameron and E. Beli], converted clade name Cameron C. B. wrote the first draft of the paper that was accepted in 2012, before we knew that *Rhabdopleura* was a living graptolite. Major changes were not permitted to the manuscript before publication in 2020, but Beli was able to make minor edits. Beli was invited to do this because of their productive years of collaboration, fruitful discussions and experiments, and for her expertise in pterobranch biology.

Chapter 3: Part V, Second Revision, Chapter 15: Subclass Graptolithina and *Incertae Sedis* Family Rhabdopleuridae: Introduction and Systematic Description
Beli E. wrote together with Maletz the generalities of living *Rhabdopleura* and provided information on the living *Rhabdopleura recondita*.

Chapter 4: On the morphological invariability of *Rhabdopleura recondita* tubes (Hemichordata, Pterobranchia, Graptolithina).
Beli designed and realized the experimental aquarium, sampled, collected and analyzed the data from this experiment and made many novel observations. Beli wrote the first draft and edited subsequent drafts.

Chapter 5: The complex chemical composition of the tubes in the graptolite *Rhabdopleura recondita*.
Beli devised the study in collaboration with Cameron. She collected the zooids and shipped them to the lab of Max Telford (UC London) who is a long-time collaborator of Cameron. She found expert collaborators in microscopy and chemistry and with prof. Cameron was awarded grants to work on the bioinformatics of the *R. recondita* genome in the lab of Telford. She analyzed the data, wrote the first draft and edited subsequent drafts of the chapter.

References

Allman, G. J. (1869). On *Rhabdopleura*, a new form of Polyzoa, from deep-see dredging in Shetland. *The Quarterly Journal of Microscopical Science*, 9, 57–63.

Allmon, W. D., & Yacobucci, M. M. (2016). Species and speciation in the fossil record. University of Chicago Press.

Argano, R., Boero, F., Bologna, M. A., Dallai, R., Lanzavecchia, G., Luporini, P., Melone, G., Sbordoni, V., & L., S. L. (2007). Zoologia: Diversità animale. Monduzzi editore.

Armstrong, W. G., Dilly, P. N., & Urbanek, A. (1984). Collagen in the pterobranch coenecium and the problem of graptolite affinities. *Lethaia*, 17, 145–152.

Arsenault, D. J., Marchinko, K. B., & Palmer, A. R. (2001). Precise tuning of barnacle leg length to coastal wave action. *Proceedings of the Royal Society of London. Series B: Biological Sciences*, 268, 2149–2154.

Barnes, R. D. (1977). New record of a pterobranch hemichordate from the Western Hemisphere. *Bulletin of Marine Science*, 27, 340–343.

Beli, E., Piraino, S., & Cameron, C. B. (2017). Fossilization processes of graptolites: insights from the experimental decay of *Rhabdopleura* sp.(Pterobranchia). Palaeontology, 60, 389–400.

Beli, E., Aglieri, G., Strano, F., Maggioni, D., Telford, M. J., Piraino, S., & Cameron, C. B. (2018). The zoogeography of extant rhabdopleurid hemichordates (Pterobranchia: Graptolithina), with a new species from the Mediterranean Sea. *Invertebrate Systematics*, 32, 100–110.

Bjerreskov, M. (1991). Pyrite in Silurian graptolites from Bornholm , Denmark. *Lethaia*, 24, 351–361.

Burdon-Jones, C. (1954). The habitat and distribution of *Rhabdopleura normani* Allman. *Universitetet I Bergen Årbok Naturvitenskapelig rekke* 11, 1–17.

Cameron, C. B. (2005). A phylogeny of the hemichordates based on morphological characters. *Canadian Journal of Zoology*, 83, 196–215.

Cameron, C. B. (2016). *Saccoglossus testa* from the Mazon Creek fauna (Pennsylvanian of Illinois) and the evolution of acorn worms (Enteropneusta: Hemichordata). *Palaeontology*, 59, 329–336.

Cannon, J. T., Kocot, K. M., Waits, D. S., Weese, D. A., Swalla, B. J., Santos, S. R., & Halanych, K. M. (2014). Phylogenomic resolution of the hemichordate and echinoderm clade. *Current Biology*, 24, 2827–2832.

Caron, J. B., Morris, S. C., & Cameron, C. B. (2013). Tubicolous enteropneusts from the Cambrian period. *Nature*, 495, 503–506.

Chapman, A. J., Durman, P. N., & Rickards, R. B. (1995). Rhabdopleuran hemichordates: new fossil forms and review. *Proceedings of the Geologists' Association*, 106, 293–303.

Dilly, P. (1971). Keratin-like fibres in the hemichordate *Rhabdopleura compacta*. *Zeitschrift für Zellforschung und Mikroskopische Anatomie*, 117, 502–515.

Dilly, P. N. (1972). The structures of the tentacles of *Rhabdopleura compacta* (Hemichordata) with special reference to neurociliary control. *Zeitschrift für Zellforschung und mikroskopische Anatomie*, 129, 20–39.

Dilly, P. N. (1973). The larva of *Rhabdopleura compacta* (Hemichordata). *Marine Biology*, 18, 69–86.

Dilly, P. N. (1975). The dormant buds of *Rhabdopleura compacta* (Hemichordata). *Cell and Tissue Research*, 159, 387–397.

Dilly, P. N. (1976). Some features of the ultrastructure of the coenecium of *Rhabdopleura compacta*. *Cell and Tissue Research*, 170, 253–261.

Dilly, P. N., & Ryland, J. S. (1985). An intertidal *Rhabdopleura* (Hemichordata, Pterobranchia) from Fiji. *Journal of Zoology*, 205, 611–623.

Durman, P. N., & Sennikov, N. V. (1993). A new rhabdopleurid hemichordate from the Middle Cambrian of Siberia. *Palaeontology*, 36, 283–296.

Graus, R. R., Chamberlain Jr, J. A., & Boker, A. M. (1977). Structural modification of corals in relation to waves and currents: reef biota. In. Frost, S. H., Weiss, M. P., Saunders, J. B. (eds.) Reefs and related carbonates ecology and sedimentology. *American Association of Petroleum Geologists*, 135–153.

Halanych, K. M. (1993). Suspension feeding by the lophophore-like apparatus of the pterobranch hemichordate *Rhabdopleura normani*. *The Biological Bulletin*, 185, 417–427.

Jullien, J. (1890). Description d'un Bryozoaire nouveau du genre *Rhabdopleura*. *Bulletin de la Société Zoologique de France* 15, 180–183.

Jullien, J., and Calvet, L. (1903). *Bryozoaires provenant des campagnes de l'Hirondelle, 1866–1888*. Vol. 23. *Résultats des campagnes scientifiques accomplies sur son yacht par Albert Ier, prince souverain de Monaco*.

Kraft, P. G., Franklin, C. E., & Blows, M. W. (2006). Predator-induced phenotypic plasticity in tadpoles: Extension or innovation? *Journal of Evolutionary Biology*, 19, 450–458.

Laubier, L. (1964). Découverte de la classe des Ptérobranches en Mediterranée. *Comptes rendues de L'Academie des Sciences, Paris* 258, 4340–4342.

Lester, S. M. (1985). *Cephalodiscus* sp. (Hemichordata: Pterobranchia): observations of functional morphology, behavior and occurrence in shallow water around Bermuda. *Marine Biology*, 85, 263–268.

Lester, S. M. (1988)a. Settlement and metamorphosis of *Rhabdopleura normani* (Hemichordata: Pterobranchia). *Acta Zoologica*, 69, 111–120.

Lester, S. M. (1988)b. Ultrastructure of adult gonads and development and structure of the larva of *Rhabdopleura normani* (Hemichordata: Pterobranchia*). Acta Zoologica*, 69, 95–109.

Loydell, D. K., Orr, P. J., & Kearns, S. (2004). Preservation of soft tissues in Silurian graptolites from Latvia. *Palaeontology*, 47, 503–513.

Maletz, J., & Cameron, C. B. (2016). Part V, Second Revision, Chapter 3: Introduction to Class Pterobranchia Lankester, 1877. *Treatise Online*, 82, 1–15.

Maletz, J., Steiner, M., & Fatka, O. (2005). Middle Cambrian pterobranchs and the Question: What is a graptolite? *Lethaia*, 38, 73–85.

Maletz, J., Mottequin, B., Olive, S., Gueriau, P., Pernègre, V., Prestianni, C., & Goolaerts, S. (2020). Devonian and Carboniferous dendroid graptolites from Belgium and their significance for the taxonomy of the Dendroidea. *Geobios*, 59, 47–59.

Marchinko, K. B. (2003). Dramatic phenotypic plasticity in barnacle legs (*Balanus glandula* Darwin): Magnitude, age dependence, and speed of response. *Evolution*, 57, 1281–1290.

Mitchell, C. E., Melchin, M. J., Cameron, C. B., & Maletz, J. (2013). Phylogenetic analysis reveals that *Rhabdopleura* is an extant graptolite. Lethaia, 46, 34–56.

Nanglu, K., Caron, J. B., & Cameron, C. B. (2015). Using experimental decay of modern forms to reconstruct the early evolution and morphology of fossil enteropneusts. *Paleobiology*, 41, 460–478.

Palumbi, S. R. (1986). How body plans limit acclimation: responses of a demosponge to wave force. *Ecology*, 67, 208–214.

Pigliucci, M. (2001). *Phenotypic Plasticity - Beyond Nature and Nurture*. The Johns Hopkins University Press.

Ramírez-Guerrero, G. M., Kocot, K. M., & Cameron, C. B. (2020). Zooid morphology and molecular phylogeny of the graptolite *Rhabdopleura annulata* (Hemichordata, Pterobranchia) from Heron Island, Australia. *Canadian Journal of Zoology*, 98, 844–849.

Rickards, R. B. & Durman, P. N. (2006). Evolution of the earliest graptolites and other hemichordates. *National Museum of Wales Geological Series* 25, 5–92.

Sato, A. (2008). Seasonal reproductive activity in the pterobranch hemichordate *Rhabdopleura compacta*. *Journal of the Marine Biological Association of the United Kingdom*, 88, 1033–1041.

Sato, A., Rickards, B., & Holland, P. W. (2008)a. The origins of graptolites and other pterobranchs: a journey from 'Polyzoa'. *Lethaia*, 41, 303–316.

Sato, A., Bishop, J. D. D., & Holland, P. W. H. (2008)b. Developmental biology of pterobranch hemichordates: History and perspectives. *Genesis*, 46, 587–591.

Schepotieff, A. (1909). Die Pterobranchier des Indischen Ozeans. Zoologische Jahrbücher. Abteilung für Systematik 28, 429–448.

Sewera, L. J. 2011. Determining the Composition of the Dwelling Tubes of Antarctic Pterobranchs. Honors thesis. Paper 48. Illinois Wesleyan University.

Silvers, W. K. (1979). *The Coat Colors of Mice - A model for mammalian gene action and interaction*. In *The Coat Colors of Mice*. Springer-Verlag.

Stebbing, A. R. D. (1970)a. Aspects of the reproduction and life cycle of *Rhabdopleura compacta* (Hemichordata). *Marine Biology*, 5, 205–212.

Stebbing, A. R. D. (1970)b. The status and ecology of *Rhabdopleura compacta* (Hemichordata) from Plymouth. *Journal of the Marine Biological Association of the United Kingdom*, 50, 209–221.

Strano, F., Micaroni, V., Beli, E., Mercurio, S., Scarì, G., Pennati, R., & Piraino, S. (2019). On the larva and the zooid of the pterobranch *Rhabdopleura recondita* Beli, Cameron and Piraino, 2018 (Hemichordata, Graptolithina). *Marine Biodiversity*, 49, 1657–1666.

West-Eberhard, M. J. (2003). *Developmental Plasticity and Evolution*. Oxford University Press.

Chapter 2

This paper was originally formatted for and published in *Phylonyms*: A Companion to the *PhyloCode* (K. de Queiroz, P. D. Cantino, and J. A. Gauthier, eds.). CRC Press, Boca Raton, FL. and is reproduced here with permission.

Cameron, C. B. and Beli, E. 2020 contributions:

Cameron C. B. wrote the first draft of the paper that was accepted in 2012, before we knew that *Rhabdopleura* was a living graptolite. Major changes were not permitted to the manuscript before publication in 2020, but Beli was able to make minor edits. Beli was invited to do this because of their productive years of collaboration, fruitful discussions and experiments, and for her expertise in pterobranch biology.

Hemichordata W. Bateson 1885 [C. B. Cameron and E. Beli], converted clade name

Registration Number: 49

Definition: The smallest crown clade containing *Cephalodiscus gracilis* Harmer 1905 and *Ptychodera flava* Eschscholtz 1825. This is a minimum-crown-clade definition. Abbreviated definition: min crown ∇ (*Cephalodiscus gracilis* Harmer 1905 & *Ptychodera flava* Eschscholtz 1825).

Etymology: Derived from the Greek *hemi* (half) and *chorde* (string), referring to the stomochord. The stomochord is derived from the endoderm and is composed of turgid cells, it is restricted to the anterior part of the body and thus is a "half-chord".

Reference Phylogeny: The primary reference phylogeny is Cameron (2005: Fig. 5). See also Cameron et al. (2000), Winchell et al. (2002), and Cannon et al. (2009).

Composition: The clade *Hemichordata* is currently thought to contain some 106 extant species of *Enteropneusta*, *Pterobranchia*, and *Planctosphaeridae*, and the extinct *Graptolithina*. An up-to-date comprehensive list of living species may be found in Cameron (2009).

Diagnostic Apomorphies: *Hemichordata* apomorphies include the prosoma: a muscular–secretory–locomotory preoral organ (enteropneust proboscis and pterobranch cephalic shield) that encloses a heart–kidney coelomic complex, including a stomochord. Further apomorphies include the paired valved mesocoel ducts and pores; and a ventral postanal extension of the metacoels (Schepotieff 1909; Horst 1939; Hyman 1959).

Synonyms: *Stomochordata* Dawydoff 1948 (approximate).

Comments: The monophyly of *Hemichordata* is supported by both molecular and morphological analyses (Cameron et al. 2000; Winchell et al. 2002; Cameron 2005). The hypothesis that the pterobranchs are the sister group of the echinoderms and the enteropneusts are the sister group of the chordates (Bateson 1885; Nielsen 2001) is no longer widely accepted. Instead, hemichordates

are widely regarded as monophyletic and the sister group of *Echinodermata* (Horst 1939; Dawydoff 1948; Hyman 1959; Halanych 1996; Cameron et al. 2000). Dawydoff (1948) created a taxon named *Stomochordata* to unambiguously include *Enteropneusta* and *Pterobranchia*; however, the name *Hemichordata*, originally applied to enteropneusts alone (Bateson 1885), had already been applied to this group in two major works (Harmer 1904; Horst 1939). *Hemichordata* is the name most commonly applied to the clade composed of pterobranchs and enteropneusts (e.g., Cameron et al. 2000; Winchell et al. 2002; Cannon et al. 2009) and was selected here for that reason. *Deuterostomia* should have precedence over *Hemichordata* in the context of phylogenies in which the two names are synonyms. Members of the monotypic taxon *Planctosphaeridae* may be long-lived enteropneust larvae (Hadfield and Young 1983).

References

Bateson, W. (1885). The later stages in the development of *Balanoglossus kowalevskii*, with a suggestion as to the affinities of the Enteropneusta. *Quarterly Journal of Microscopical Science*, 25, 81–122.

Cameron, C. B. (2005). A phylogeny of the hemichordates based on morphological characters. *Canadian Journal of Zoology*, 83, 196–215.

Cameron, C. B. (2009). A comprehensive list of extant hemichordate species with links to images. Available online at https://www.webdepot.umontreal.ca/Usagers/cameroc/MonDepotPublic/Cameron/Species.html

Cameron, C. B., Garey, J. R., & Swalla, B. J. (2000). Evolution of the chordate body plan: new insights from phylogenetic analyses of deuterostome phyla. *Proceedings of the National Academy of Sciences*, 97, 4469–4474.

Cannon, J. T., Rychel, A. L., Eccleston, H., Halanych, K. M., & Swalla, B. J. (2009). Molecular phylogeny of hemichordata, with updated status of deep-sea enteropneusts. *Molecular Phylogenetics and Evolution*, 52, 17–24.

Dawydoff, C. (1948). *Classe des entéropneustes*. Pp. 369–453 in *Traité de zoologie* (P. P. Grassé, ed.). Masson, Paris.

Hadfield, M. G., & Young, R. E. (1983). *Planktospaera* (Hemichordata: Enteropneusta) in the Pacific Ocean. *Marine Biology*, 73, 151–153.

Halanych, K. M. (1996). Convergence in the feeding apparatuses of lophophorates and pterobranch hemichordates revealed by 18S rDNA: an interpretation. *The Biological Bulletin*, 190, 1–5.

Harmer, S. F. (1904). *Hemichordata*. Pp. 3–111 in *The Cambridge Natural History* (S. F. Harmer

and A. E. Shipley, eds.). Vol. 7. Macmillan & Co., London.

van der Horst, C. J. (1939). *Hemichordata*. In *Klassen und Ordnungen des Tier-Reichs wissenschaftlich dargestellt in Wort und Bild* (H. G. Bronns, ed.). Band 4, Abt. 4, Buch 2, Tiel 2. Akademische Verlagsgesellschaft, Leipzig.

Hyman, L. H. (1959). *The Invertebrates: Smaller Coelomate Groups*. Vol. 5. McGraw-Hill Book Company, New York.

Nielsen, C. (2001). *Animal Evolution: Interrelationships of the Living Phyla*. 2nd edition. Oxford University Press, Oxford. 578pp.

Schepotieff, A. (1909). Die Pterobranchier des Indischen Ozeans. *Zoologische Jahrbücher. Abteilung für Systematik*, 28, 429–448, plates 7–8.

Winchell, C. J., Sullivan, J., Cameron, C. B., Swalla, B. J., & Mallatt, J. (2002). Evaluating hypotheses of deuterostome phylogeny and chordate evolution with new LSU and SSU ribosomal DNA data. *Molecular Biology and Evolution*, 19, 762–776.

Chapter 3

This paper was originally formatted for and published on *Treatise Online* in the *Treatise on Invertebrate Paleontology*, and is reproduced here with permission.

Maletz, J. and Beli, E. 2018 contributions:

Maletz J. wrote the first draft of this paper.
Beli E. wrote together with Maletz the generalities of living *Rhabdopleura* and provided information on the living *Rhabdopleura recondita*.

Part V, Second Revision, Chapter 15: Subclass Graptolithina and *Incertae Sedis* Family Rhabdopleuridae: Introduction and Systematic Descriptions

Subclass Graptolithina Bronn 1849

[Graptolithina Bronn, 1849, p. 149] [=Rhabdophora Allman, 1872, p. 380] [incl. order Rhabdopleurida Fowler, 1892, p. 297; order Rhabdopleuroidea Beklemishev, 1951, p. 414; order Graptovermida Kozłowski, 1949, p. 204, herein]

Pterobranchs with a colonial habit, building a tubarium from individual fusellar rings and half rings or, in some instances, featureless membranes; rigid stolon system (black stolon) connects the individual, clonally produced zooids attached to stolon by highly flexible and extendable zooidal stalk. Cambrian (*Terreneuvian*, *Fortunian*)–*Holocene* (extant): worldwide.

Mitchell et al. (2013) defined the taxon based on a detailed cladistic analysis of Paleozoic benthic graptolites and extant pterobranchs and regarded serial budding from an interconnected stolon system as the defining synapomorphy. The Graptolithina can be characterized as pterobranchs with a clonal, colonial development, secreting a tubarium from individual fusellar rings and half rings, as was described by Mitchell et al. (2013) and Maletz (2014).

Fossil taxa can be recognized through the preservation of the tubarium. More rarely, the black stolon and the diaphragm complexes are preserved. These are not formed from fusellar tissue and have often not been recognized as pterobranch remains. Several authors (e.g., Mierzejewski 1986; Urbanek and Dilly 2000; Maletz 2014) identified stolonal remains, initially identified as hydroids, as putative stolonal fragments of Graptolithina. Mierzejewski (1986) was able to convincingly combine the remains of *Kystrodendron longicarpus* (Eisenack 1937) (stolon with cysts) and *Eorhabdopleura urbaneki* Kozłowski 1970 (tubes of fusellar construction) into a single rhabdopleurid taxon.

Graptolithina? *Incertae Sedis*

A few apparently colonial genera are here tentatively identified as Graptolithina? *incertae sedis* following Maletz and Steiner (2015), even though the final recognition of fusellar construction for

their complex fossils is lacking and the material is poorly preserved. They differ considerably in the construction of their tubaria from the remaining taxa of the Graptolithina, as thecal apertures are recognized only at the distal end of the stipes and not at the branching segments. It is impossible to refer the material to the recognized families included in the Graptolithina.

Dalyia Walcott 1919, p. 237 [**D. racemata*; OD]. Colonial organism with long, slender, almost parallel-walled thecal tubes(?) and prominent internal thread; axes both erect and creeping, with whorls of thecal tubes radiating at specific branching points; circular attachment structures at base of branching points. *Cambrian (Series 3, Stage 5*, Ptychagnostus praecurrens *Biozone*): Canada.——Fig. 1,1. **D. racemata*, lectotype, USNM 354117, Burgess Shale, loc. 35K, British Columbia, Canada, scale bar, 10 mm (Maletz and Steiner 2015, fig. 16).

Malongitubus Hu 2005, p. 185 [**M. kuangshanensis*; OD] [=?*Cambrohydra* Hu 2005, p. 188 (type, *C. ercaia*; OD)]. Colonial organism(?) formed from parallel-sided tubes(?), branching at irregular distances to form whorls of radiating tubes of next order; number of tubes forming at branching division variable from two to at least six; distal tubes may be open-ended; length of the longest tubular branch measures at least 6 cm. *Cambrian (Series 2, Stage 3*, upper Eoredlichia–Wutingaspis *Zone*): China.——Fig. 1,2. **M. kuangshanensis*, holotype, NIGP 165032, Kuangshan, Yunnan Province, China, scale bar, 10 mm (Hu 2005, pl. 18).

Graptolithina Families *Incertae Sedis*

The precise status of the families of the benthic graptolites within the subclass Graptolithina has not yet been established. Thus, they are discussed here as families *incertae sedis* and are considered to represent preliminary taxonomic units of uncertain value. Their diagnoses are based on strongly limited features of fragmentary material.

Incertae Sedis Family Rhabdopleuridae Harmer 1905

[Rhabdopleuridae Harmer 1905 p. 5] [incl. Chaunograptidae Bulman 1955, p. 36, *partim*; Idiotubidae Kozłowski, 1949, p. 144, *partim*; Stolonodendridae Bulman 1955, p. 43; Rhabdopleuroididae Mierzejewski 1986, p. 176; Rhabdopleuritidae Mierzejewski 1986, p. 177; ?Rhabdohydridae Mierzejewski 1986, p. 151]

Colonial pterobranchs with encrusting tubarium, showing irregular fusellar rings or regular zigzag sutures in creeping and erect tubes; resorption foramen for the origination of new tubes; erect thecal tubes parallel-sided or slowly widening, with simple or ornamented apertures; zooids connected through robust stolon system showing diad budding with diaphragm complexes and dormant bud capsules (cysts); sicular zooid secretes featureless dome. *Cambrian (Terreneuvian, Fortunian)–Holocene* (extant): worldwide.

The Rhabdopleuridae represent a group of encrusting benthic organisms, restricted to the marine environment. They possess a complex life cycle with a planktic, swimming larval stage and a benthic stage, growing through asexual production of clonal zooids and forming encrusting colonies with various structures, known only from extant taxa. Rhabdopleurids occur from the shallow intertidal zone to the deep marine regions, from the tropical equatorial regions to Arctic and Antarctic regions. The fossil remains of their tubaria can easily be compared to the tubaria of a number of extant species. The modern taxa provide the only information of the soft body anatomy of the rhabdopleurids.

Morphology

The complexities of the tubarium of the Rhabdopleuridae are known in some detail from the extant genus *Rhabdopleura* Allman in Norman 1869, but details of fossil taxa are difficult to interpret, as they are often based on highly fragmented material. Two main features have to be differentiated: (1) the tubarium secreted from fusellar rings and half rings by the zooids; and (2) the stolon system (pectocaulus) formed as a dermal construction on the surface of the living tissues of the gymnocaulus with all its additional developments in the form of thecal cones, dormant bud capsules, cysts, and diaphragm complexes. Schepotieff (1907) described the early colony development in *Rhabdopleura normani* Allman in Norman 1869. His description shows the presence of the “Embryonalblase” (dome) and an “Embryonalring” (initial circular part of the stolon), formed from the stolon. The rhabdopleurid tubarium starts with the dome, sometimes homologized with the prosicula of the Graptoloidea (see Maletz, Steiner, and Fatka 2005; Mitchell et al. 2013). The dome is secreted by the sicular zooid as a featureless membrane in which the larva morphs into the mature zooid. It generally has an ovoid shape and is attached to the substrate on one side. The zooid emerges from one side of the dome by resorbing a foramen into the membrane and starts to secrete the first fusellar rings. In most *Rhabdopleura*, even the earliest fuselli form

half rings and a dorsal zigzag suture on the developing metasicular tube (Dilly 1986). The sicular zooid produces a horizontal, encrusting thecal tube with a distinct dorsal zigzag suture and a flat basal surface, with which it is attached to the substrate. In other (fossil) taxa, the initial fuselli may be irregularly formed, but details are available from few specimens.

Sars (1872), Lankester (1884), and Schepotieff (1907) described and illustrated the tubarium of the extant *Rhabdopleura normani* in some detail and provided the most complete understanding of any rhabdopleurid tubarium. The tubarium of *Rhabdopleura compacta* Hincks 1880 is largely comparable in its construction (see Hincks 1880; Stebbing 1970a, 1970b), but the presence of a permanent terminal zooid is not confirmed. All rhabdopleurids produce a tubarium in the shape of interconnected tubes for the individual zooids. These tubaria possess a number of characteristics not found in other pterobranchs. Early rhabdopleurids appear to possess irregularly placed fusellar sutures, for example, *Sphenoecium wheelerensis* Maletz and Steiner 2015 (see Maletz and Steiner 2015), but details are only available from a few specimens. *Sphenoecium obuti* (Durman and Sennikov 1993) (see Durman and Sennikov 1993; Sennikov 2015) from the middle Cambrian of Siberia already shows a relatively regular development of the sutures closely resembling the zigzag suture of extant *Rhabdopleura*.

The most remarkable character of the *Rhabdopleura normani* tubarium is the monopodial development of the main stem, the branching axis (Lankester 1884, p. 625) or "Hauptröhre" of Schepotieff (1907, p. 213), but a comparable feature is not known in most other *Rhabdopleura* taxa. Colony growth is achieved through the increasing length of the main stem and the addition of new thecal tubes ("Wohnröhren" in Schepotieff 1907, p. 213) at the sides of this stem. The permanent terminal zooid (Fig. 2.1) produces fusellar half rings and increases the length of the stipe. At regular or irregular distances, transverse septa are formed to separate individual segments of the stem into compartments for the developing zooids (Lankester 1884; Schepotieff 1907; Urbanek and Dilly 2000). The development of the transverse septa starts from the inner wall of the tubes, as incompletely developed septa indicate (Schepotieff 1907, p. 220).

The zooids resorb an opening into one side of the main stem, invariably at the distal end of the compartment (see Schepotieff 1907, p. 220; Kozłowski 1949, fig. 14E) and start to build erect thecal tubes from fusellar full rings. These tubes can reach considerable lengths and are inhabited

by a single zooid attached to the stolon system with a highly flexible gymnocaulus. While the main stem invariably bears a dorsal zigzag suture in *Rhabdopleura*, the thecal tubes show full fusellar rings with a single oblique suture. A distinct collar is often also present in the fuselli of the thecal tubes but in fossil material may be difficult to recognize.

The interconnection between the zooidal development and the tubarium construction in *Rhabdopleura normani* and possibly in other members of the genus is an important observation. Lankester (1884, p. 627) noted that the creeping (recumbent) tubes with their characteristic zigzag sutures are invariably secreted by immature zooids before arms have developed. The mature zooids with their two, fully formed arms secrete the full rings of the erect thecal tubes. Thus, the zooids morph in their initial compartments into fully grown organisms before they break through the tube wall and start secreting the thecal tubes. The permanent terminal zooid represents the model of an immature zooid before the maturation process is finished.

Branching of the main stem can be produced irregularly and appears to be through a resorption foramen and the immediate development of a dorsal zigzag suture of the new branch (Fig. 3.1). An illustration of Kozłowski (1949, fig. 14A) shows the original branch and the laterally originating secondary branch, at the base of which truncated fuselli of the previous branch can be seen. A transverse septum separates the continuing part of the main branch. Branching of the thecal tubes is generally not noted, but Kozłowski (1949, fig. 14C) illustrated a fragment that appears to show an unusual resorption foramen and the growth of a secondary thecal tube (Fig. 3.3). Regeneration of thecal tubes is more common (Fig. 3.2) and can be seen by the irregular break across a tube and the subsequent addition of fusellar full rings (Rigby 1994). Often, the new addition is also less strongly colored than the older part of the tubarium.

One of the most conspicuous features of the Rhabdopleuridae is the stolon system connecting the individual zooids. The fully developed stolon system is a black rod either lying free within the main tube or attached to the ventral tube wall, which develops as the gymnocaulus hardens to form the stolon system (black stolon) and is surrounded by denser, dark material (Lankester 1884, p. 636). This dark stolonal material is formed from dense crassal fabric, as is the stolon system of other graptolites (Urbanek and Towe 1974; Bates and Urbanek 2002; Saunders et al. 2009). In extant

rhabdopleurids, the stolon is often easily visible through the translucent tubarium (see Urbanek and Dilly 2000).

Initially, the stolon (gymnocaulus) is naked and flexible and begins to lengthen behind the terminal zooid and its developing buds (Fig. 2.1). When a number of buds are formed and separated into their individual chambers, the gymnocaulus within these chambers subsequently and slowly thickens and hardens, attaining a dark coloration and losing its original flexibility (Lankester 1884).

A short branch of the stolon connects to the zooidal stalk of the zooids (Fig. 2.1). At the tip of the zooidal stolon, a diaphragm complex (Urbanek and Dilly 2000) develops (Fig. 4), representing the encysting shell of a dormant bud or a resting stage of the developing zooid, also called the pigmented peridermal capsule (Urbanek and Dilly 2000, p. 210). These capsules were first recognized by Lankester (1884) as "hibernacula." Later, Schepotieff (1907) referred to them as "sterile Knospen" (sterile buds). Stebbing (1970a) showed that these buds were able to develop into zooids and introduced the term dormant buds. In thecal tubes of active zooids, these capsules are open distally and can be seen as an inner lining of the tube over considerable distances, adhering closely to the fusellar wall (Urbanek and Dilly 2000, p. 214). The zooid is independent of this thecal lining, as can be seen from retracted zooids with a coiled zooidal stalk in the terminal diaphragm complex (Urbanek and Dilly 2000, fig. 9).

When Kozłowski (1949) introduced the order Graptovermida, he described them as tubes of unknown origin, possessing a flat basal surface indicating an encrusting habit. He documented the presence of fuselli in some specimens. The Graptovermida can be included in the Rhabdopleuridae as they are easily interpreted as remains of a tigmophyllic *Rhabdopleura*-like species. Kozłowski (1949, p. 206) indicated the presence of an ovoid initial part or dome in *Graptovermis spiralis* Kozłowski 1949, termed a cul-du-sac ovale. The vermiform tubes represent the creeping tubes of the tubarium, showing zigzag suture lines on the upper surface of the tubes. The erect tubes with their collared full fusellar rings may not be preserved. Mierzejewski (1988) discussed the graptovermids in some detail based on chemically isolated material from Öland, Sweden. The material consisted of stolonal developments with strongly elongated cysts or buds, similar to the diaphragm complexes of extant rhabdopleurids. Mierzejewski (1988) interpreted them as resting

stolothecae of encrusting graptolites. However, the ultra- structure of the graptovermids has not yet been investigated.

Evolution

The evolutionary origin of the Rhabdopleuridae is uncertain, but a number of observations have led to some understanding. Earliest rhabdopleurid fossils originate from the middle Cambrian and may be referred to the genus *Sphenoecium* (Maletz and Steiner 2015). They clearly show the clonal, colonial development through the presence of interconnected thecal tubes in encrusting colonies with erect, unbranched distal thecal tubes. *Sphenoecium wheelerensis* and *Sphenoecium mesocambricus* (Öpik 1933) belong to the oldest members of the group. However, *Sphenoecium obuti* appears to be the oldest well-preserved rhabdopleurid. Very little is known about the diversification of the Graptolithina in the upper Cambrian, and even the cladistic analysis (Mitchell et al. 2013) did not provide sufficient evidence for an evolutionary interpretation of the early origins of the group. Rhabdopleurids with numerous modern tubarium features are present in the Ordovician (Skevington 1965; Mierzejewski 1986), but may not be referred to the genus *Rhabdopleura*. Chemically isolated material of *Sokoloviina* Kirjanov 1968 may represent the oldest rhabdopleurid record in the Lower Cambrian (Fortunian), as it shows fusellar construction and collars on the tubes.

The earliest taxon referable to the extant genus *Rhabdopleura* may be *Rhabdopleura hollandi* Rickards, Chapman, and Temple 1984 from the Silurian *Spirograptus turriculatus* Biozone of Wales (Rickards, Chapman, and Temple 1984), while older rhabdopleurids can be referred to the genus *Kystodendron* Kozłowski 1959 (see Mierzejewski and Kulicki 2001, 2002, 2003).

Chapman, Durman, and Rickards (1995) identified fragmentary material from the Ordovician (upper Darriwilian) of China as *Rhabdopleura sinica* Kozłowski 1959, fig. 10. *Rhabdopleura graysoni* Chapman, Durman, and Rickards 1995 from the Asbian (Carboniferous) resembles the extant *Rhabdopleura compacta*, but little detail of the tubarium development is available. Another record from the Carboniferous is *Rhabdopleura delmeri* Mortelmans 1955 from Belgium. Fossil records of rhabdopleurids from the Mesozoic and Cenozoic are rare, and few specimens have been described. Kozłowski (1956) described *Rhabdopleura vistulae* Kozłowski 1956 from the Danian (Cretaceous) of Poland, and Kulicki (1969, 1971) recorded the species *Rhabdopleura kozlowskii*

Kulicki 1969 from the Callovian (Jurassic) of Poland. A single record of *Rhabdopleura* exists from the Eocene of England (Thomas and Davies 1949a, 1949b, 1950).

Rhabdopleura Allman in Norman 1869, p. 311 [**R. normani*; M] [=*Halilophus* Sars 1868, p. 255 (type, *H. mirabilis*; nom. nud., herein)]. Rhabdopleurids with thigmophyllic to thigmophobic tubarium; creeping tubes with fusellar half rings and dorsal zigzag sutures, sutures on ventral sides indistinct or lacking; sicular zooid forms dome from which the metasicula and first autotheca develop; creeping tubes show irregularly to regularly produced partitions; erect tubes with irregularly placed sutures and full fusellar rings; branching occurs only in creeping tubes; apertures simple, straight; fuselli on erect tubes with distinct collar; stolon system with diad budding and complex diaphragm complexes. *?Silurian* (*Llandovery*, *Spirograptus turriculatus* Biozone)–*Holocene* (extant): worldwide.——Fig. 5,1. **R. normani*, part of tubarium, Shetland Sea, ~165 m depth, scale bar, ~1 mm (Allman 1869, pl. 8,1).

Archaeolafoea Chapman 1919, p. 390 [* *A. longicornis*; M] [=*Archaeocryptolaria* Chapman 1919, p. 392 (type, *A. skeatsi*; SD Bulman 1970, p. 55): Maletz and Steiner 2015, p. 1097]. Tubarium construction of colonial pterobranch formed from organic tubes; creeping and branching, elongated central tube with erect and unbranched lateral tubes bearing simple, straight apertures; parallel-sided lateral tubes formed from fusellar half rings or full rings, possibly with irregularly developed oblique sutures; stolon and zooidal development unknown. *Cambrian (Series 3)–?Ordovician*: Australia (Victoria).——Fig. 5,2a. **A. longicornis*, holotype, NMVP 13112, scale bar, 1 mm (new).——Fig. 5,2b. *Archaeocryptolaria skeatsi* Chapman, 1919, holotype, NMVP 13114, scale bar, 1 mm (new).

Chaunograptus Hall 1882, p. 225 *[*Dendrograptus* (*Chaunograptus*) *novellus*; M] [=*Desmohydra* Kozłowski 1959, p. 227 (type, *D. flexuosa*; OD): Mierzejewski 1986, p. 163] [=*Epallohydra* Kozłowski 1959, p. 230 (type, *E. adhaerensis*; OD): Mierzejewski 1986, p. 163]. Tubarium formed from organic tubes; creeping and branching, elongated central tube with unbranched lateral tubes bearing simple, straight apertures; fusellar construction; stolons and zooidal development unknown. *Cambrian (Series 3, Stage 5*, Ptychagnostus praecurrens Biozone)–*Silurian (Wenlock)*: Poland, USA.——Fig. 5,*4a–b*. **C. novellus* Hall 1882; 4a, syntype, NYSM 3170/1, specimens attached to *Spirifera radiata*, scale bar, 10 mm (Hall 1882,

pl. 1); 4b, syntype, UC 11989, specimen attached to *Eucalyptocrinus*, scale bar, 1 mm (new).——Fig. 5,4c. *C. flexuosus* (Kozłowski 1959), holotype, ZPAL material, Poland, glacial boulder, scale bar, 1 mm (Kozłowski 1959, fig. 10).——Fig. 5,*4d*. *C. adhaerensis* (Kozłowski 1959), holotype, ZPAL material, Poland, glacial boulder, scale bar, 1 mm (Kozłowski 1959, fig. 10).

Sokoloviina Kirjanov, 1968, p. 22 [**S. costata*; OD]. Small- to medium-sized tubes of black color with collars in the form of sharp-pointed or circular annular growths. *Lower Cambrian (Terreneuvian, Fortunian)*: Ukraine (Podolia).——Fig. 5,3a-b. **S. costata; 3a*, syntype, tube fragment, scale bar, 1 mm (Kirjanov 1968, pl. 3,8); *3b*, chemically isolated fragment, scale bar, 10 μm (Sokolov 1997,pl. 9,*4*).

Epigraptus Eisenack 1941, p. 25 [**E. bidens*; M] [=*Idiotubus* Kozłowski 1949, p. 144 (type, *I. typicalis;* OD): Mierzejewski 1978, p. 566]. Encrusting thecoriza of unknown form; erect portions of autothecae arising directly from surface of thecorhiza; autothecal apertural apparatuses in form of single or two lamelliform or bifurcate process; stolon system unknown. *Lower Ordovician (Tremadocian)–Upper Ordovician*: Estonia, Germany, Poland, Sweden (glacial boulder).—— Fig. 6,1a–b. **E. bidens*. 1a, neotype, GPIT S.G. 158, Nr. (Eisenack 1974, p. 671); 1b, holotype (not preserved), Wesenberg D1, Estonia (Eisenack 1941, fig. 1). Scale bars, 1 mm.——Fig. 6,1c. *Epigraptus* sp., small colony with part of dome, whereabouts unknown, scale bar, 1 mm (Andres 1977, fig. 27).——Fig. 6,1d. *E. typicalis* (Kozłowski 1949), holotype, ZPAL material, Poland, scale bar, 1 mm (Kozłowski 1949, pl. 13,1).

Graptovermis Kozłowski 1949, p. 206 [**G. spiralis*; OD]. Rhabdopleurids with thigmophyllic tubarium; creeping tubes with fusellar development; thecal apertures and erect tubes unknown; sicular zooid forms dome; details of tubarium unknown. *Lower Ordovician (Tremadocian)*: Poland (glacial boulder).——Fig. 6,2a–c. **G. spiralis*. 2a–b, holotype, ZPAL material, in dorsal (a) and ventral (b) views; 2c, paratype, ZPAL material, showing spiral development from ventral side, scale bars, 1 mm (6,2a–c, Kozłowski 1949, pl. 36).——Fig. 6,2d. *G. intestinalis* Kozłowski 1949, holotype, ZPAL material, scale bar, 1 mm (Kozłowski 1949, pl. 35,6).

Haplograptus Ruedemann 1933, p. 323 [**H. wisconsinensis*; OD]. Branched, encrusting to erect tubes with elongate conical or vermiform, erect theca forming irregularly dendroid tubarium. *Cambrian (Furongian)–Middle Ordovician (Darriwilian)*: China, Canada, USA.——Fig. 6,4.

**H. wisconsinensis* Ruedemann 1933, holotype. Repository unknown. scale bar, 1 mm (Ruedemann 1947, pl. 40,6).

Kystodendron Kozłowski 1959, p. 252 [**Chitinodendron longicarpus* Eisenack 1937, p. 237; OD] [=*Eorhabdopleura* Kozłowski 1970, p. 4 (type, *E. urbaneki*; OD); *nom. dub.*, Mierzejewski 1986, p. 184] [=*?Cylindrotheca* Eisenack 1934, p. 66 (type, *C. profunda*; OD); *nom. dub.*, Mierzejewski 1986, p. 183]. Zooidal and stolonal tubes similarly developed as in *Rhabdopleura*; major stolon and peduncular stolons of cysts of sterile buds without diaphragms; sterile bud cysts circular in cross section, simple or composite. *Ordovician*: Poland (glacial boulder).——Fig. 7,2a. **K. longicarpus*, holotype, ZPAL material, stolon with cysts, scale bar, 1 mm (Eisenack 1937, fig. 18).——Fig. 7,2b–c, *Eorhabdopleura urbaneki* Kozłowski 1970, holotype, ZPAL material, thecal tube, scale bar, 0.1 mm (Kozłowski 1970, fig. 1).

Rhabdopleurites Kozłowski 1967, p. 126. [**R. primaevus*; OD]. Colony encrusting, with dendroidal part underdeveloped, composed of stolonal and zooidal tubes; fuseIlar tubes varying from 0.3 to 0.6 mm in width and fuselli 60 to 100 μm wide; fusellar collars varying in size, sometimes very large; some stolonal tubes nonfusellar; stolons without diaphragms; sterile bud cysts missing. *Ordovician (Darriwilian)*: Germany, Poland, Sweden (glacial boulder).——Fig. 7,1a–b. **R. primaevus.* 1a, syntype, ZPAL material, thecal tube; 1b, syntype, ZPAL material, thecal tube, scale bars, 0.5 mm (Kozłowski 1961, fig. 13).

Rhabdopleuroides Kozłowski 1961, p. 4 [**R. expectatus*; M]. Tubarium exclusively composed of creeping stolonal and zooidal tubes; stolons without cysts of sterile buds. *Middle Ordovician (Darriwilian)–Upper Ordovician (Sandbian)*: Poland (glacial boulder).——Fig. 7,3a–d. **R. expectatus*. 3a–b, holotype, not preserved (Mierzejewski 1986, p. 177); 3c, paratype, ZPAL material; 3d, lectotype (designated by Mierzejewski 1986, p. 177), ZPAL material (Kozłowski 1961, 1970, fig. 2). Scale bars, 0.5 mm.

Sphenoecium Chapman and Thomas 1936, p. 205 [**Sphenothallus filicoides* Chapman 1917, p. 92; SD Bulman 1970, p. 57] [pro *Sphenothallus* Chapman 1917; non J. Hall 1847, p. 261 (type, *Sphenothallus angustifolius* Hall, 1847, p. 261; SD Moore and Harrington 1956, p. 65); =*Cnidaria* Van Iten, Cox, and Mapes (1992, p. 143)] [=*Rhabdotubus* Bengtson and Urbanek, 1986 (type, *R. johannssoni*; OD): Maletz and Steiner 2015, p.1098] [=*Fasciculitubus* Obut and

Sobolevskaya 1967, p. 56 (type, *F. tubularis*; OD): Maletz and Steiner 2015, p.1098]. Tubarium construction of colonial pterobranchs formed from organic tubes; short creeping and branching tubes with distally erect and unbranched, slowly widening tubes with simple, straight apertures; tubes formed from fusellar half rings or full rings with irregularly developed oblique sutures; colony shapes often dependent on the availability of suitable surface for attachment, from small and circular to elongate, or with multiple branchings covering larger areas. *Cambrian (Series 3, Stage 5)–Ordovician*: worldwide.——Fig. 6,3a. *S. wheelerensis* Maletz and Steiner, 2015, Spence Shale, Wellsville Mountains, Utah, USA, scale bar, 1 mm (photo, Maletz and Steiner 2015, fig. 17C).——Fig. 6,3b. **S. filicoides*, NMVP 47737, well-preserved specimen, scale bar, 1 mm (photo, Maletz and Steiner 2015, fig. 12C).

Stolonodendrum Kozłowski 1949, p. 194 [**S. uniramosum*; OD]. Branched stolonal tubes with cysts and elongated thecal tubes with fusellum showing irregular sutures; interpreted as creeping tubes of Rhabdopleuridae (Bengtson and Urbanek 1986, p. 294). *Ordovician (Tremadocian)*: Poland (glacial boulder).——Fig. 7,4. **S. uniramosum*, holotype, ZPAL material, scale bar, 1mm (Kozłowski 1949, pl. 32,2).

Possible Rhabdopleurid Stolons

Numerous fragments of strings or slender tubes of organic material—sometimes with attached rounded or elongated bodies and showing distinct branching patterns—have been found in the Paleozoic and have often been identified as hydroid remains (e.g., Kozłowski 1959). Mierzejewski (1986) erected the family Rhabdohydridae for the genera *Rhabdohydra* Kozłowski 1959 and *Palaeotuba* Eisenack 1934 and regarded it as an extinct group related to the hydrozoan suborder Athecata Hincks 1868. A number of taxa originally described as possible hydroids have subsequently been referred to the Pterobranchia (see Mierzejewski 1986; Bates and Urbanek 2002; Maletz 2014). Muscente, Allmon, and Xiao (2015, p. 79) especially questioned the hydroid fossil record in the Paleozoic and suggested a hemichordate origin for many remains. They recognized that lower Paleozoic putative hydroid fossils are either preserved as carbonaceous microfossils or as alumosilicate "films" (pressure shadow minerals, see Underwood 1992; Maletz and Steiner 2015), while younger taxa are commonly preserved as bioimmured fossils. Keupp, Doppelstein, and Maletz (2016) described the rare occurrence of the stolon system of a rhabdopleurid preserved in situ on a Lower Jurassic hardground.

Calyxhydra Kozłowski, 1959, p. 221 [**C. gemellithecata*; OD; =rhabdopleurid stolon, Mierzejewski 1986, p. 168]. Branching system with more or less regular dichotomous diversions; terminal branches with conical tubes; no diaphragms. *Ordovician*: Poland (glacial boulder).——Fig. 8,1. **C. gemellithecata*, holotype, ZPAL material, scale bar, 0.5 mm (Kozłowski 1959, fig. 3).

Chitinodendron Eisenack 1937, p. 236 [**C. bacciferum*; SD Kozłowski 1959, p. 251; =?rhabdopleurid stolon, herein]. Branched stolon system with irregularly placed oval cysts. *Ordovician–Silurian*: Estonia, Poland.——Fig. 8,6. **C. bacciferum*, holotype, ZPAL material, scale bar, 0.5 mm (Eisenack 1937 fig. 13).

Diplohydra Kozłowski 1959, p. 240 [**D. longithecata*; OD; =Rhabdopleuroidea Beklemishev 1951, p. 19: Mierzejewski and Kulicki 2002, p. 171]. Stolon system devoid of diaphragms, peduncular stolons, and true capsules of the dormant buds; major stolon with irregularly arranged lateral offshoots; lateral offshoots form diads composed of the two daughter stolons; as a rule, one of the daughter stolons is strongly inflated and sometimes forms an imperfect composite cyst. *Ordovician–Permian (Roadian)*: Norway (Barents Shelf), Poland (glacial boulder).——Fig. 8,2. **D. longithecata*, holotype, ZPAL material, scale bar, 1 mm (Kozłowski 1959, fig. 16).

Flexihydra Kozłowski 1959, p. 225 [**F. undulata*; OD; =?rhabdopleurid remains, herein]. Short stolons with elongated, flexible thecal cups; fusellum unknown. *Ordovician:* Poland (glacial boulder).——Fig. 8,4a–b, **F. undulata*, syntype, ZPAL material, scale bar, 0.5 mm (Kozłowski 1959, fig. 7).

Lagenohydra Kozłowski 1959, p. 245 [**L. phragmata*; OD; =rhabdopleurid stolon, Mierzejewski 1986, p. 193]. Stolon system with distinct thecal dimorphism; each node bears two differently shaped thecae; fusellum unknown. *Ordovician*: Poland (glacial boulder).——Fig. 8,3. **L. phragmata*, holotype (specimen not preserved, see Mierzejewski 1986, p. 194), scale bar, 0.5 mm (Kozłowski 1959, fig. 22A).

Palaeokylix Eisenack 1932, p. 266 [**P. chitinosus*; OD; *nom. dub.*, herein]. Simple branched stolon with thecal cup; fusellum unknown. *Ordovician– Silurian?*: Oblast Kaliningrad (formerly

Samland), Russia (glacial boulder).——Fig. 8,9. **P. chitinosus*, holotype, ZPAL material, scale bar, 0.1 mm (Eisenack 1932, pl. 11,22).

Palaeotuba Eisenack 1934, p. 54 [**P. polycephala*; OD; =?rhabdopleurid stolon, Mierzejewski 1986, p. 179]. Stolon system with multiple branchings. *Upper Ordovician* (*lower Sandbian*, Kukruse Stage): Estonia, Poland (glacial boulder).——Fig. 8,7. **P. polycephala*, holotype, repository unknown, scale bar, 1 mm (Eisenack 1934, pl. 4,5).

Phragmohydra Kozłowski 1959, p. 238 [**P. articulata*; OD; =?rhabdopleurid remains, herein]. Stolon system with complex peduncular diaphragms; fusellum unknown. *Ordovician*: Poland (glacial boulder).——Fig. 8,5. **P. articulata*, holotype, ZPAL material, scale bar, 0.5 mm (Kozłowski 1959, fig. 15a).

Rhabdohydra Kozłowski 1959, p. 235 [**R. tridens*; OD; =?rhabdopleurid remains, herein]. Stolon system with multiple peduncular diaphragms; fusellum unknown. *Ordovician*: Poland (glacial boulder).——Fig. 8,8. **R. tridens*, ZPAL material, holotype, scale bar, 0.5 mm (Kozłowski 1959, fig. 14a).

ABBREVIATIONS FOR MUSEUM REPOSITORIES

GPIT: Geologisch-Paläontologisches Institut der Universität Tübingen, Germany

NIGP: Nanjing Institute of Geology and Palaeontology, Academia Sinica, Nanjing, China

NMVP: Museum Victoria, Melbourne, Australia NYSM: New York State Museum, Albany, New York, USA

UC: Field Museum of Natural History, Chicago, Illinois, USA

USNM: US National Museum of Natural History, Washington, DC, USA

ZPAL: Institute of Palaeobiology, Polish Academy of Sciences, Warsaw, Poland (older ZPAL materials do not have type numbers)

References

Allman, G. J. (1869). On *Rhabdopleura*, a new form of Polyzoa, from deep-sea dredging in Shetland. *Quarterly Journal of Microscopical Science*, 9, 57–63, pl. 8.

Allman, G. J. (1872). On the morphology and affinities of graptolites. *Annals and Magazine of Natural History (series 4)*, 9, 364–380.

Andres, D. (1977). Graptolithen aus ordovizischen Geschieben und die frühe Stammesgeschichte der Graptolithen. *Paläontologische Zeitschrift*, 51, 52–93.

Bates, D. E. B., & Urbanek A. 2002. The ultrastructure, development, and systematic position of the graptolite genus *Mastigograptus*. *Acta Palaeontologica Polonica*, 47, 445–458.

Beklemishev, V. N. 1951. [Russian editions in 1951, 1964] Osnovy sravnitelnoi anatomii bespozvonochnykh. 2 volumes, 430, 478 p. Sovetskaya nauka, Moskva. [German edition: Grundlagen der vergleichenden Anatomie der Wirbellosen 1958 (Band 1. Promorphologie); 1960 (Band 2. Organologie). VEB Deutscher Verlag der Wissenschaften, Berlin.] [English edition: Beklemishev, V.N. 1970. Principles of Comparative Anatomy of Invertebrates. Vol. 1, 490 p.; vol. 2, 529 p.; Oliver and Boyd. Edinburgh.]

Beli, E., Aglieri, G., Strano, F., Maggioni, D., Telford, M. J., Piraino, S. & Cameron, C. B. (2018). The zoogeography of extant rhabdopleurid hemichordates (Pterobranchia: Graptolithina), with a new species from the Mediterranean Sea. *Invertebrate Systematics*, 32, 100–110.

Bengtson, S., & Urbanek A. (1986). *Rhabdotubus*, a Middle Cambrian rhabdopleurid hemichordate. *Lethaia*, 19, 293–308.

Bronn, H. G. (1849). Handbuch der Geschichte der Natur. Dritter Band, Zweite Abtheilung. II. Theil: Organisches Leben (Schluß). Index palaeontologicus oder Ueberblick der bis jetzt bekannten fossilen Organismen. Schweizerbart. Stuttgart. 1106 p.

Bulman, O. M. B. (1955). *Graptolithina*. In *Treatise on Invertebrate Paleontology, Part V*. (R. C. Moore, ed.). The Geological Society of America & The University of Kansas Press. New York & Lawrence. xvii + 101 p.

Bulman, O. M. B. (1970). *Graptolithina*. In: C. Teichert, ed., *Treatise on Invertebrate Paleontology, Part V*. (C. Teichert, ed.). second edition. Geological Society of America & University of Kansas Press. Boulder & Lawrence. xxxii + 163 p.

Chapman, A. J., Durman, P. N., & Rickards, R. B. (1995). Rhabdopleuran hemichordates: New fossil forms and review. *Proceedings of the Geologists' Association*, 106, 293–303.

Chapman, F. (1917). The Heathcote Fauna. *Records of the Geological Survey of Victoria*, 4, 89–102, pl. 6–7.

Chapman, F. (1919). On some hydroid remains of Lower Palaeozoic age from Monegetta, near Lancefield. *Proceedings of the Royal Society of Victoria* (new series), 31, 388–393, pl. 19–20.

Chapman, F., & Thomas, D. E. (1936). The Cambrian Hydroidea of the Heathcote and Monegeeta Districts. *Proceedings of the Royal Society of Victoria* (new series), 48, 193–212, pl. 14–17.

Dilly, P. N. (1986). Modern pterobranchs; Observations on their behaviour and tube building. *Palaeoecology and biostratigraphy of graptolites*. *Geological Society Special Publication*, 20, 261–269.

Durman, P. N., & Sennikov, N. V. (1993). A new rhabdopleurid hemichordate from the Middle Cambrian of Siberia. *Palaeontology*, 36, 283–296.

Eisenack, A. (1932). Neue Mikrofossilien des baltischen Silurs II. (Foraminiferen, Hydrozoen, Chitinozoen u. a.). *Paläontologische Zeitschrift*, 14, 257–277, pl. 11–12.

Eisenack, A. (1934). Neue Mikrofossilien des baltischen Silurs III. und neue Mikrofossilien des böhmischen Silurs. I. *Paläontologische Zeitschrift*, 16, 52–76, pl. 4–5.

Eisenack, A. 1937. Neue Mikrofossilien des baltischen Silurs. IV. *Paläontologische Zeitschrift*, 19, 217–242, pl. 15–16.

Eisenack, A. (1941). *Epigraptus bidens* n. g., n. sp., eine neue Graptolithenart des baltischen Ordoviciums. *Zeitschrift für Geschiebeforschung und Flachlandsgeologie*, 17, 24–28.

Eisenack, A. (1974). Einige neue Graptolithen aus dem Ordovizium des Baltikums, ferner über Epigraptus und andere Idiotubidae. *Neues Jahrbuch für Geologie und Paläontologie*, Monatshefte 1974, 664–674.

Fowler, G. H. (1892). The morphology of *Rhabdopleura* Allman. Festschrift zum 70ten Geburtstag Rudolf Leuckarts. Verlag Wilhelm Engelmann. Leipzig. p. 293–297.

Hall, J. (1847). *Paleontology of New York*. Volume I. Containing descriptions of the organic remains of the Lower Division of the New-York System (equivalent to the Lower Silurian rocks of Europe). C. Van Benthuysen. Albany. 338 p.

Hall, James. (1882). *Descriptions of the species of fossils found in the Niagara Group at Waldron, Indiana*. Indiana Department of Geology and Natural History, 11th Annual Report. p. 217–345, 12 fig., pl. 1–36.

Harmer, S. F. (1905). The Pterobranchia of the Siboga-Expedition with an account on other species. *Siboga Expedition Monograph*, 26, 1–133, pl. 1–14.

Hincks, T. (1868). *A history of the British Hydroid zoophytes*. Van der Voorst. London. Vol. 1: p. i–lxviii +1–338; Vol. 2: pl. 1–67.

Hincks, T. (1880). *History of British marine Polyzoa*. Van Voorst. London. Vol. I: cxli+601 p., Vol. II: 83 pl.

Hu, S. (2005). Taphonomy and palaeoecology of the early Cambrian Chengjiang biota from eastern Yunnan, China. *Berliner Paläobiologische Abhandlungen*, 8, 1–189.

Keupp, H., Doppelstein, B., & Maletz, J. (2016). First evidence of in situ rhabdopleurids (Pterobranchia, Hemichordata) from the Lower Jurassic of southern Germany. *Neues Jahrbuch für Geologie und Paläontologie, Abhandlungen*, 282, 263–269.

Kirjanov, V. V. (1968). Paleontology and stratigraphy of the Baltic deposits in the Volhyn-Podolia. *Paleontology and Stratigraphy of the Lower Paleozoic of Volhyn-Podolia. Naukova Dumka*, Kiev. p. 5–27.

Kozłowski, R. (1949). Les graptolithes et quelques nouveaux groups d'animaux du Tremadoc de la Pologne. *Palaeontologia Polonica*, 3, 1–235, pl. 1–42.

Kozłowski, R. (1956). Sur *Rhabdopleura* du Danien de Pologne. *Acta Palaeontologica Polonica*, 1, 3–21.

Kozłowski, R. (1959). Les Hydroïdes ordoviciens à squelette chitineux. *Acta Palaeontologica Polonica*, 4, 209–271.

Kozłowski, R. (1961). Découverte d'un Rhabdopleuridé (Pterobranchia) ordovicien. *Acta Palaeontologica Polonica*, 6, 3–16.

Kozłowski, R. (1967). Sur certain fossiles ordoviciens à teste organique. *Acta Palaeontologica Polonica*, 12, 99–132.

Kozłowski, R. (1970). Nouvelles observations sur les rhabdopleuridés (Ptérobranches) ordoviciens. *Acta Palaeontologica Polonica*, 4, 3–17.

Kulicki, C. (1969). The discovery of *Rhabdopleura* (Pterobranchia) in the Jurassic of Poland. *Acta Palaeontologica Polonica*, 14, 537–551.

Kulicki, C. (1971). New observations of *Rhabdopleura kozlowskii* (Pterobranchia) from the Bathonian of Poland. *Acta Palaeontologica Polonica*, 16, 415–428.

Lankester, E. R. (1884). A contribution to the knowledge of *Rhabdopleura*. *Quarterly Journal of Microscopical Science*, 24, 622–647, pl. 37–41.

Maletz, J. (2014). The Classification of the Graptolithina Bronn, 1849. *Bulletin of Geosciences*, 89, 477–540.

Maletz, J., & Steiner, M. (2015). Graptolite (Hemichordata, Pterobranchia) preservation and identification in the Cambrian series 3. *Palaeontology*, 58, 1073–1107.

Maletz, J., Steiner, M., & Fatka, O. (2005). Middle Cambrian pterobranchs and the question: What is a graptolite? *Lethaia*, 38, 73–85.

Mierzejewki, P. (1978). Tuboid graptolites from erratic boulders of Poland. *Acta Palaeontologica Polonica*, 23, 557–575.

Mierzejewki, P. (1986). Ultrastructure, taxonomy and affinities of some Ordovician and Silurian organic microfossils. *Palaeontologia Polonica*, 47, 129–220, pl. 19–37.

Mierzejewski, P. (1988). Nature of graptovermids (Graptolithina). *Acta Palaeontologica Polonica*, 33, 267–272, pl. 14–15.

Mierzejewski, P., & Kulicki, C. (2001). Graptolite-like fibril pattern in the fusellar tissue of Palaeozoic rhabdopleurid pterobranchs. *Acta Palaeontologica Polonica*, 46, 349–366.

Mierzejewski, P., & Kulicki, C. (2002). Discovery of Pterobranchia (Graptolithoidea) in the Permian. *Acta Palaeontologica Polonica*, 47, 169–175.

Mierzejewski, P., & Kulicki, C. (2003). Cortical fibrils and secondary deposits in periderm of the hemichordate *Rhabdopleura* (Graptolithoidea). *Acta Palaeontologica Polonica*, 48, 99–111.

Mitchell, C. E., Melchin, M. J., Cameron, C. B., & Maletz, J. (2013). Phylogenetic analysis reveals that *Rhabdopleura* is an extant graptolite. *Lethaia*, 46, 34–56.

Moore, R. C., & Harrington, H. J. (1956). *Conulata*. In *Treatise on Invertebrate Paleontology: Part F: Coelenterata*. R. C. Moore, ed., The Geological Society of America & The University of Kansas Press. New York & Lawrence. p. 54–66.

Mortelmans, G. (1955). Découverte d'un Ptérobranche, *Rhabdopleura delmeri* nov. sp., dans le Viséen terminal du Sondage de Turnhaut. *Bulletin de la Societé Belge de Géologie, de Paléontologie et d'Hydrologie*, 64, 52–66.

Muscente, A. D., Allmon, W. D., & Xiao, S. (2015). The hydroid fossil record and analytical techniques for assessing the affinities of putative hydrozoans and possible hemichordates. *Palaeontology*, 59, 71–87.

Norman, A. M. (1869). Shetland Final Dredging Report. Part 2. On the Crustacea, Tunicata, Polyzoa, Echinodermata, Actinozoa, Hydrozoa and Porifera. *Reports of the British Association of the Advancement of Science*, 38, 247–336.

Obut, A. M., & Sobolevskaya, R. F. (1967). Nekotoryye stereostolonaty pozdnego kembriya I ordovika Norilskogo rayona [Some stereostolonates of the late Cambrian and Ordovician of the Norilsk Region]: In *Novyye dannye pobiostratigrafii nishnego paleozoya Sibirskoy platiformy* [New data on biostratigraphy of Lower Paleozoic of the Siberian platform]. Ivanovskiy, A. A., & B. S. Sokolov, eds. Nauka Moskva. p. 45–64, pl. 6–19.

Öpik, A. (1933). Über einen kambrischen Graptolithen aus Norwegen. *Norsk Geologisk Tidsskrift*, 13, 113–115.

Rickards, R. B., Chapman, A. J., & Temple, J. T. (1984). *Rhabdopleura hollandi*, a new pterobranch hemichordate from the Silurian of the Llandovery district, Powys, Wales. *Proceedings of the Geologist's Association*, 95, 23–28.

Ridewood, W. G. (1907). Pterobranchia. *Cephalodiscus*. National Antarctic Expedition 1901–1904. *Natural History Zoology (Vertebrata: Mollusca: Crustacea)*, 2, 1–67, pl. 1–7.

Rigby, S. (1994). Erect tube growth in *Rhabdopleura compacta* (Hemichordata: Pterobranchia) from off Start Point, Devon. *Journal of Zoology*, London 233, 449–455.

Ruedemann, R. (1933). Cambrian graptolite faunas of North America. *Milwaukee Public Museum Bulletin* 12, 307–348.

Ruedemann, R. (1947). *Graptolites of North America*. Vol. 19. Geological Society of America. New York. 652 p.

Sars, G. O. (1872). *On some remarkable forms of animal life from the great deeps off the Norwegian coast I*. Partly from posthumous manuscripts of the late Professor Dr. Michael Sars. University Programm for the 1st half-year 1869. Brogger & Bristiff. Christiania. 82 p., 6 pl.

Sars, G. O. (1874). On *Rhabdopleura mirabilis* (M. Sars). *Quarterly Journal of Microscopical Science* (new series), 14, 23–44, 1 pl.

Sars, M. (1868). Fortsatte Bemærkninger over det dyriske livs udbredning i havets dybder. Særskilt aftryt af Videnskabers-selskap forhandlinger for 1868, 245–275 (reprint with separate pagination 1–32).

Saunders, K. M., Bates, D. E. B., Kluessendorf,J., Loydell, D. K., & Mikulic, D. G. (2009). *Desmograptus micronematodes*, a Silurian dendroid graptolite, and its ultrastructure. *Palaeontology*, 52, 541–559.

Sennikov, N. V. (2015). *The morphology of Cambrian rhabdopleurids exoskeleton and soft tissues. Morphogenesis in the individual and historical growth: Stability and variability.* Geobiological systems in the Past. Moscow. Paleontological Institute Press. 237–255.

Schepotieff, A. (1907). Die Pterobranchier. Anatomische und histologische Untersuchungen über *Rhabdopleura normanii* Allman und *Cephalodiscus dodecalophus* M'Int. 1. Teil. *Rhabdopleura normanii* Allman. 2. Abschnitt. Knospungsprozess und Gehäuse von *Rhabdopleura*. *Zoologische Jahrbücher. Abteilung für Anatomie und Ontogenie der Tiere*, 24, 193–238, pl. 17–23.

Skevington, D. (1965). Graptolites from the Ontikan limestones (Ordovician) of Öland, Sweden. 2. Graptoloidea and Graptovermida. *Bulletin of the Geological Institutions of the University of Upsala,* 43, 1–74.

Sokolov, B. S. (1997). *Essays on the Advent of the Vendian System*. KMK Scientific Press Ltd. Moscow. 156 p., 24 pl. (ISBN 5-87317-032-0). Two different versions exist with 142 p. and 156 p. They have the same ISBN number but different covers. Longer version has photos in the text.

Stebbing, A. R. D. 1970a. Aspects of the reproduction and life cycle of *Rhabdopleura compacta* (Hemichordata). *Marine Biology*, 5, 205–212.

Stebbing, A. R. D. 1970b. The status and ecology of *Rhabdopleura compacta* (Hemichordata) from Plymouth. *Journal of the Marine Biological Association of the United Kingdom*, 50, 209–221.

Thomas, H. D., & Davis, A. G. (1949a). The pterobranch *Rhabdopleura* in the English Eocene. *Bulletin of the British Museum* (Natural History) Geology, 1, 1–19, pl. 1–3.

Thomas, H. D., & Davis A. G. (1949b). A fossil species of the pterobranch *Rhabdopleura*. *Abstracts, proceedings of the Geological Society*, London 1450, 79.

Thomas, H. D., & Davis A. G. (1950). A fossil species of the pterobranch *Rhabdopleura*. *Quarterly Journal of the Geological Society of London*, 106, 133.

Underwood, C. J. (1992). Graptolite preservation and Deformation. *Palaios*, 7, 178–186.

Urbanek, A., & Dilly, N. P. (2000). The stolon system in *Rhabdopleura compacta* (Hemichordata) and its phylogenetic implications. *Acta Palaeontologica Polonica*, 45, 201–226.

Urbanek, A., & Towe, K. M. (1974). Ultrastructural studies on graptolites, 1: The periderm and its derivatives in the Dendroidea and in *Mastigograptus*. *Smithsonian Contributions to Paleobiology*, 22, 1–48.

Van Iten, H., Cox, R. S., & Mapes, R. H. (1992). New data on the morphology of *Sphenothallus* HALL: Implication for its affinities. *Lethaia*, 25, 135–144.

Walcott, C. D. (1919). Cambrian geology and paleontology IV. Middle Cambrian algae. *Smithsonian Miscellaneous Collections*, 67, 217–260.

Figures

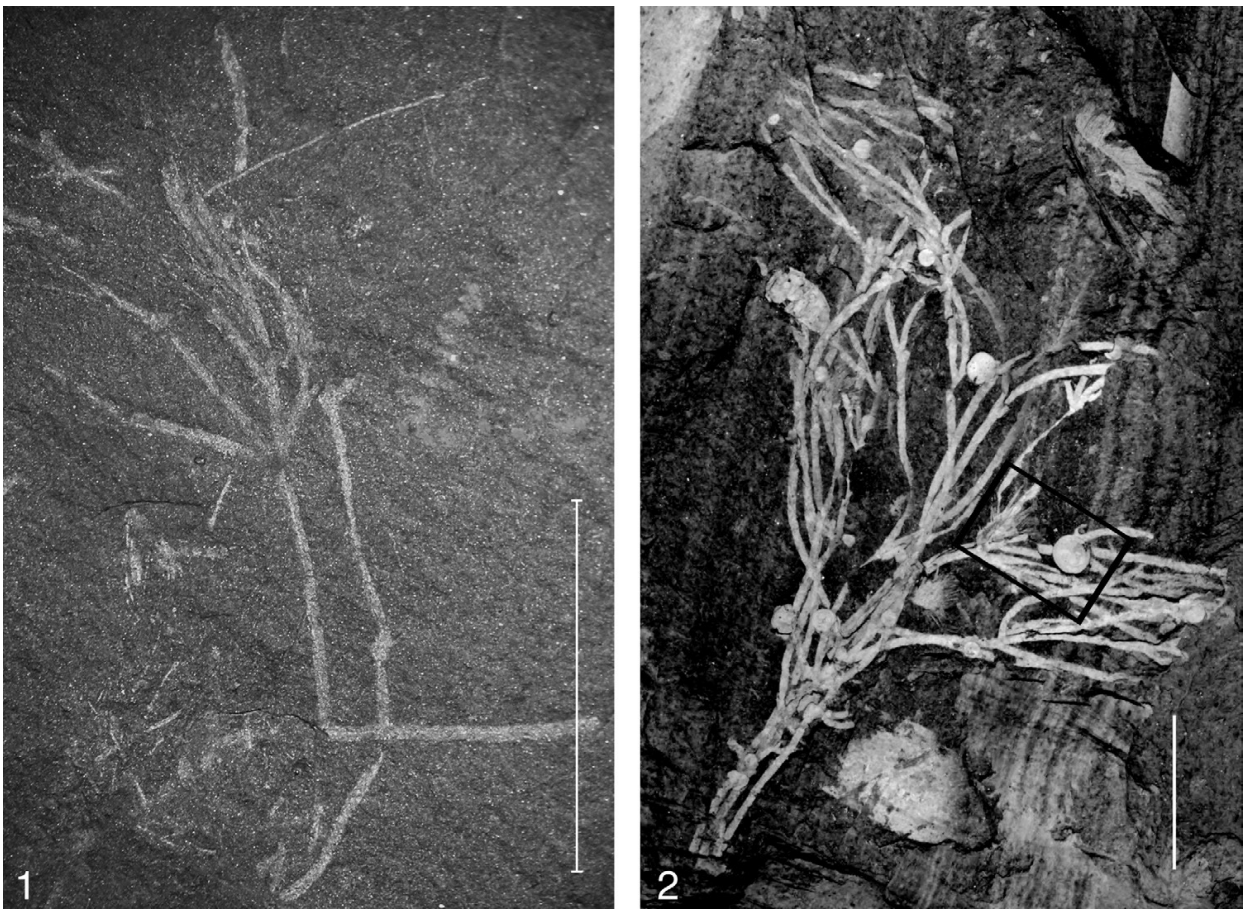

Dalyia Malongitubus

Fig. 1. Graptolithina? *incertae sedis* (p. 1–2).

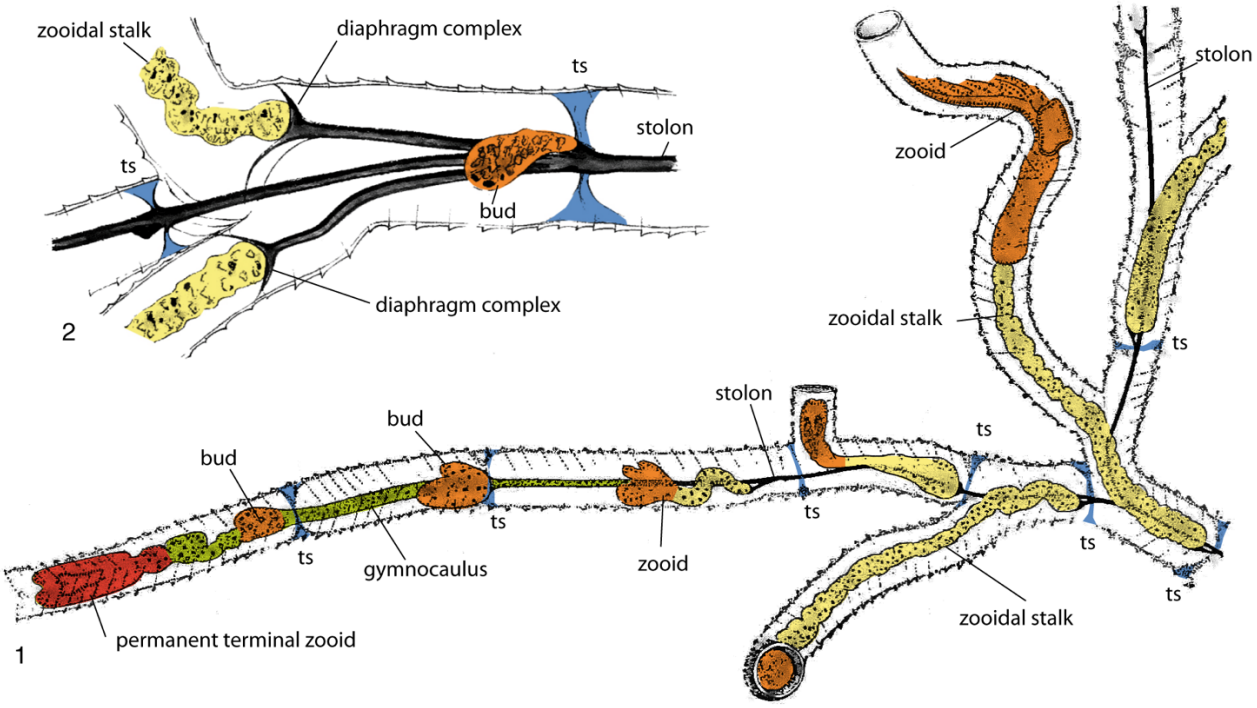

Fig. 2. *Rhabdopleura normani* Allman in Norman 1869, monopodial growth and stolon system with diaphragm complexes. 1, Growing end of colony showing monopodial growth with permanent terminal zooid (adapted from Ridewood 1907, fig. 7). 2, Branching point; ts, transverse septum (adapted from Lankester 1884).

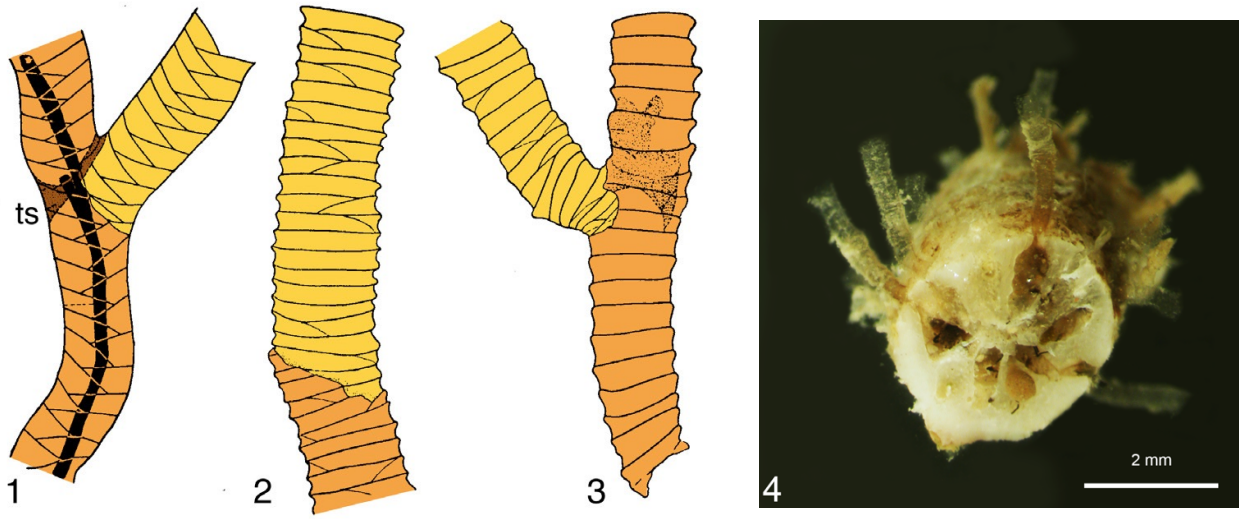

Fig. 3. Branching of tubarium. 1, Main stem with branching, see stolon and transverse septum (ts); 2, Part of erect thecal tube with regeneration. 3, Erect tube with unusual lateral branching. (adapted from Kozłowski, 1949, fig. 14). 4, *Rhabdopleura recondita* Beli et al. 2018 finds shelter inside the dead branches of bryozoan hosts, erect tubes project from the pores (new; photo courtesy of Stefano Piraino).

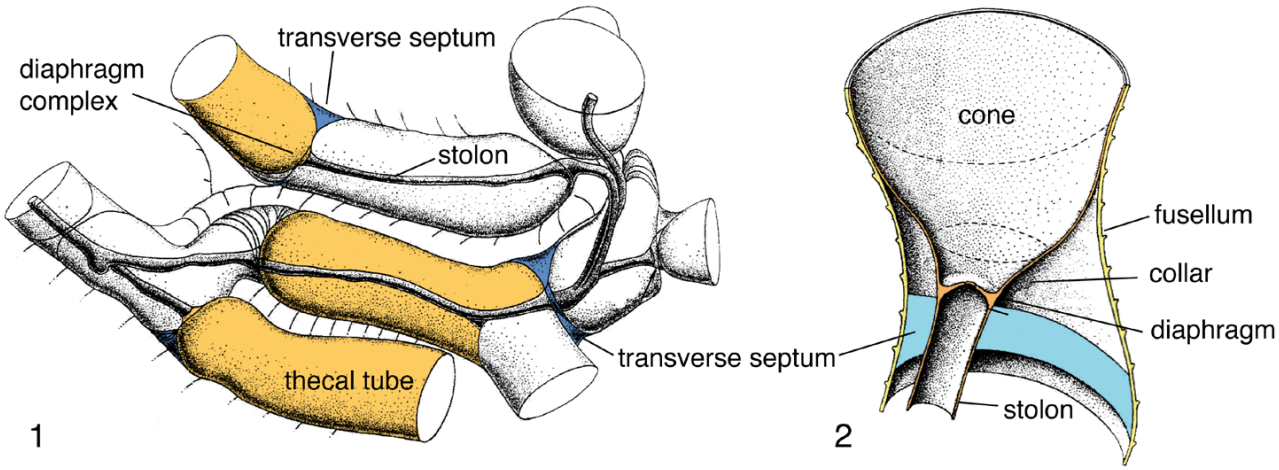

Fig. 4. The stolon system. 1, Stolon and inner lining (cone) of thecal tubes. 2, Diaphragm complex and connection to the fusellar tube (adapted from Urbanek & Dilly 2000).

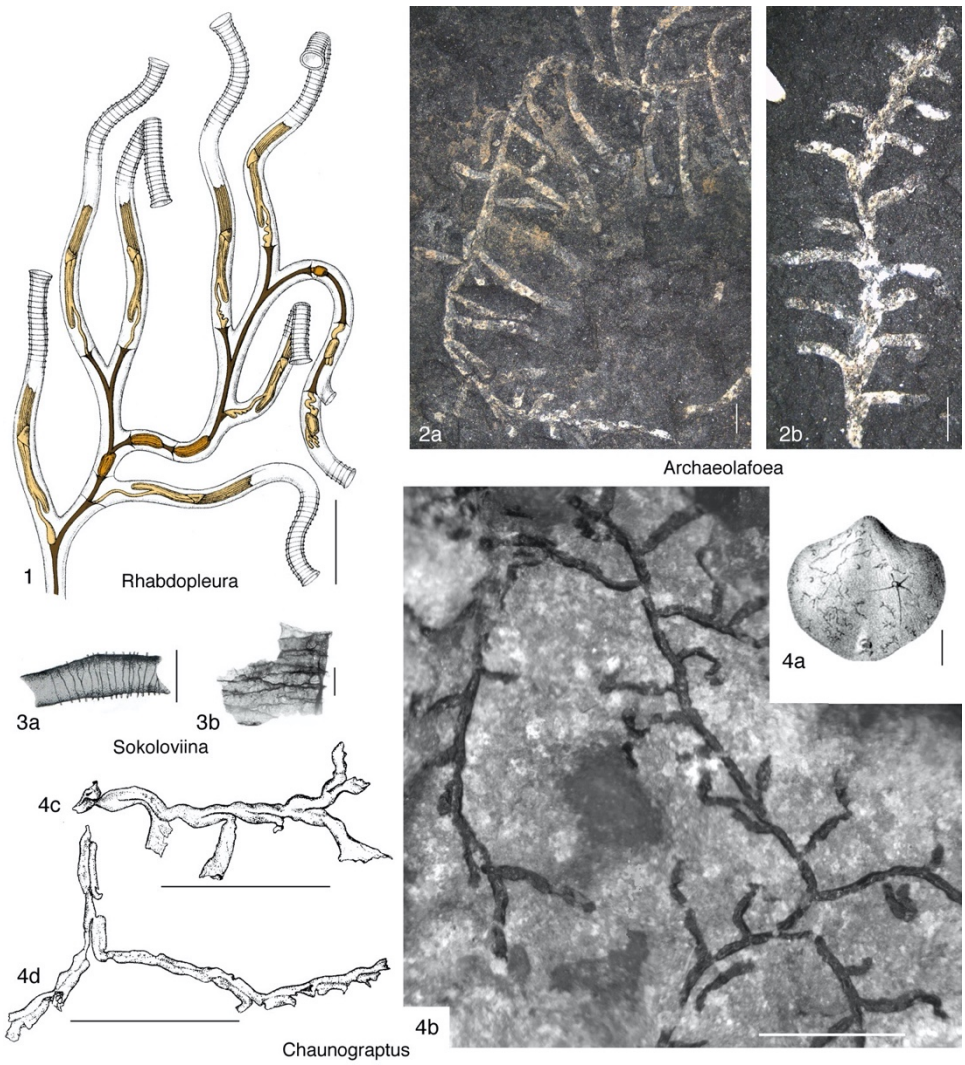

Fig. 5. Rhabdopleuridae (p. 7).

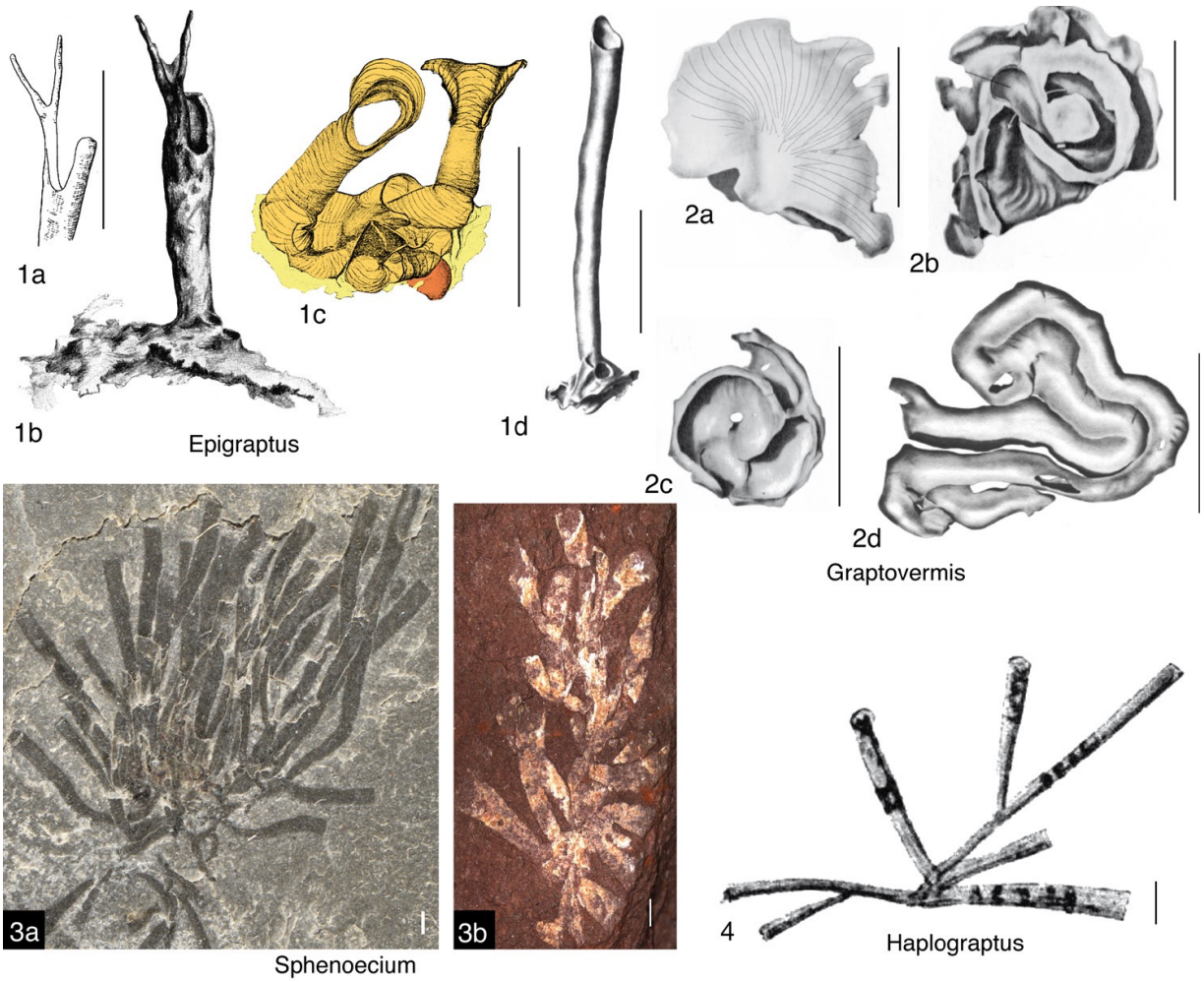

Fig. 6. Rhabdopleuridae (p. 7–10).

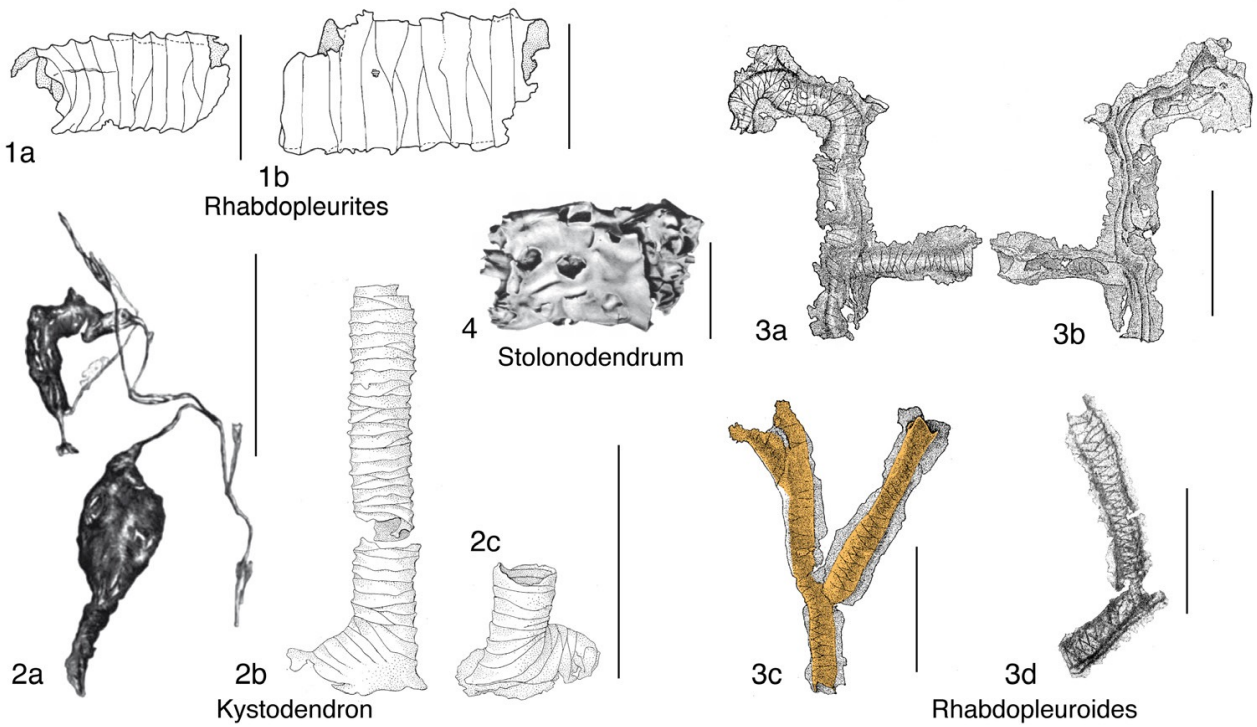

Fig. 7. Rhabdopleuridae (p. 8–10).

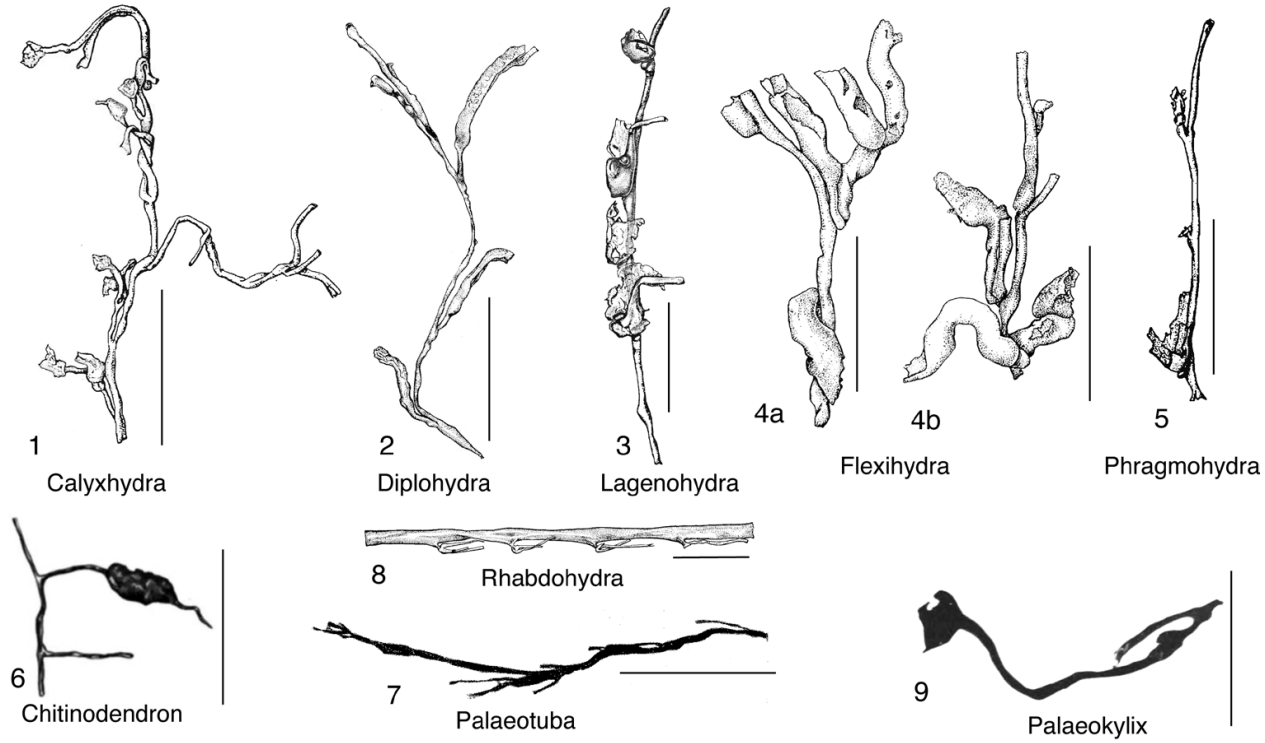

Fig. 8. Rhabdopleurid stolons (p. 10–11).

Chapter 4

This chapter is a paper in preparation, here reproduced with the permission of all the authors.

Beli, E., De Castro Mendonça, L. M., Piraino, S. and Cameron, C. B. contributions:

Beli designed and realized the experimental aquarium, sampled, collected and analyzed the data from this experiment and made many novel observations. Beli wrote the first draft and edited subsequent drafts.
Mendonça, L. M. C. performed the statistical tests, wrote the relative part in materials and methods, and reviewed the draft.
Piraino S. gave access to lab facilities at the University of Salento, provided funds for experiments and sampled.
Cameron C. B. conceived the idea for this project, guided the experiments, and contributed to its writing.

On the development and morphological invariability of the graptolite *Rhabdopleura recondita* tubes in response to water flow velocity

Abstract

Graptolites dominated the Paleozoic seas. The graptolite fossil record begins in the Middle Cambrian, then shows a considerable adaptive radiation between the Ordovician and Silurian periods, before disappearing in the Middle Carboniferous. The fossil record consists of the decay-resistant tubaria, so abundant that they are used as sedimentary layer index fossils. Graptolites are diverse and the variability of form between higher taxonomic levels is the most disparate of any extracellular, secreted, matrix structure. Taxonomic definitions of early benthic encrusting graptolites can be small. Here we make observations on larvae and zooids of the extant graptolite *Rhabdopleura recondita*. Larval settlement, the secretion of the larval dome, and metamorphosis show that they are possible in the absence of a bryozoan matrix, but further colony development may require the bryozoan matrix. Continued growth and tube secretion probably require that the larva is hidden inside of the host matrix. This obligate developmental dependence on the bryozoan host may constrain the development of *R. recondita* tube and tubaria, compared to the other *Rhabdopleura* species that develop without a host. We also make a first attempt to test the response of *R. recondita* under variable flow velocities. We removed the original tubes but found no significant variation in the number of new tubes formed or tube length. These findings suggest that *R. recondita* resides in a narrow velocity range and that tube and tubarium development are largely invariable.

Introduction

Hemichordates are a phylum of marine animals comprised of the solitary enteropneusts and the colonial, tubicolous pterobranchs, the latter include the Cephalodiscidae and Graptolithina. Graptolites are known primarily from the fossil record of the Middle Cambrian to the Middle Carboniferous (Maletz and Beli 2018; Maletz et al. 2020). A graptolite colony starts from a larva that secretes a dome (or prosiculum) where it metamorphoses into the foundational sicular zooid. The zooid emerges from the prosiculum and then secretes, using glandular cells on the ventral cephalic shield, the first tube of the colony (Stebbing 1970a fig. 4; Strano et al. 2019). Subsequent colonial development is by asexual budding from a common, connecting stolon. Each zooid may

contribute a new tube, or tubes to the colony giving rise to a tubarium, or coenecium, that is flexible and transparent tending to brown with age (Maletz et al. 2016). It is composed of a chitin-like polysaccharide, fatty acids and occluded particles from the environment (Ch. 6). Tubes may be creeping or erect and are made of rings and half rings called fuselli (Maletz 2014; Maletz and Beli 2018). An individual tube may be used by several generations of zooids. The colony tubarium, with some exception (Maletz 1996) is usually a few millimeters to a few centimetres in size and may take a dizzying variety of forms. The defining feature of graptolites are the tube fuselli, prosicula and a stolon that links individual zooids.

An enduring challenge for paleontologists is the species definition of fossils based solely on morphology. Fossils provide no evidence of reproductive isolation that is frequently used by biologists to define a living species (Allmon and Yacobucci 2016) and in the absence of genetic data, there is no way to determine heritable characteristics including variation, from non-heritable ones. The species, especially if fossil species are defined by their unique or unique combinations of traits (Allmon and Yacobucci 2016). Adding to this challenge is the morphological phenotypic plasticity in response to a new environment (West-Eberhard 2003). In marine environments, the flow velocity of the water is a potent selective force (see Graus et al. 1977; Palumbi 1986; Marchinko 2003), animals that are sessile animals are susceptible to damage from biomechanical drag, or variations in the availability of food. Dramatic phenotypic plastic responses to flow have been documented in sponges, barnacles, bryozoans and colonial tunicates (Arsenault et al. 2001; Marchinko 2003). Benthic graptolites may also be expected to show a plasticity in the tube and tubarium form in response to flow.

With the exception of a few tentative zooid impressions (Rickards and Stait 1984; Bjerreskov 1991; Durman and Sennikov 1993; Chapman et al. 1995; Loydell et al. 2004), the graptolite fossil record consists entirely of tubes and tubaria. The earliest forms including rhabdopleurids (Zhang et al. 2007; Maletz and Beli 2018), were benthic encrusting Dendroids that had creeping and erect tubes. *Rhabdopleura*, the subject of this study, is the last surviving genus of the Graptolithina. The evolutionary radiation of the planktonic Graptoloidea tubaria are among the most extraordinary examples of diverse extracellular secreted structures in nature (Maletz and Cameron 2016; Maletz 2019). The peak of this radiation was Early Ordovician through the Silurian period, after which

they went almost entirely extinct. The fossils are so abundant, with global distributions, that they are used to date strata of rocks into graptolite biozones. They are the topic of hundreds of scientific papers and books (Maletz and Beli 2018). There are tens of thousands of fossils, and thousands of species, the systematics of which are known only from their organic tubes (Maletz et al. 2005).

Rhabdopleura recondita is a benthic graptolite distributed throughout the Mediterranean (Beli et al. 2018). It is a typical rhabdopleurid, except that the colonies reside inside of the matrix of dead bryozoans *Myriapora truncata* and *Schizoretepora serratimargo*. The matrix provides habitat for the zooids, and the creeping tubes are smooth and lack fuselli. They conform to the walls of the bryozoan lacunae where the zooids reside. The erect tubes are a few millimeters in length and extend perpendicularly from the bryozoan matrix into the water column, and are typically graptolite-like, with fuselli (Fig. 1). Here we make observations on *R. recondita* kept in captivity. We observe i) dome secretion, larval metamorphosis, tube secretion and tube repair by adult zooids and ii) we evaluate the phenotypic plastic response of the tubes and tubarium to different water flow velocities, hypothesizing a pattern of shorter tubes with higher density at high velocity where zooids would face stronger mechanical stress, and gradually a number of longer tubes with lower density at slower velocity.

Materials and Methods

Rhabdopleura recondita colonies are not visible to the naked eye because they are concealed inside of clumps of dead bryozoan matrix of *S. serratimargo* and *M. truncata*. These clumps were collected by hand by SCUBA diving between 10 and 20 meters depth along the Salento coast, south of Otranto, Italy. They were transported in thermally insulated coolers to the University of Salento where they were kept in aquarium at 19 °C, the temperature of the collection site. Colonies were kept at a 12-hour photoperiod alternating between light and dark.

Larval and adult tube building

Larvae, zooids and tube building behaviour were observed daily with a Leica MZ6 ocular stereo microscope, and pictures taken with a Sony-RX100-I camera. The search for larvae occurred by breaking the bryozoan matrix using steel probes and chisels. We found six larvae which were recovered with a pipette and transferred to six water bowls with 3 ml of filtered sea water at 19°C.

The bowls were covered with a nylon mesh and immersed together in a one litre vessel of seawater with aerator. The vessel also held fragments of colonised bryozoans. i) Five larvae, one per bowl, were observed without a substrate to evaluate their ability to settle, metamorphose and build a colony; and ii) one larva was provided with a deeply fragmented *M. truncata* to let it feel inside a host allowing instead external observation.

Rhabdopleura recondita zooids were collected in the same manner as the larvae and placed into bowls to evaluate their ability to build tubes and colonies. We prepared a total of five bowls, covered with a nylon mesh. Zooids were fed coral food twice a week (H&O by Sicce) and kept together in a one litre vessel with aerator. i) Into three separate bowls, to observe progress in tube building, we isolated one developing zooid and two adult zooids exposed naked, which means without an erect tube, but with attached stolon, creeping tube and bryozoan calcium carbonate zoarium where they could not shelter. ii) In the fourth bowl, we observed the behavior of two zooids exposed partially naked, attached to a common stolon, and with a reduced capacity to shelter inside of the bryozoan zoarium. iii) In a fifth bowl, to observe the ability of zooids to secrete new tubes and the timing of tube development, we cut all the 23 standing tubes from a 1.5 cm bryozoan fragment containing a *R. recondita* colony and observed it over time.

Finally, one colony was fixed in alcohol and placed in vinegar overnight to remove the bryozoan calcium carbonate matrix. This treatment made it possible to observe the colony in the absence of the host matrix.

Flow-induced response

To test the phenotypic plastic response of *R. recondita* tube secretion and development to different water velocities, a preliminary trial was performed for four colonies deprived of tubes and exposed to 4.8 cm/s.

After the preliminary experiment, 16 colonies were permitted to form tubes in channels with lower velocities. These velocities were based on speeds measured at the collection sites as reported in the Istituto Superiore per la Protezione e Ricerca Ambientale (ISPRA 2012).

These colony fragments were chosen after finding evidence of abundant *R. recondita* tubes and zooids, though hidden nature of zooids inside of the bryozoan matrix meant that it was impossible

to know the number of zooids in one of the experimental colony fragments. Images were captured at a SMZ 25 stereo microscope equipped with DS-Ri2 video camera and a video-interactive image analysis system NIS–Elements BR 4.30.02 Nikon Instruments software, and with a Sony RX100 digital camera. Colonies were drawn with particular attention paid to the number and position of erect tubes. The tubes were then removed using tweezers, measured and washed in filtered sea water and preserved in Picric Acid-Formaldehyde-Glutaraldehyde (PAFG).

These 16 colonies, denuded of erect tubes with pliers (Fig. 2), were then placed into flow channels with one of four experimental flow velocities.
Colonies were numbered from 1 to 16 based on the flow velocity treatment. Numbers 1 thru 4 were maintained at 1.6 cm/s; 5-8 were maintained at 2 cm/s; 9-12 were maintained at 3.3 cm/s; and the control colonies 13 thru 16 were maintained at 0 cm/s. The aquarium was equipped with a 12,300 l/h pump, a filtering and refrigerating system and taps to regulate the flow rate through four parallel channels (Fig. 3). Filtered sea water from the *Rhabdopleura* collection site was used at temperature of 19 °C maintained with a refrigerator pump. Salinity, dissolved oxygen, pH were checked weekly and kept at 38‰, 7 mg/l, 8.2 respectively. Distilled water was sometimes added to counter evaporation. Full spectrum fluorescent bulbs were set to a 12-hour daylight photoperiod.
To set the flow velocity, a fluorescein dye was used close to the pump, the pump in turn distributed the colour uniformly in the channels. In doing so, it was possible to set the velocities with taps.
After ten running with the same settings the mean velocity of 1.6 cm/s, 2 cm/s and 3.3 cm/s were obtained.

Four colonies were placed in each channel where flow was laminar. The control channel at velocity of 0 cm/s had a drip that prevented stagnation, though no flow could be detected. To minimize a boundary layer effect, colonies were attached to a weighted Plexiglas base that was 1cm deep and projected them upwards into the centre of the flow channel (Fig. 4). Animals were fed twice a week with a coral food (H&O by Sicce) and allowed to secrete new tubes for 40 days. The progress of tube construction was observed and photographed every eight days (i.e. days 0, 8, 16, 24, 32 and 40).

Statistical analysis

Initially, the data related to the number of new tubes formed and the length of tubes (original and new tubes) were tested to homogeneity and normality using graphical analysis and the Shapiro-Wilk (1965) test. No data tested fit the assumptions of normality and non-parametric tests were performed. We used the Kruskal-Wallis (1952) analysis to test if i) the number of new tubes formed differ significantly between speed treatments and ii) the new tubes lengths differ significantly between speed treatments. If the result of the Kruskal-Wallis were significant, the Dunn (1964) post-hoc test was performed to highlight the significance of the differences between treatments.

Additionally, we tested if there were differences between the new tubes length and the original ones, considering the speed treatments: to test if there was difference in tube length before and after the experiment (new length versus original length) and, if the differences, if existent, was conditioned to the speed treatment, was performed a General Linear Models (GLMs). First, a complete model was created using the new tube length as response variable and the original length and speed treatment as explanatory variables. With the model created, a family selection was made to determine the best distributional family to this model. To select the family we compare them with the Akaike criteria. With the best family selected, the model was tested to highlight the significance, if there was any. In addition, the adjustment for the model was observed using graphs (model vs residuals). All analysis were performed using the R software (R DEVELOPMENT CORE TEAM, 2011). The level of significance adopted in this study was 5%.

Results

Larval and adult tube building

Discerning between an alive or dead larva (as well as zooid) is simple. When living, these soft-bodied organisms are turgid and move, or react to stimuli. Their surface is covered with moving cilia, sometimes visible at the stereo microscope. When dead, they show signs of decomposition within few hours. We initially observed the development of six larvae. i) From the five larvae without a substratum, one of them settled, produced a dome, metamorphosed and secreted a short creeping tube within the tenth day (Fig. 5a), but then the development stopped and the newly metamorphosed zooid died. Four larvae settled, two of them showed the ability to creep and swim during dome secretion (Fig. 5b), the other two were able to swim during metamorphosis (Fig. 5c), however the larvae died within 24 hours showing clear signs of decomposition.

ii) One larva was cultured with a deeply fragmented bryozoan matrix. This larva crept among the fragments, stopped protected by some of them and extended its anterior upward. It remained in the same position at each observation until, at the 26th day we noticed a dome in which it was able to rotate, while it appeared to continue secreting the dome fabric. Twenty-nine days after, the larva ceased its rotation and started the metamorphosis. After 37 days from start of the observation, the zooid resorbed a part of the dome and from that hole it built a transparent creeping tube. At the time of the creeping tube secretion, the zooid was tripartite, with distinct cephalic shield, collar and trunk, but lacked fully developed arms, tentacles and gut. No further development was observed (Fig. 6). At day 40 two additional larvae, each in a dome were discovered, and at day 47 another larva settled and formed a dome. These three additional larvae emerged from the colonised bryozoan fragments that were kept in the larger vessel that housed the experimental treatment bowls.

Parallel experiments were done to determine the success of tube building by adult zooids. Here we discovered that zooids that were isolated from the colony did not secrete tube material. i) In the three bowls with one zooid each, one immature and two adults, which were attached to a length of stolon and a piece of calcium carbonate zoarium that offered no shelter, no tubes were secreted. The immature zooid survived eight days. One adult zooid survived 24 hours and the second adult survived 18 days without secreting a tube (Fig. 7). ii) A fourth bowl had two zooids that were united by a common stolon and partially exposed on top of a bryozoan zoarium fragment. These zooids survived and at 20 days had secreted new erect tubes. One zooid was able to move marginally deeper inside of the zoarium and built a normal tube with a smooth base and 10 fuselli (Fig. 8a). The more exposed zooid built an irregularly shaped tube that was flared distally, providing some protection for its fragile body (Fig. 8b). In the fifth bowl we put an entire colony but removed from it 23 erect tubes. After 10 days, three short new tubes of the original 23, each with about five fuselli, were re-secreted. Other tubes were not remade though zooids were seen alive and perched from the bryozoan apertures. The new tube material was transparent in part due to the absence of included foreign particulates. On those new tubes a kind of “scar” was visible at the junction of the old and the new tubes sections, with the margin of the old tube left lacerate and the new tube secreted on a deeper fusellum (Fig. 9). After 90 days of observation, no further growth

of the tubes was observed. The scarce number of tubes rebuilt in this experiment, reminds what was observed after, during the flow experiments, below.

One last colony was treated in vinegar to remove the calcium carbonate matrix of the bryozoan. Here we discovered that *R. recondita* is unusual in that it lacked a creeping tube with fuselli (Beli et al. 2018). Instead, it lines the inside of the bryozoan lacunae with smooth sheets of cortical material. The creeping tubes take the form of the walls of the host matrix, and no zigzag fuselli were found, whereas the erect tubes had typical fuselli. Interestingly, we observed a brood chamber made of a spirally formed smooth creeping tube that contained, from the outside to the inside, a degenerated female zooid and four larvae, from younger to older (Fig. 10a). A degenerated female zooid is characterized by reduced tentacles and reduced internal organs, and sometimes a gonad is visible (Fig. 10b). It is possible these individuals do not feed themselves (Maletz and Cameron 2016).

Flow-induced response

In the preliminary experiment, with colonies exposed to 4.8 cm/s, no new tubes were made, so we continued with lower speed as follows.

Sixteen colonies were maintained in flow channels of four velocities. Numbers 1 thru 4 were maintained at 1.6 cm/s; 5-8 were maintained at 2 cm/s; 9-12 were maintained at 3.3 cm/s; and the control colonies 13 thru 16 were maintained at 0 cm/s. Colonies were alive for the duration of the 40 days experimental period. Zooids are delicate, and rapidly withdraw into the lacunae of the bryozoan matrix when disturbed by shadows, vibrations and experimental manipulation. Other zooids may not have emerged from the matrix. For this reason, it was not possible to evaluate the number of living zooids in each colony before the removal of the original tubes, but for each observation during the flow speed treatment we noticed the presence of at least one zooid. Many zooids that we observed did not secrete new tubes. Of the sixteen experimental colonies, eleven formed new tubes; 9/11 of which were exposed to water velocities, and 2/11 belonged to the controls exposed to 0 cm/s flow (Fig. 11, Tab. 1). The intermediate velocities treatments seem to favour tube regrowth (Fig. 12, 13a, 14), with a higher number of tubes formed at 1.6 cm/s and 2 cm/s (mean 7.5 and 7.8, respectively) and fewer tubes were formed at 0 cm/s and the highest

velocity of 3.3 cm/s (mean 1.5 and 2.5, respectively). However these differences were not significant (p=0.541).

Concerning the relationship between water velocity and tube length (Fig. 13b, see also Table 2): at 0 cm/s the mean tube length of the new tubes was 0.3 mm; at 1.6 cm/s the mean tube length was greatest at 0.42 mm; at 2 cm/s mean tube length was 0.33 mm and at 3.3 cm/s mean tube length was 0.31 mm. The statistical test did not show significance to the effect of water velocity on the tube length (p=0.083). However, the differences between the new tube length (secreted during the experiment) and the original ones from the colonies collected in the field (mean length: 1.14, 1.14, 1.05, 1.08 mm from slower to faster flow) was significant ($p=7.65e^{-05}$) (Fig. 15), but the difference was not influenced by the treatments (1.6 cm/s p=0.138; 2 cm/s p=0.575; 3.3 cm/s p=0.892).

The bulk of tube formation occurred during the first 16-24 days of the experimental trials. Growth seemed to stop after 32 days (Fig. 12), but from the trend lines in figure 14, there seems to be a potential for tube growing, especially in the medium velocity treatments (1.6 and 2 cm/s) with a higher slope. In this case, however, only the regression line of 0 cm/s treatment shows significance (p=0.04). An unexpected observation made during these flow treatments was the presence of a closed lid on some of the shortest tubes in each colony, at all flow velocity treatments, presumably secreted by the zooids (Fig. 16).

Discussion

The observations and experiments made here with the larvae and zooids, highlight the adaptation and perhaps constrains to the hidden life of *R. recondita*. Congeneric species typically develop on exposed surfaces, frequently of calcium carbonate, though occasionally they occupy internal cavities (Schepotieff 1909; Johnston 1937; Stebbing 1970b; Barnes 1977; Lester 1988a). During this study, we have not observed *R. recondita* build a new colony or enlarge a pre-existing colony outside of the bryozoan host. Larvae settled without bryozoan substrate and began the process of dome secretion (Fig. 5ab), all but one failed to develop beyond the larval morphology, suggesting that a host matrix increases normal settlement and metamorphosis. The larvae were still capable of swimming after the dome secretion or metamorphosis started (Fig. 5bc). In this respect they were like *R. normani*. This truncation to development and dome secretion is probably because the larvae

were disturbed, not in the ideal conditions (Lester 1988b), or lacking bryozoan zoarium as a cue to metamorphosis. Only one larva without the substratum settled and complete the metamorphosis within 10 days (Fig 5a). By contrast, the larva in the bowl with the bryozoan fragments secreted a dome and metamorphosis took more than 25 days (Fig. 6). In this case, following its metamorphosis, additional larvae emerged from the fragments, aggregated, settled and metamorphosed. This result supports the finding that host fragments may increase metamorphosis and suggests that larval settlement may induce conspecific larval settlement and metamorphosis.

Fertilization and early cleavage of pterobranch embryos is known from few observations (Lester 1988b) and observations of larvae are almost as rare (Stebbing 1970a; Dilly 1973; Sato 2008). After carbon carbonate excision, we observed a *R. recondita* brood chamber. Brood chambers are known for *R. normani* (Lester 1988b), and one with a female zooid, embryos and larvae has been documented for *R. compacta* (Sato 2008). The brood chamber of *R. recondita* had four larvae at different stages of maturity demonstrating asynchronous brood development. The most mature larva was positioned the most distant from the tube aperture. It would need to squeeze past the other larvae and the parent zooid to exit the colony tubarium (Dilly 1973).

Three experiments were done to observe tube building by adult zooids. Three bowls were cultured with two adults and one immature zooid that were isolated. These did not reform a new tube, the immature zooids did not develop further, and none formed a stolon or budded new zooids (Fig. 7ab). They survived few hours or days supporting the idea that the absence of other connected zooids and a tubarium, are incompatible with life (Maletz and Cameron 2016). The two zooids connected by a common stolon and cultured in the presence of host matrix survived and secreted erect tubes with fuselli (Fig. 8ab). Figure 8a shows that the one zooid that moved marginally deeper inside the tubarium built a normal shaped erect tube with fuselli. The second zooid (Fig. 8b) secreted a distally flared and abnormal shaped tube. This difference in tube form may suggest that normal tube secretion depends not only on host material, but the ability to hide inside of it. Alternatively the flared tube may be a response to exposure. In either case, this observation shows that *R. recondita* colony formation is adapted and constrained to life inside of a bryozoan host zoarium matrix.

In a fifth bowl a fragment of bryozoan zoarium that contained a *R. recondita* colony, demonstrated by zooids that extended their arms for filter feeding (Fig. 9a), had the erect tubes removed. The absence of tubes did not appear to disturb normal emergence and feeding activities. Those zooids rebuilt only three of the 23 dissected tubes, similar to what we found in our colonies that were subjected to flow velocities, below, where we discuss possible reasons for this finding.

The finding that a few zooids within a colony will secrete new tubes begged the question, does tube number or tube form vary when secreted under four different flow velocities? This is the first analysis of the potential for induced phenotypic plasticity in a graptolite. The rationale for this study was twofold. First, the thousands of graptolite species, including the benthic Dendroidea (with *Rhabdopleura*) and the planktonic Graptoloidea, exhibit an incredible disparity of tube and colony form. Taxonomic definitions of early benthic graptolites can be small (Ramírez-Guerrero and Cameron 2021). These minor morphological differences are a conundrum to graptolite systematists who have debated the validity of traits to define a species. Is the difference due to the fossilization process, to genetic variability within the species, or to the environment? Phenotypic plasticity may account for the majority of variation with a species tube and colony form (Erdtmann et al. 1987; Erdtmann 1988; Štorch 1995; Lenz and Melchin 2008; Blackett et al. 2009; Maletz et al. 2016), because the tubes are extracellular secreted structures that result from an individual zooids tube building behavior. The second rationale is that phenotypic plasticity responses to flow are common in benthic invertebrates. It has been reported in the ostia of sponges (Vicente 1978), and in barnacle legs (Marchinko 2003) where at low velocities, appendages must extend through a thicker boundary layer to access food in the water column. Flow velocity is an important selective force (Graus et al. 1977; Palumbi 1986; Marchinko 2003) even in hemichordates (Vo et al 2019).

We expected a pattern of shorter tubes with higher density at high velocity where zooids would face stronger mechanical stress, and gradually a number of longer tubes with lower density at slower velocity. Instead, we found a tendency for a higher number of tubes build at intermediate flow speeds and no difference in newly secreted tube length. The number of new erect tubes formed by zooids of *R. recondita* exposed to different flow velocities (0, 1.6, 2 and 3.3 cm/s) showed a higher regrowth and potential for growing (Fig. 13a, 14) at 1.6 and 2 cm/s, though these differences were not statistically significant. *Rhabdopleura recondita* is the best of the five living

rhabdopleurids to conduct experiments because it is the only one that can be collected abundantly with relative ease. *Rhabdopleura recondita* may be, on the other hand, a poor species for some studies, because the colonies are hidden inside of the bryozoan zoarium host. In this study, the peculiar habit made it impossible to know the number of zooids in a given colony at the start of the experiment, and therefore the number of zooids that could potentially remake new tubes. This species is the least ideal to study tubarium astogeny, or overall colony form with respect to flow because the spacing of the tubes is mediated by the availability of channels and exit pores from the bryozoan zoarium. More significant results may be obtained with a larger sample size, but we think it is unlikely. Our interpretation of these results is that *R. recondita* lives in a low and narrow velocity range and does not vary tube secretion based on flow velocity.

We found no difference in the length of new tubes among the four velocity treatments, but a difference in length between the original and new tubes was significant (Fig. 15). This latter result may indicate that the experimental conditions for tube building was not ideal, or that more time was needed to achieve the original length (Maletz 2017). It may also indicate that *R. recondita* in the wild occupy microhabitats that have little to no flow, and in this narrow range tube form is invariable. This narrow range of flow velocities may be the range of balance between successful food capture (Sebens et al. 1997) and limited mechanical stress on the feeding zooids.

Assuming that the tubarium where tubes were removed housed a zooid, the low resecretion ratio may be explained as one of six possibilities. i) The food that we used, developed for corals, was too limited or chemically inadequate for ideal colony growth. Nothing is known about culturing *Rhabdopleura* in captivity (Cavers 2005). Alternatively, the food we provided may have been so abundant that secreting a new tube was unnecessary. ii) Tube secretion and colony enlargement may be seasonal, or sporadic (Cavers 2005). iii) Tube formation is rare because tubes are used from generation to generation (Stebbing 1970a; Rigby 1994; Briggs et al. 1995). Related to this is that at the beginning of our experiment, colonies had more tubes than zooids to re-build all the experimentally excised tubes. iv) The boundary layer effect may have exposed zooids to lower velocities than those set in each channel, which in turn may have reduced the gas exchange. v) Colonies may require much more time to rebuilt in terms of number and length (Maletz 2017). vi) Stress caused by the loss of all the tubes in a given colony and the energy supply required for their

reconstruction. We observed zooids that lacked erect tubes emerge from the zoarium to feed, but perhaps that did not have the energy to secrete new tubes. At the terminal end of some excised tubes we observed a lid on the aperture. We do not know why they secrete those lids and what they do inside the tubarium after secretion, but we know rhabdopleurids can produce dormant buds to overcome adverse periods (Stebbing 1970a; Maletz and Beli 2018) and these lids may be the sign of zooids encystment to face stressful conditions caused by tube removal and aquarium environment.

These results show that *R. recondita* tube secretion and form exhibit no significant variation in response to water flow velocity. Together, the results of preliminary experiments where we found no tube secretion in flow velocities over 3.3 cm/s, suggest that *R. recondita* occupies a niche that includes low velocity. Within the narrow range of velocities that it does form new tubes, tube development appears canalized (i.e., fixed). It is invariable in response to flow velocity. It suggests that small differences that distinguish primitive, encrusting graptolite species may be real. Of course, other living rhabdopleurids, especially those with tubaria that are free of a host, may have a phenotypic plastic response to flow, food, predation or temperature. It is also possible that the developmental toolkit including plasticity of Paleozoic graptolites was quite different from that of *R. recondita*. Peterson et al. (2009) hypothesized that an accumulation of microRNAs over geological time may have increased the silencing and post-translational regulation of gene expression. Unfortunately, we cannot experiment with the phenotypic plasticity of fossil forms (Pigliucci 2001) nor can we sequence their microRNAs. Others have quantified the number and variation of forms over time and concluded that these are largely determined by extinctions, and not developmental constraints (Bapst et al. 2012). Our results suggest that tube form of *R. recondita* may in fact be constrained, but we do not extend this finding to other species, dead or alive. As with other speciose groups, it is likely that some species and clades exhibited tremendous tubarium evolvability, and others did not. In the case of *Rhabdopleura*, its evolvability has nothing to do with survivability. Its lineage has survived five major extinction events and it is the only graptolite genus that survives to this day.

References

Allmon, W. D., & Yacobucci, M. M. (2016). *Species and speciation in the fossil record*. University of Chicago Press.

Arsenault, D. J., Marchinko, K. B., & Palmer, A. R. (2001). Precise tuning of barnacle leg length to coastal wave action. *Proceedings of the Royal Society of London. Series B: Biological Sciences*, 268, 2149–2154.

Bapst, D. W., Bullock, P. C., Melchin, M. J., Sheets, H. D., & Mitchell, C. E. (2012). Graptoloid diversity and disparity became decoupled during the Ordovician mass extinction. *Proceedings of the National Academy of Sciences*, 109, 3428–3433.

Barnes, R. D. (1977). New record of a pterobranch hemichordate from the western hemisphere. *Bulletin of Marine Science*, 27, 340–343.

Beli, E., Aglieri, G., Strano, F., Maggioni, D., Telford, M. J., Piraino, S., & Cameron, C. B. (2018). The zoogeography of extant rhabdopleurid hemichordates (Pterobranchia: Graptolithina), with a new species from the Mediterranean Sea. *Invertebrate Systematics*, 32, 100–110.

Bjerreskov, M. (1991). Pyrite in Silurian graptolites from Bornholm , Denmark. *Lethaia*, 24, 351–361.

Blackett, E., Page, A., Zalasiewicz, J., Williams, M., Rickards, B., & Davies, J. (2009). A refined graptolite biostratigraphy for the late Ordovician-early Silurian of central Wales. *Lethaia*, 42, 83–96.

Briggs, D. E., Kear, A. J., Baas, M., de Leeuw, J. W., & Rigby, S. (1995). Decay and composition of the hemichordate *Rhabdopleura*: implications for the taphonomy of graptolites. *Lethaia*, 28, 15–23.

Cavers, P. (2005) Quantifying Variation in a Population of *Rhabdopleura compacta*. Unpublished Zoology Honours thesis, University of Edinburgh, Edinburgh.

Chapman, A. J., Durman, P. N., & Rickards, R. B. (1995). Rhabdopleuran hemichordates: new fossil forms and review. *Proceedings of the Geologists' Association*, 106, 293–303.

Dilly, P. N. (1973). The larva of *Rhabdopleura compacta* (Hemichordata). *Marine Biology*, 18, 69–86.

Dunn, O. J. (1964). Multiple comparisons using rank sums. *Technometrics*, 6: 241–252.

Durman, P. N., & Sennikov, N. V. (1993). A new rhabdopleurid hemichordate from the Middle Cambrian of Siberia. *Palaeontology*, 36, 283–296.

Erdtmann, B. D. (1988). The earliest Ordovician nematophorid graptolites: Taxonomy and correlation. *Geological Magazine*, 125, 327–348.

Erdtmann, B. D., Maletz, J., & Marco, J. C. G. (1987). The new Early Ordovician (Hunneberg Stage) graptolite genus *Paradelograptus* (Kinnegraptidae), its phylogeny and biostratigraphy. *Paläontologische Zeitschrift*, 61, 109–131.

Graus, R. R., Chamberlain Jr, J. A., & Boker, A. M. (1977). Structural modification of corals in relation to waves and currents: reef biota. In. Frost, S. H., Weiss, M. P., Saunders, J. B. (eds.) Reefs and related carbonates ecology and sedimentology. *American Association of Petroleum Geologists*, 135–153.

ISPRA. (2012). Strategia per l'ambiente marino - valutazione iniziale -sottoregione Mar Adriatico - caratteristiche fisiche. ISPRA. http://www.strategiamarina.isprambiente.it/consultazioni/consultazione-2012/files/3.1%20mar_adr%20caratteristiche%20fisiche.pdf

Johnston, T. H. (1937). A note on the occurrence of *Rhabdopleura annulata* in South Australian waters. *Records of the South Australian Museum* 6, 105–107.

Kruskal, W. H. & Wallis, W. A. (1952). Use of Ranks in One-Criterion Variance Analysis. *Journal of the American Statistical Association*, 47, 583–62.

Lenz, A. C., & Melchin, M. J. (2008). Convergent evolution of two Silurian graptolites. *Acta Palaeontologica Polonica*, 53, 449–460.

Lester, S. M. (1988)a. Settlement and metamorphosis of *Rhabdopleura normani* (Hemichordata: Pterobranchia). *Acta Zoologica*, 69, 111–120.

Lester, S. M. (1988)b. Ultrastructure of adult gonads and development and structure of the larva of *Rhabdopleura normani* (Hemichordata: Pterobranchia). *Acta Zoologica*, 69, 95–109.

Loydell, D. K., Orr, P. J., & Kearns, S. (2004). Preservation of soft tissues in Silurian graptolites from Latvia. *Palaeontology*, 47, 503–513.

Maletz, J. (1996). The identity of *Didymograptus* (*Expansograptus*) *suecicus* (Tullberg) and related species (Graptoloidea, Dichograptidae). *Paläontologische Zeitschrift*, 70, 203–212.

Maletz, J. (2014). The classification of the Pterobranchia (Cephalodiscida and Graptolithina). *Bulletin of Geosciences*, 1977, 477–540.

Maletz, J. (2019). Tracing the evolutionary origins of the Hemichordata (Enteropneusta and Pterobranchia). *Palaeoworld*, 28, 58–72.

Maletz, J., & Cameron, C. B. (2016). Part V, Second Revision, Chapter 3: Introduction to Class Pterobranchia Lankester, 1877. *Treatise Online*, 82, 1–15.

Maletz, J., & Beli, E. (2018). Part V, Second Revision, Chapter 15: Subclass Graptolithina and *Incertae Sedis* Family Rhabdopleuridae: Introduction and Systematic Descriptions. *Treatise Online*, 101, 1–14.

Maletz, J., Steiner, M., & Fatka, O. (2005). Middle Cambrian pterobranchs and the Question: What is a graptolite? *Lethaia*, 38, 73–85.

Maletz, J., Lenz, A. C., & Bates, D. E. B. (2016). Part V, Second Revision, Chapter 4: Morphology of the Pterobranch Tubarium. *Treatise Online*, 76, 1–63.

Maletz, J. (2017). Graptolites: fossil and living. *Geology Today*, 33, 233–240.

Maletz, J., Mottequin, B., Olive, S., Gueriau, P., Pernègre, V., Prestianni, C., & Goolaerts, S. (2020). Devonian and Carboniferous dendroid graptolites from Belgium and their significance for the taxonomy of the Dendroidea. *Geobios*, 59, 47–59.

Marchinko, K. B. (2003). Dramatic phenotypic plasticity in barnacle legs (*Balanus glandula* Darwin): Magnitude, age dependence, and speed of response. *Evolution*, 57, 1281–1290.

Palumbi, S. R. (1986). How body plans limit acclimation: responses of a demosponge to wave force. *Ecology*, 67, 208–214.

Peterson, K. J., Dietrich, M. R., & McPeek, M. A. (2009). MicroRNAs and metazoan macroevolution: insights into canalization, complexity, and the Cambrian explosion. *Bioessays*, 31, 736–747.

Pigliucci, M. (2001). *Phenotypic plasticity: beyond nature and nurture*. The Johns Hopkins University Press.

Ramírez-Guerrero, G. M., Cameron, C. B. (2021). Systematics and evolution of pterobranchs from the Cambrian Period Burgess Shales of Canada. *Bulletin of Geosciences*, 96, 1–18.

R Development Core Team. (2011). R: A language and environment for statistical computing. R Foundation for Statistical Computing, Vienna, Austria. http://www.R-project.org/.

Rickards, R., & Stait, B. (1984). *Psigraptus*, its classification, evolution and zooid. *Alcheringa*, 8, 101–111.

Rigby, S. (1994). Erect tube growth in *Rhabdopleura compacta* (Hemichordata: Pterobranchia) from off Start Point, Devon. *Journal of Zoology*, 233, 449–455.

Sato, A. (2008). Seasonal reproductive activity in the pterobranch hemichordate *Rhabdopleura compacta*. *Journal of the Marine Biological Association of the United Kingdom*, 88, 1033–1041.

Schepotieff, A. (1909). Die Pterobranchier des Indischen Ozeans. *Zoologische Jahrbücher. Abteilung für Systematik* 28, 429–448.

Sebens, K. P., Witting, J., & Helmuth, B. (1997). Effects of water flow and branch spacing on particle capture by the reef coral *Madracis mirabilis* (Duchassaing and Michelotti). *Journal of experimental marine biology and ecology*, 211, 1–28.

Shapiro, S. S. & Wilk, M. B. (1965). An analysis of variance test for normality (complete samples). *Biometrika*, 52: 591–611.

Stebbing, A. R. D. (1970)a. Aspects of the reproduction and life cycle of *Rhabdopleura compacta* (Hemichordata). *Marine Biology*, 5, 205–212.

Stebbing, A. R. D. (1970)b. The status and ecology of *Rhabdopleura compacta* (Hemichordata) from Plymouth. *Journal of the Marine Biological Association of the United Kingdom*, 50, 209–221.

Štorch, P. (1995). Biotic crises and post-crisis recoveries recorded by Silurian planktonic graptolite faunas of the Barrandian area (Czech Republic). *Geolines*, 3, 59–70.

Strano, F., Micaroni, V., Beli, E., Mercurio, S., Scarì, G., Pennati, R., & Piraino, S. (2019). On the larva and the zooid of the pterobranch *Rhabdopleura recondita* Beli, Cameron and Piraino, 2018 (Hemichordata, Graptolithina). *Marine Biodiversity*, 49, 1657–1666.

Vicente, V. P. (1978). An ecological evaluation of the West Indian demosponge *Anthosigmella varians* (Hadromerida: Spirastrellidae). *Bulletin of Marine Science*, 28, 771–779.

Vo, M., Mehrabian, S., Étienne, S., Pelletier, D., & Cameron, C. B. (2019). The hemichordate pharynx and gill pores impose functional constraints at small and large body sizes. *Biological Journal of the Linnean Society*, 127, 75–87.

West-Eberhard, M. J. (2003). *Developmental Plasticity and Evolution*. Oxford University Press.

Zhang, Y., Chen, X., & Goldman, D. (2007). Diversification patterns of Early and Mid Ordovician graptolites in south China. *Geological Journal*, 42, 315–337.

Figures

Fig. 1. A transversal section of the bryozoan *Myriapora truncata* colonized by *Rhabdopleura recondita*. Erect semi-transparent tubes of *R. recondita* project from bryozoan host. Scale bar 2 mm.

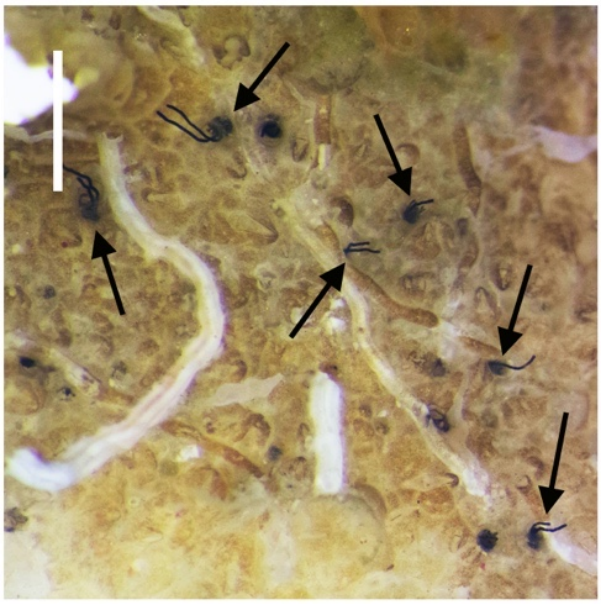

Fig. 2. Colony deprived of tubes. A few individuals are visible (arrows). Scale bar 1 mm.

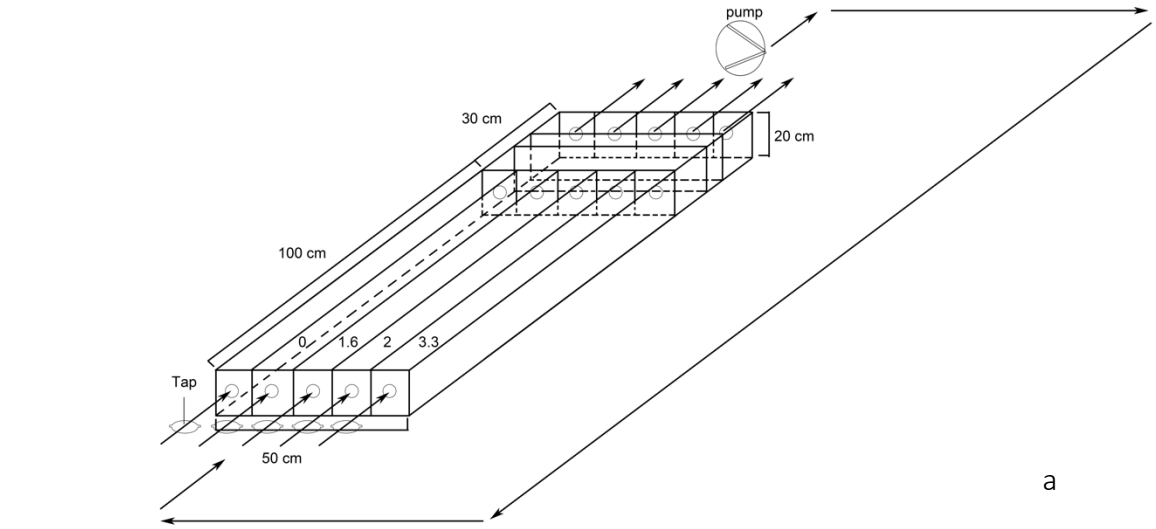

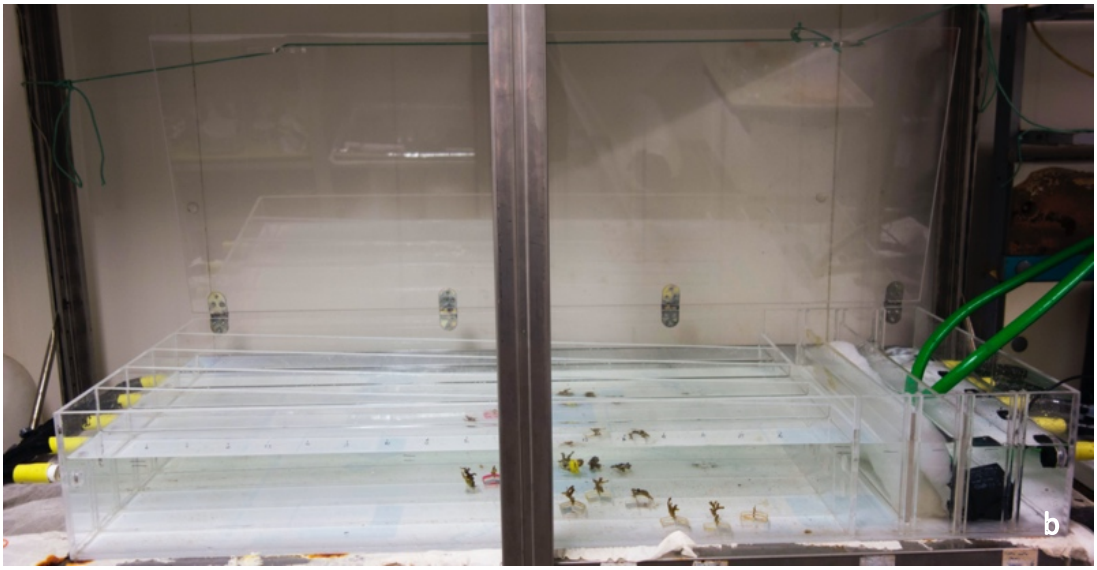

Fig. 3. a, A drawing and b, Photograph of the experimental aquarium with flow channels. One channel was used for control, with 0 cm/s flow, and three channels were maintained at flow velocities of 1.6 cm/s, 2 cm/s, and 3.3 cm/s. In figure a, arrows indicate the direction of flow, and velocities in cm/s are reported on each channel.

Fig. 4. Photos of the 16 experimental colonies, maintained in place by Plexiglas weights. Velocities were: 1-4 at 1.6 cm/s; 5-8 at 2 cm/s; 9-12 at 3.3 cm/s; 13-16 at 0 cm/s. Scale bar 3 cm.

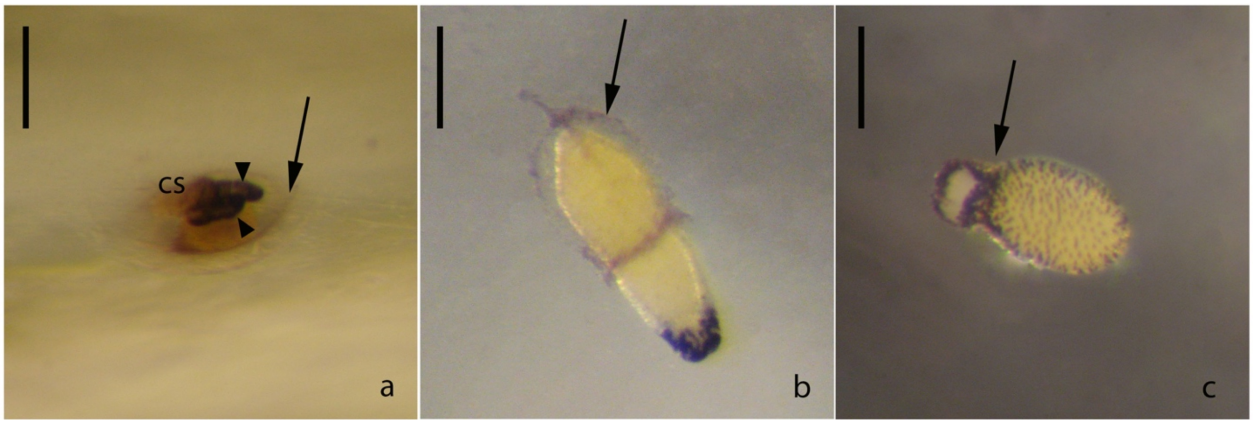

Fig. 5. *Rhabdopleura recondita* metamorphosing larvae. a, A metamorphosing larva shows the dome (arrow), arms (arrowheads) and cephalic shield (cs). b, A larva started the secretion of the dome (arrow). c, A furrow between the trunk and the cephalic shield (arrow) is a sign of metamorphosis. Larvae in b and c can still swim. Scale bar 100 µm.

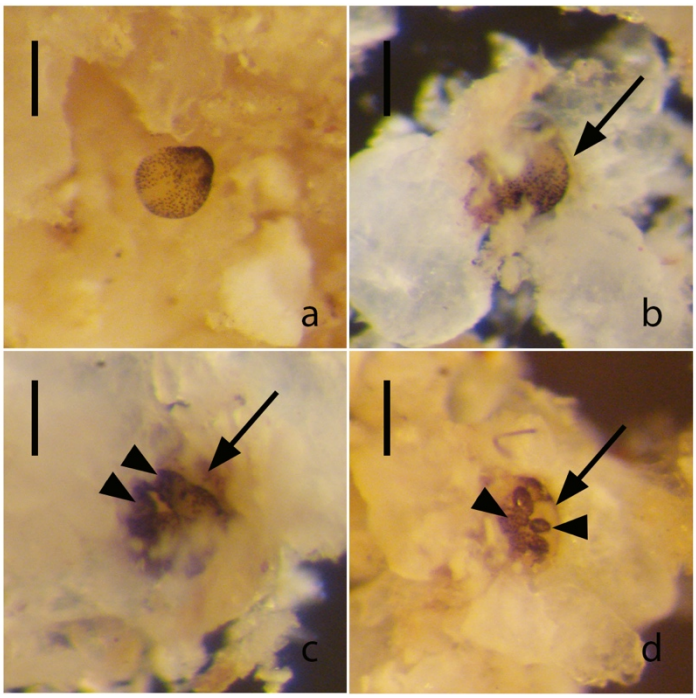

Fig. 6. *Rhabdopleura recondita* larval development on a bryozoan fragmented matrix. a, The larva stopped with the anterior part upward. b, The larva started secreting the dome. c, After 29 days from settlement the metamorphosis begun, the buds of naked arms are visible beyond the dome. d, The zooid is tripartite, lack developed tentacles and pierce the dome to form creeping tube after 37 days from settlement. Arrows show the dome, arrowheads the naked arms. Scale bars 100 µm for a, b, d, 150 µm for c.

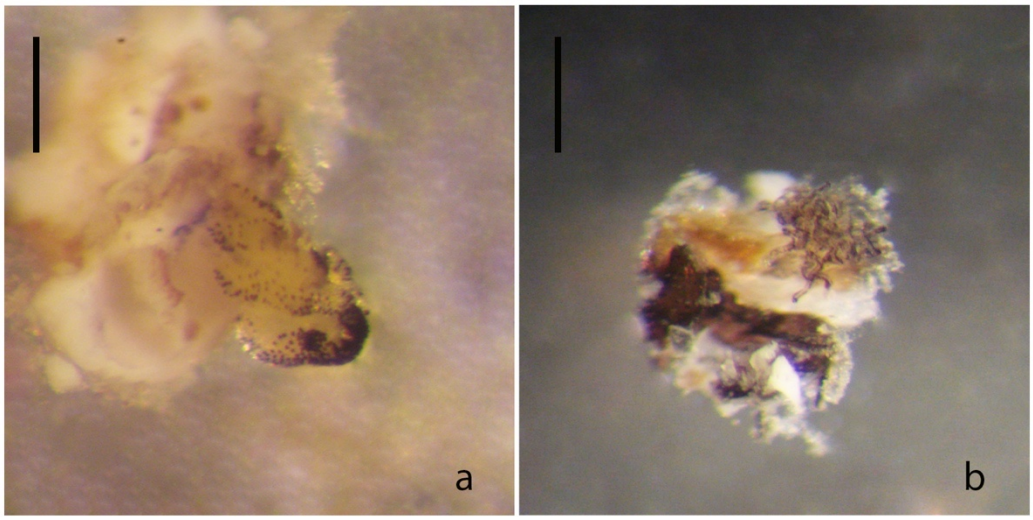

Fig. 7. a, A developing zooid survived eight days with no further development. b, One of the two naked zooids with a creeping tube, and stolon embedded in a bryozoan fragment. Scale bars 200 µm for a, 300 µm for b.

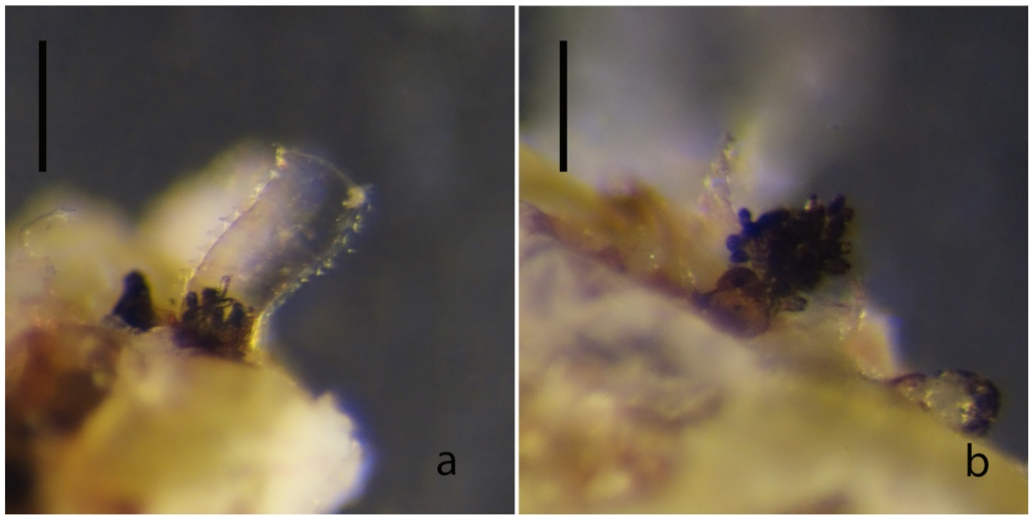

Fig. 8ab. Two zooids united by a common stolon and exposed following fracturing of the bryozoan matrix. a, The zooid able to descend into the host matrix built a normal erect tube. b, The zooid more exposed built an unusual flared tube. Scale bar 300 µm.

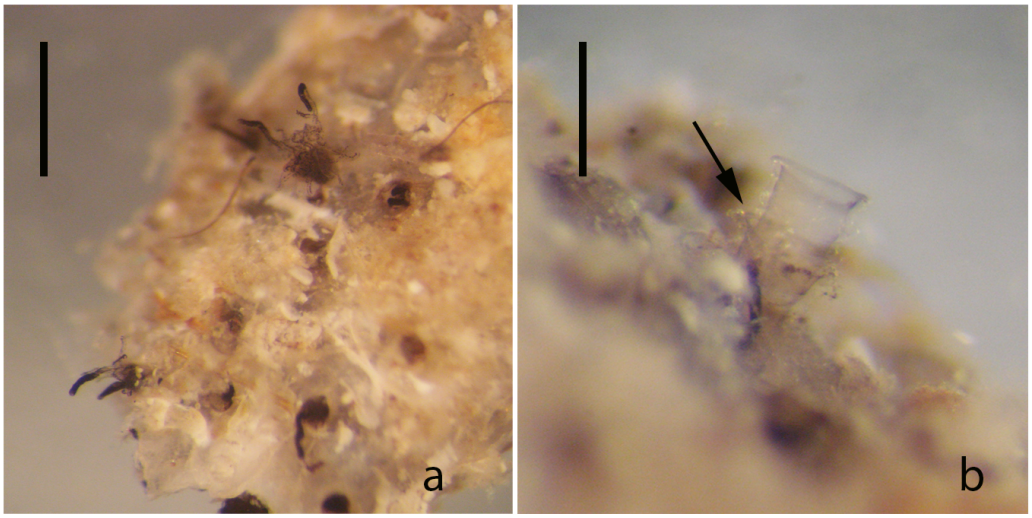

Fig. 9. a, *Rhabdopleura recondita* zooids perched from the bryozoan zoarium apertures after tube removal. b, A new tube rebuilt, arrow indicate the rim of the old tube. Scale bars 500 µm for a, 300 µm for b.

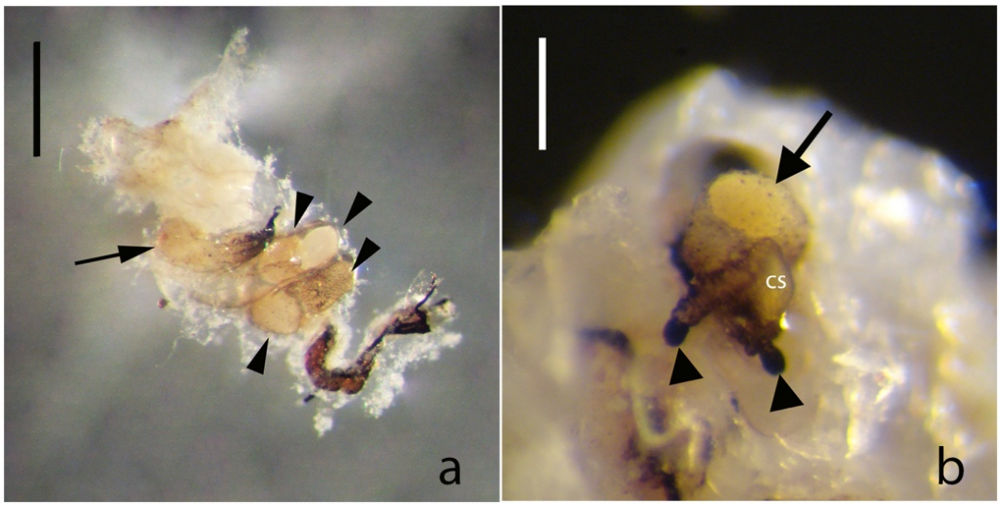

Fig. 10. a, A brooding chamber made of a smooth and spiralised creeping tube. Female zooid (arrow) and larvae (arrowheads). b, Female zooid with ovary (arrow) and reduced tentacles (arrowheads). cs: cephalic shield. Scale bars 400 µm for a, 200 µm for b.

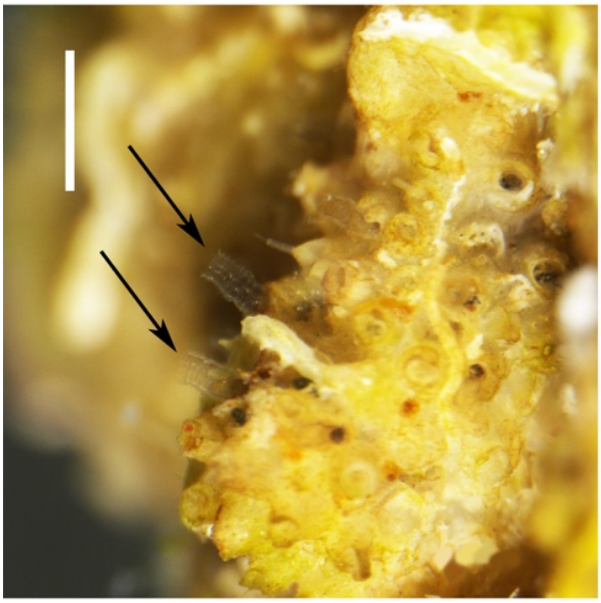

Fig. 11. Two new tubes are indicated by arrows. Scale bar: 1 mm.

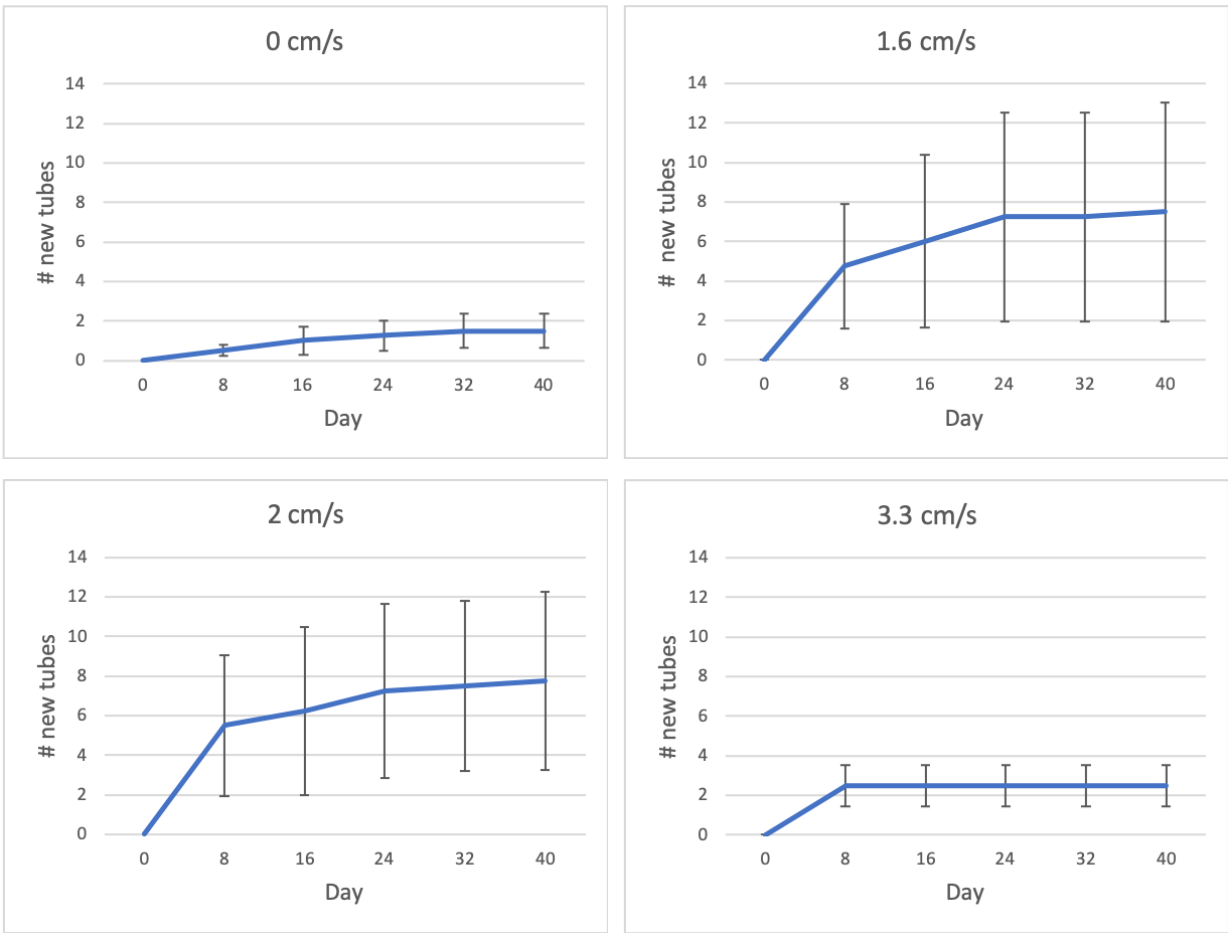

Fig. 12. A plot for each treatment. On the abscissa the days, on the ordinate the mean number of new tubes rebuilt with error bar.

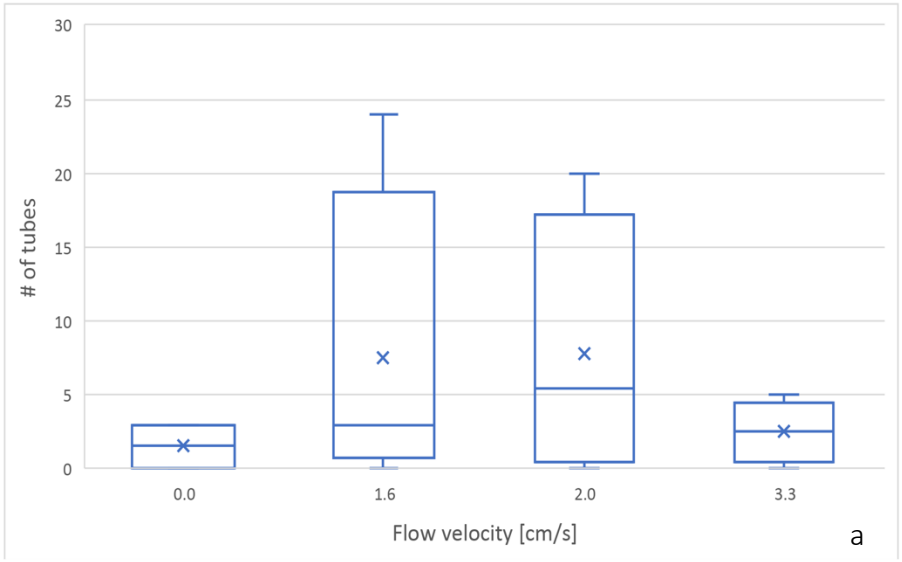

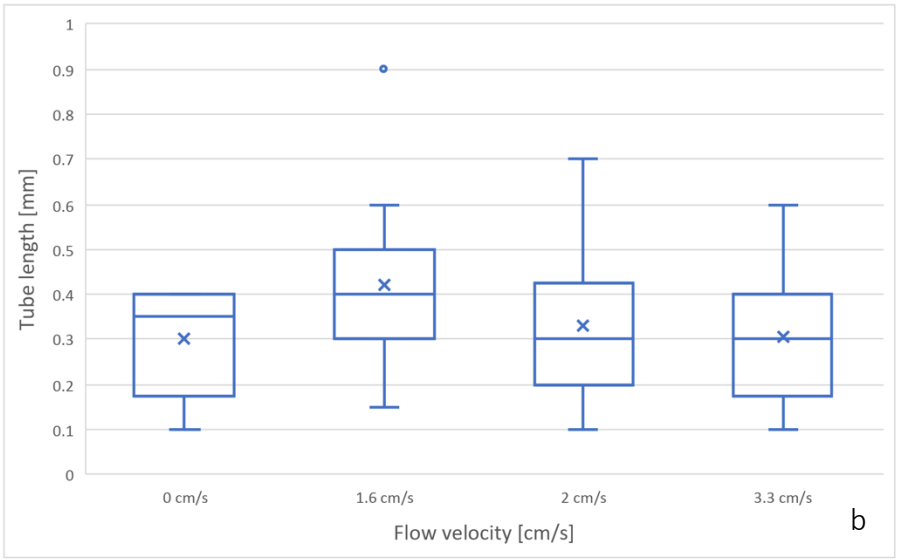

Fig. 13. a, The number of tubes re-built in function of the flow velocity. b, The length of tubes rebuilt in function of flow velocity.
Each box delimits the distance between the first and third quartile, the median is the horizontal bar in the box and the "x" is the mean value. The whiskers reach the lowest and largest data point excluding the outliers (dot).

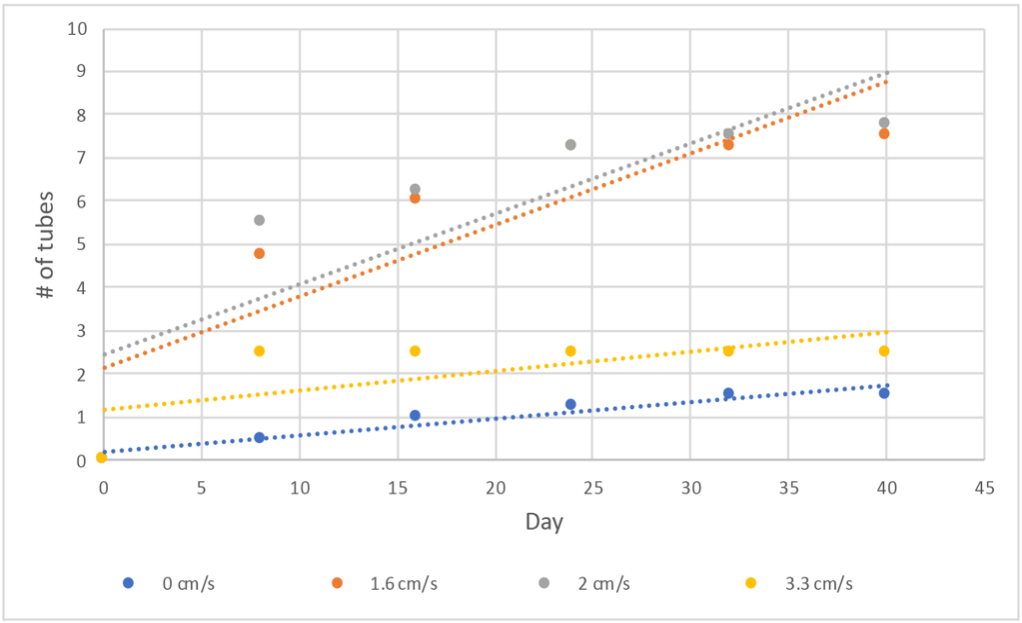

Fig 14. Number of new tubes built per day grouped by speed treatment, plotted together for comparison. Trend lines used the method of least squares to find the regression line.

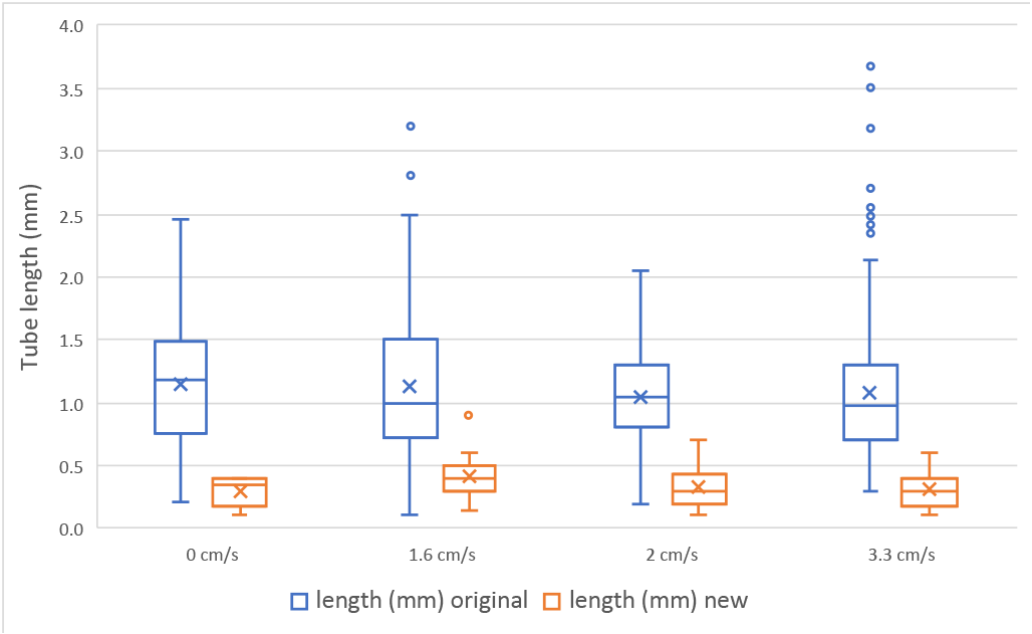

Fig. 15. Differences in tube length between the original tubes (blue) and the new tubes (orange) for each treatment. Each box delimits the distance between the first and third quartile, the median is the horizontal bar in the box and the "x" is the mean value. The whiskers reach the lowest and largest data point excluding the outliers (dots).

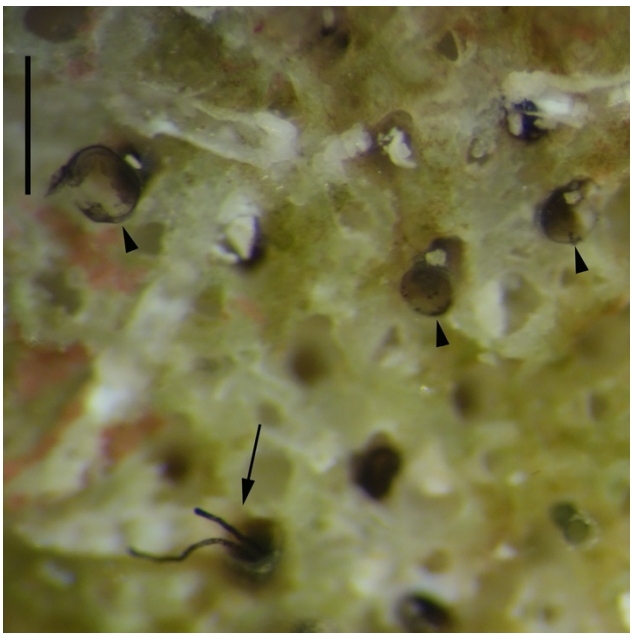

Fig. 16. Some of the removed erect tubes were closed with a lid secreted by the zooids (arrowheads). The lid on the left is broken. Arrow indicates the naked arm tips of a zooid. Scale bar 100 μm.

Tables

Table 1. Number of new tubes reformed for each colony and flux treatment.

# colony	1.6 cm/s	2 cm/s	3.3 cm/s	0 cm/s (controls)
	# new tubes/ # original tubes	# new tubes/ # original tubes	# new tubes/ # original tubes	# new tubes/ # original tubes
1	24/152			
2	3/102			
3	0/32			
4	3/115			
5		2/27		
6		9/68		
7		20/121		
8		0/13		
9			2/35	
10			5/63	
11			3/22	
12			0/27	
13				3/13
14				3/38
15				0/27
16				0/44

Table 2. Mean tube length for each colony, before and after the flow-induced response.

# colony	1.6 cm/s		2 cm/s		3.3 cm/s		0 cm/s (controls)	
	Mean length original tubes	Mean length new tube	Mean length original tubes	Mean length new tube	Mean length original tubes	Mean length new tube	Mean length original tubes	Mean length new tube
1	1.21	0.43						
2	1.38	0.25						
3	1.15	0						
4	0.87	0.2						
5			0.90	0.45				
6			1.07	0.32				
7			1.05	0.35				
8			1.15	0				
9					1.09	0.6		
10					0.96	0.29		
11					0.67	0.3		
12					1.70	0		
13							0.89	0.33
14							0.89	0.27
15							1.27	0
16							0.92	0

Chapter 5

This chapter is a paper in preparation, here reproduced with the permission of all the authors.

Beli, E., Giotta, L., Guascito, M. R., Natsidis, P., Pagliara, P., Schiffer, P., Telford, J. M., Piraino, S. and Cameron, C. B. contributions:

Beli devised the study in collaboration with Cameron. She collected the zooids and shipped them to the lab of Max Telford (UC London) who is a long-time collaborator of Cameron. She found expert collaborators in microscopy and chemistry and with prof. Cameron was awarded grants to work on the bioinformatics of the *R. recondita* genome in the lab of Telford. She analyzed the data, wrote the first draft and edited subsequent drafts of the chapter.

Giotta, L. and Guascito M. R. performed the FTIR and XPS analysis and wrote the first draft of the corresponding section of this chapter.

Natsidis P., Telford, J. M. and Schiffer P. performed *Rhabdopleura recondita* DNA and RNA extractions, assembled the transcriptome and genome, analyzed the data, and helped write this section of the chapter. Telford J. M. also coordinated Beli's research stage in his lab at the University College London.

Pagliara P. helped perform Hoechst and immunohistochemistry, and revised the writing of this section of the chapter.

Piraino S. gave access to lab facilities at the University of Salento, and sampled.

Cameron C. B. conceived the idea for this project, gave access to lab facilities at the University of Montreal, and contributed to its writing.

The complex chemical composition of the tubes in the graptolite *Rhabdopleura recondita*

Abstract

Hemichordata play an important role in our understanding the origin of the deuterostomes. Whereas enteropneusts are solitary worms and relatively simple to study, the sister group of colonial and tubicolous graptolites is composed almost exclusively of fossil taxa, with the exception of five living *Rhabdopleura* species. *Rhabdopleura recondita* has a Mediterranean distribution and builds colonies of a few millimeters inside of dead bryozoan zoaria. The chemical composition of graptolite tubes is an enduring debate and includes chitin, keratin, cellulose and collagen. Here we integrate bioinformatics, spectroscopic and immunohistochemical analysis, and reject the keratin protein and cellulose hypotheses. Instead, we find eight chitin synthesis genes in the *R. recondita* genome. FTIR and XPS analysis of the tubes reveal a chitin-like polysaccharide with a complex of other unexpected elements, along with a protein and fatty acid components. Seventy-nine chitin synthesis genes are found in enteropneusts, leading to the hypothesis that the tubes of the stem group acorn worms were composed of similar chitin-like polysaccharides.

Introduction

Graptolites are a group of colonial animals belonging to the Hemichordata phylum. Hemichordates and echinoderms form the Ambulacraria which, together with chordates, are the deuterostomes. Graptolites are largely extinct, they dominated Paleozoic seas from the Middle Cambrian to the Middle Carboniferous (Maletz and Beli 2018; Maletz et al. 2020). The fossils consist of tubes that are arranged in a myriad of forms. They were so abundant and ubiquitous that they are used as index fossils, revealing the same sedimentary layers in rocks around the planet. Thousands of species have been described from a vast literature. The fossils paleo-geography, the tube shape including details of their microstructure, and the development of the overall colony structure (or astogeny) are well studied topics of interest to paleontologists, sedimentologists and taxonomists (Maletz 2017; Potter et al. 1980). The chemical compositon of graptolite tubes, and fossils in general, is unknown because they have been subject to diagenetic changes. The pressure of burial and tectonic forces and the resultant chemically transformation have made it very difficult to know their original composition.

A phylogeny based on the morphology of the tubes of graptolites and the living pterobranchs *Rhabdopleura* and *Cephalodiscus* placed the graptolites inside of the Pterobranchia and revealed that *Rhabdopleura*, including five extant species, is an extant graptolite (Mitchell et al. 2013). *Cephalodiscus* is sister to the subclass Graptolithina which together form the class Pterobranchia. This phylogeny has permitted us an understanding of the biology of the group including the gross anatomy of the zooids, which are almost completely unknown from the fossil record. Moreover, we have details of the ultrastructure of the zooid tissues including the ciliated and secretory cells that comprise the epithelia, the connective tissue, the coeloms, the musculature, the circulatory, nervous and digestive systems (Dilly 1971, 1972; Lester 1988; Strano et al. 2019). We know the roles that arms and tentacles play in capturing food particles (Dilly 1972; Halanych 1993). Gametogenesis, larval development, settlement, and metamorphosis is also known for *Rhabdopleura* (Stebbing 1970; Sato 2008). Similarly, observations have been made on the secretion of the tubes, the fine details of the tubes, the form of the tubarium, and the taphonomic decay of the zooids, tubes and stolons (Dilly 1986; Maletz et al. 2016; Beli et al. 2017).

Graptolite tubaria begin their development by one larva that secretes a dome-shaped prosiculum, inside the prosiculum, the larva metamorphoses into a zooid with the characteristic body subdivision into metasome (trunk), mesosome (collar with two tentacled arms) and prosome (cephalic shield). The tubes are secreted by the cephalic shield of the adult zooids. The first tube emerges from an aperture on the prosiculum ("dome" in *Rhabdopleura*), the zooid starts to build a tubarium and other zooids will bud from a common black stolon. The colony is usually built up with creeping tubes adorned with half-rings and erect tubes with complete rings called fuselli. In most *Rhabdopleura* species, the tubarium is composed of creeping tubes that adhere to a hard surface and erect tubes from which a single zooid may emerge. *Rhabdopleura recondita* from the Mediterranean Sea is unusual in that it resides inside the skeleton of erect and dead bryozoans (Beli et al. 2018). The smooth creeping tubes are modified to line the internal cavities of the bryozoan skeletal matrix, whereas erect tubes project from the matrix into the water column. Only the erect tubes exhibit complete fuselli. At the ultrastructural level, tubes are characterized by a matrix of overlapping sheets, called cortical tissue, that is intercalated with fibres (Mierzejewski and Kulicki 2003). *Rhabdopleura*'s tubes are made of an organic matter partially mixed with foreign material

joined after secretion. The chemical composition of the tubes is unknown and remains a subject of intensive debate.

Rhabdopleura tubarium composition is probably similar to that of the first graptolites if not to that of the primitive enteropneust tubes (Caron et al 2013; Nanglu et al. 2016), with this study we give a substantial contribution to the knowledge of the extinct graptolites and hypothetically to the common hemichordate ancestor. It is possible in fact that modern enteropneust lost the ability to build tubes whereas it was kept in pterobranchs (Cameron 2018).

Hypotheses on the chemical composition of pterobranch tubes include chitin (Kraft 1926), keratin (Dilly 1971), collagen (Armstrong et al. 1984), and cellulose (including tunicin) (Sewera 2011). Early authors wrote about chitinous tubes and chitinous fibres (Allman 1869; Kozłowski 1948; Sars 1874) but it was more a conventional thought (Kozłowski 1966). Wiman (1901) undertook the first chemical analysis of graptolite fossils and concluded that it was unlikely to contain chitin, although Kraft (1926), using what he believed to be specific stains, insisted on its chitinous nature. Chitin is a N-acetylglucosamine chain linked with β-(1→4) linkages. It is a major component of arthropod carpaces and fungal cell walls (Gullan and Cranston 2010) but is diffused in many other metazoan taxa including sponges, cnidarians and vertebrates. Chitin synthesis (CSs) genes have been characterized from vertebrates (Zakrzewski et al. 2014). Rudall in 1955 rejected the hypothesis that chitin is present in the tubes of *R. normani* based on chemical digestion of tubes. He found that they disintegrate in boiling dilute alkali and do not have an X-ray chitin pattern. Foucart et al. (1965) using an enzymatic and chromatographic method, stated that the tubarium of the pterobranchs does not contain any chitin and the proteinaceous part is collagen because of the high proportion of glycine.

Dilly (1971) investigated the composition of the tubes of *Rhabdopleura compacta* and tentatively concluded that they are composed of keratin. He found some weak evidence for sulphur and disulphide bonds but remarked that these results need to be further verified. Dilly (1971) also used transmission electron microscopy (TEM) to show three kinds of fibres which he supposed to be keratin. Keratins are intermediate filaments that form heterodimers and are intracellular proteins with high-sulphur content. Their function is to protect tissues like epidermis, nails, hair and horns. In hagfish, keratin fibres are secreted with the mucus for defense (Wang et al. 2016). Bairati (1972)

was critical of the pterobranch tube keratin hypothesis from Dilly (1971) because it is based solely on morphological data, and failed to show a diffractographic pattern and high sulphur content.

Urbanek (1976) concluded there is no evidence of high sulphur content amino acid, or of collagen-like fibrils nor from the amino acid analysis result collagen markers like hydroxyproline or hydroxylisine in living *Rhabdopleura*, whereas Armstrong et al. (1984) claimed they found collagen fingerprints during amino acid analysis of *Rhabdopleura normani*. Collagen is a major component of connective tissues that makes up tendons, ligaments, skin, and muscles, and is a defining characteristic of the animal kingdom. It is formed by three α-chains containing repetition of GXY amino acids, where X and Y are often proline and hydroxyproline amino acids; the α-chains assemble to form a coiled triple helix, the tropocollagen or collagenous domain which is interrupted by non-collagenous domain (Garrone 1998; Ehrlich 2010; Jürgen and Chiquet 2011).

Finally, Sewera (2011) investigated the tubes of *Cephalodiscus nigrescens* using microscopy, histology and purification techniques. He investigated the possibility of cellulose, including a form called tunicin, because it is a component of the mantle, or tunic of tunicates (Sagane et al. 2010). Cellulose is the most abundant polysaccharide on earth made of β(1→4) linked D-glucose units. It is found in prokaryotes and plants where it gives structural support. Tunicin of tunicates probably arrived from a prokaryote via transposable elements (Nakashima et al. 2004). The study of Sewera (2011) was largely inconclusive, revealing a protein component of uncertain nature and probably no cellulose or chitin present.

Here we characterize the chemical composition of the tubes of *R. recondita* (Beli et al. 2018) via bioinformatics analyses of the *R. recondita* transcriptome and genome, and chemical analyses of the tubes via Fourier-transform infrared spectroscopy (FTIR), X-ray photoelectron spectroscopy (XPS), and immunohistochemistry.

Materials and Methods

Colonies of *R. recondita* were collected by SCUBA diving in January 2019 at about 20 m depth in the Adriatic Sea, south of Otranto, Lecce, Italy. Samples were then moved to the Dipartimento di Scienze e Tecnologie Biologiche e Ambientali (DiSTeBA), University of Salento, into an aquarium with the sea water temperature of the place of collection (19 ºC). Zooids reside in tubes that are in

turn inside of the skeletal matrix of dead bryozoans. Zooids and tubes were removed from the matrix using tweezers and needles and separated. Zooids were fixed for genomics, and tubes were dried or fixed for spectroscopy and immunochemistry, as detailed below. We started with a bioinformatics search of chitin and cellulose/tunicin synthases, and keratin genes to obtain a prediction of the presence of chitin, cellulose/tunicin and keratin molecules. Based on the results we tried an immunohistochemistry approach and at the same time performed a Hoechts, a Fourier-transform infrared spectroscopy (FTIR), an X-Ray Photoelectron Spectroscopy analysis (XPS).

Genomics

Zooids were fixed in RNAlater (Ambion Europe Ltd., Huntingdon, Cambridgeshire, UK) and mailed to the University College London for genome sequencing. Sequencing, genome assembly and bioinformatics analysis were conducted in the University College London and Natural History Museum laboratories.

DNA extraction and library preparation

Genomic DNA was extracted from batches of 5-10 pooled *R. recondita* specimens using the Zymo Research Quick-DNA Microprep kit. The lysis buffer alone did not succeed in dissolving the specimens, so a pestle was used to manually crush the animals before adding the lysis buffer.
According to Qubit measurements, the extractions yielded 5-20ng of DNA. Libraries for genomic DNA sequencing were prepared with NEBNext Ultra II FS DNA Library Prep Kit for Illumina, which includes an enzymatic fragmentation step and PCR amplification of the input DNA before sequencing. The aimed fragment size during the fragmentation step was ~500bp, for a target paired-read length of 150bp. The fragmentation size profile for each library was assessed using a TapeStation instrument.

Genome sequencing and assembly

The sequencing was performed in a NextSeq Illumina instrument. Two libraries were successfully sequenced, yielding 65,015,822 and 45,909,334 read pairs. The quality of the raw reads was checked using FastQC and MultiQC. After quality check, Trimmomatic was employed to cut the reads and remove low-quality base calls and potential adapter sequences. The settings that were selected in Trimmomatic are: ILLUMINACLIP:adapters.fasta:2:30:10 LEADING:3 TRAILING:3

SLIDINGWINDOW:4:15 MINLEN:36. FastQC and MultiQC reports were created for trimmed reads as well.

Jellyfish software was used to estimate the genome sizes from the trimmed reads, using a k-mer counting approach. Using a k-mer size of k=21, the genome size of *Paratomella* was estimated at ~1.1Gbp and of *Rhabdopleura* at ~178Mbp. The trimmed reads were assembled into contigs and scaffolds using SPAdes with the parameters -k 21,33,55,77 –careful. Potential contaminant contigs were investigated with BlobTools. Contigs with length <500bp and/or coverage <10X were filtered out of the assembly. Furthermore, RNA-Seq reads were incorporated with Rascaf to improve the scaffolding by connecting contigs from different exons.

The dataset of genome and transcriptome fasta files was built considering the metazoans for their known ability to synthetize the molecules of interest: chitin, keratin, cellulose/tunicin (for the sources see Table 1). The transcriptomes were processed using 'getorf' with the option '-minsize 150' and the longest orf was kept for each transcript. To assess the completeness of each gene-set we ran BUSCO analysis (Simão et al. 2015) using the Metazoa lineage library. OrthoFinder (Emms and Kelly 2015) was employed to search for orthologs among these organisms. We searched the resulting orthogroups for genes of interest, that have been characterized in other species, i.e., chitin synthase genes (CSs) from *Caenorhabditis elegans, Ciona intestinalis* for cellulose/tunicin synthesis enzymes, *Homo sapiens* for keratin, and we retrieved all those orthogroups including a sequence of interest together with one or more *R. recondita* sequences. The selected orthogroups were aligned with MAFFT (Katoh et al. 2002) and a phylogenetic tree was built using RAxML (Stamatakis 2015) with the option '-m PROTGAMMAAUTO' and 100 bootstrap replicates to estimate branch support values.

A second OrthoFinder run was limited to the 21 Ambulacraria species, in order to gain insights about presence and evolution of interesting genes in this clade. *Rhabdopleura recondita* genes of interest from the first OrthoFinder were used to retrieve the corresponding Ambulacraria-only orthogroups. Alignments and gene trees were also produced for these orthogroups.

Fourier-transform infrared spectroscopy* (*FTIR)

Rhabdopleura recondita tubes were collected and rinsed gently with distilled water several times to remove potential contaminant particles from the outer surface, cut in small transversal fragments and dried at room temperature. The spectroscopic characterization of the tubes was performed in the analytical chemistry lab of the DiSTeBA. Infrared spectra were recorded with a Perkin Elmer Spectrum One Fourier transform infrared (FTIR) spectrometer, equipped with a deuterium triglycine sulphate (DTGS) detector and an attenuated total reflection (ATR) apparatus. The internal reflection element (IRE) was a three-bounce diamond microprism with a 4 mm diameter. The tube sample was placed onto the ATR microprism. A suitable mechanical press was used for achieving the tight contact between the tubes and the IRE, thus favouring the proper penetration of the evanescent wave within the sample. Typically, 16 interferograms were acquired and averaged for each spectrum. The resolution was 4 cm^{-1}. ATR-FTIR spectra of a series of standard compounds and biological samples were also acquired to guide IR band assignment in the tube spectra. Standard compounds, analysed as dry powders and fragments, were chitosan from crab shells (48165 – Sigma-Aldrich) and chitin from shrimp (C9213 – Sigma-Aldrich) respectively. Biological samples, suitably rinsed and dried, were a squid pen (as a reference for β-chitin) and a bee leg (as a reference for α-chitin).

X-Ray Photoelectron Spectroscopy (XPS)

The analysis of dried tubes was performed in the analytical chemistry lab of the DiSTeBA, using an AXIS ULTRA DLD (Kratos Analytical) spectrometer equipped with a monochromatic AlKa (1486.6 eV) radiation source, operating at 10 kV and 15mA. Base pressure in the analysis chamber was 3.0x10-9 torr. Survey spectra were acquired in fixed analyzer transmission (FAT) mode at a pass energy of E0 = 160 eV and energy step of 1 eV. The hybrid lens mode was used for all measurements with analysis area of about 700 µm ×300 µm. During the data acquisition a system of neutralization of the charge has been used. The peak assignments (uncertainty on BEs of ± 0.1 eV) refer to literature data and to the NIST (National Institute of Standards and Technology) database.

Hoechst and Immunohistochemistry

Hoechst and immunohistochemistry analysis were performed in collaboration with the Zoology and the Human Anatomy Lab at the DiSTeBA. For Hoechst, tubes of *R. recondita* were recovered from colonies kept in aquarium, rinsed in filtered sea water (FSW) (0.45 µm), and incubated in 10 mg mL^{-1} Hoechst solution (33258 – Sigma-Aldrich), in the dark for 15 minutes, at room temperature. The samples were then rinsed in FSW three times for 5 minutes in the dark and observed with a Nikon Eclipse 50i epifluorescence microscope (filter ex 340-380; ba 435-485).

For immunohistochemistry, *R. recondita* tubes and black stolons were washed in FSW, fixed in paraformaldehyde (4% in FSW), paraffin-embedded and serially cut into 10 µm sections (Leica RM2155 microtome). Serial sections were processed for immunohistochemical analysis on glass slides: experimental and control samples were rinsed in PBS three times for 10 minutes at room temperature, then pre-incubated with Bovine Serum Albumin (BSA) for 40 minutes at room temperature and Normal Donkey Serum (NDS) for 40 minutes at room temperature. Rabbit anti-chitin primary antibodies made against crab chitin, kindly provided by Michael Horst (Darling Marine Center, University of Maine) were then used to incubate experimental samples overnight at 4 °C, together with dried shrimp chitin (C9213 – Sigma-Aldrich) as positive control.

Negative controls, including *Rhabdopleura* tubes, stolon sections and dried shrimp chitin, were kept in a humid chamber over night at 4 °C without primary antibodies. Control and experimental sections, as well as shrimp chitin, were then washed and biotinylated goat anti-rabbit secondary antibody (Millipore - AP 132B) was applied for 1h, washed, treated with streptavidin peroxidase for 1h and washed again. To develop colour reaction, one drop of 3,3'-Diaminobenzidine (DAB) was applied for 20 mins and then rinsed. A mounting medium was applied to glue the coverslip (Bio Mount HM - Bio Optica). The positive reaction, appeared as brown colour, was observed under a Nikon Eclipse E800 microscope equipped with a Nikon Digital Sight DS-5M camera.

Results

OrthoFinder

The first OrthoFinder analysis of the whole dataset recovered two orthogroups for CSs sequences based on annotated *C. elegans* sequences, for which we built phylogenetic trees. The second OrthoFinder analysis was limited to the Ambulacraria dataset. We used *R. recondita* sequences from the first OrthoFinder search to recover seven orthogroups and build five phylogenetic trees

(two orthogroups were composed of only two sequences), for a total of seven phylogenetic trees (Fig. 1-7 and supplementary materials).

The search for keratin or cellulose/tunicin sequences belonging to *Rhabdopleura* and based on annotated sequences of *H. sapiens* and *C. intestinalis* respectively, recovered no *Rhabdopleura* orthologues.

Chitin synthase - complete dataset OG0000859

The first CSs tree (Fig. 1) encompasses 37/40 taxa of the complete dataset. Here hemichordates and echinoderms are sister taxa (red), supporting Ambulacraria. Pterobranchia (fuchsia box) is sister to enteropneusts. Among chordates (blue), arthropod and nematode sequences (green) are less clustered. The placement of the appendicularian *Oikopleura dioica* as sister to the protostomes rather than within the chordates, and one *Clytia hemishphaerica* (black) sequence within the chordates may be due to the so called "long branch attraction effect" (Felsenstein 1981), meaning that they could be sequences that evolved rapidly and secondarily acquired similarity to the protostome and chordate CSs sequences. The hydromedusa *C. hemisphaerica* sequence is sister to the bilaterians, and the sponge *Amphimedon queenslandica* is the outgroup taxon. There are six *R. recondita* sequences from both genome (two sequences) and transcriptome (four sequences). *Rhabdopleura annulata*, the sole other *Rhabdopleura* sequence available, is absent from both CSs trees. There are also 79 chitin synthase genes from four enteropneust families. Looking at this tree we can say that the CSs presence is predicted in *R. recondita*.

Chitin synthase - complete dataset OG0004142

The second CSs phylogenetic tree (Fig. 2) encompasses the whole dataset of CSs sharing organisms, including 18/40 taxa. There is an overall coherent clustering of protostomes (green), ambulacrarians (red) and chordates (blue), with exceptions that are likely due to long branch attraction. The chordate sequences are arranged step-wise as sister to the Ambulacraria plus protostomes, rather than as a monophyletic group. Among chordates there are long branches of two nematodes species (in green) sequences that probably evolved rapidly and secondarily acquired a similarity to chordate chitin synthase sequences. *Rhabdopleura recondita* is present with two genome sequences, different from the first chitin tree and the transcriptome is not present,

suggesting this CSs in *Rhabdopleura recondita* is predicted and correctly clustered but might be not expressed.

Chitin synthase - Ambulacrarian datasets OG0006824 OG0012451 OG0012607 OG0023337 OG0040366

Overall, the CSs trees are clustered as expected: enteropneusts (green), pterobranchs (red) and echinoderms (blue) are well separated. In OG0006824 (Fig. 3) two *R. recondita* sequences, one from the genome and a second from the transcriptome, are sister to the *Cephalodiscus* sequence and the pterobranch sequences evolved in turn as sister clade to enteropneusts. Similarly, in OG0012451, OG0012607 and OG0023337 (Fig. 4-6), *Cephalodiscus* was not present, but the predicted CSs in *R. recondita* is sister to the enteropneusts. The OG0040366 (Fig. 7) is composed of only four sequences including two from the crinoid *Florometra serratissima*, which do not form a monophyletic group.

FTIR and XPS analysis

ATR-FTIR spectra of standard compounds, namely chitosan from crab (Fig. 8, pink trace) and chitin from shrimps (Fig. 8, blue trace), presented the typical marker signals of these polysaccharides. The high crystallinity of chitin and chitosan powders, resulted in poor flexibility and elasticity, and hampered a tight contact between sample and diamond surface, which made it difficult for the evanescent wave to reach the sample. This agreed with the very low intensity of signals at higher wavenumbers corresponding to smaller penetration depths. The spectrum of chitin from shrimps presented a split of the amide I band at 1654 cm^{-1} and 1621 cm^{-1}, which is typical of α-chitin polymorph (Jang et al. 2004). The acetamide groups account for the signals at 1551 cm^{-1} (amide II band) and 1376 cm^{-1} (-CH_3 bending). Analogous acetamide spectral features were detectable, although less intense, in chitosan spectrum (see band at 1377 cm^{-1}), suggesting a certain acetylation degree. However, marker bands typical of primary amines (N-H deformation band at 1587 cm^{-1} and N-H stretching band at around 3300 cm^{-1}) testify the presence of -NH_2 moieties replacing acetamide in chitosan structure. Moreover, broader bands in chitosan spectrum are consistent with its chemical heterogeneity (partial deacetylation) and with the lower crystallinity degree compared with α-chitin.

The spectrum of squid pen (Fig. 8, green trace) was consistent with its high β-chitin content. This chitin polymorph presented a different arrangement of intra-chain H-bonds resulting in a single amide I band centered at 1632 cm^{-1}. Further bands ascribable to chitin, based on comparison with the α-chitin spectrum, are evident at 1543 cm^{-1}, 1378 cm^{-1}, 1319 cm^{-1}, 1202 cm^{-1}, 1154 cm^{-1} and 951 cm^{-1}. The good adhesion of squid pen sample pressed on the ATR crystal surface was likely responsible for the better penetration of the IR beam within the sample, which enabled the detection of more intense bands at higher frequencies, compared to the case of the poor contact in the purified chitin sample. As recently shown by Cuong et al. (2016), SEM image, X-ray powder diffraction (XRD) pattern and FTIR spectrum of β-chitin extracted from squid pen is very similar to that of the raw material, despite the significant reduction of protein content achieved with the deproteinization step (from 57.20% to 0.63%). However, the major effect of squid pen deproteinization on FTIR spectra reported by Cuong et al. (2016) is the relative decrease of amide I and amide II bands, where the contribution of peptide amides from proteins is more significant. In our case, the comparison with the spectrum of α-chitin from shrimps allowed ascribing to squid pen proteins the higher intensity of amide I and amide II bands and the appearance of new bands at 1445 cm^{-1} and 1237 cm^{-1}, which can be assigned to methylene groups of amino acid residues (>CH_2 bend) and to peptide amide groups (amide III band) respectively. As in squid pen, the natural association of chitin with proteins is common to all living organisms. In general, the chitin-protein complexes found in marine species show greatly variable ratios between chitin and covalently bound proteins, and each species presents its own protein binding matrix.

Moving from squid pen to an arthropod sample such as the bee leg (Fig. 8, red trace) the contribution of protein components to the FTIR spectrum appears much more pronounced, considering the strong reduction of chitin marker bands with respect to amide I and amide II bands, whose maxima fell at 1630 cm^{-1} and 1536 cm^{-1}. It should be highlighted that in arthropod cuticle, chitin does not occur in the epicuticle, but is confined to the procuticle (Hackman and Goldberg 1978). Since the typical thickness of the outermost epicuticle layer is around 300-600 nm, the low chitin contribution to the ATR-FTIR spectrum of bee leg is consistent with a low number of photons reaching the chitin matrix. Moreover, chitin occurs in cuticles as microfibrils surrounded by proteins covalently and non-covalently bound and in addition, in sclerotized cuticles, protein chains are covalently bound together by reaction of a quinonoid tanning agent. This means that the

infrared photons reaching the chitin matrix intercept functional groups not ascribable to chitin alone, further hampering the detectability of chitin marker bands in the infrared spectrum. Consequently, main features in bee leg spectrum may be assigned to proteins, included bands at 1446 cm^{-1} (>CH_2 bend) and 1232 cm^{-1} (amide III band), found also in squid pen spectrum. On the other side, the broad absorption appearing at 1100-1000 cm^{-1} is too intense to be ascribable only to proteins and can be attributed to a saccharide component. The stretching of several ether and alcoholic C-O bonds in pyranose rings indeed produces diverse and intense absorption bands in this wavenumber interval, such as in the case of α-chitin and chitosan spectra (Fig. 8, pink and blue traces). Therefore, on the basis of the well-known chemical composition of arthropod biomass, the absorption at 1100-1000 cm^{-1} in bee leg spectrum was assigned mainly to α-chitin, consistently with the higher penetration depth of photons in this low frequency region, enabling the interaction of IR beam with procuticle chitin matrix. Nevertheless, the superimposition with bands of extra-chitin components produces signals much broader than those observed in pure chitin spectrum. Sharper signals at 1204 cm^{-1} and 1154 cm^{-1} can be likewise attributed to sugar vibrations, being well evident also in chitosan, α-chitin and squid pen spectra. Surprisingly, the spectrum of bee leg presents an intense sharp signal at 874 cm^{-1}, which is characteristic of carbonate ion. It is well known that this inorganic species produces a further band, much broader, between 1490 cm^{-1} and 1410 cm^{-1}, where the bee leg spectrum presents a clear absorption signal, thus confirming the presence of carbonate in the bee sample. This puzzling result may be explained with the ability of honey bees to accumulate airborne particulate matter, such as calcium carbonate particles, in the inner surface of the hind legs (Negri et al. 2015), thus acting as living samplers and pollution sentinel species.

The ATR-FTIR spectrum of *R. recondita* tubes (Fig. 8, black trace) presents some similarities with spectra of standard compounds and the representative biological samples described above, which allowed us to gain information on the chemical composition of the tube surface. The high signal to noise ratio and the relative intensity of bands suggested a tight contact between the ATR prism and the *Rhabdopleura* tubes. The spectrum is consistent with the dual contribution from both saccharide and protein components. Major marker signal for protein is the peak at 1234 cm^{-1} (peptide amide III band), which is present in squid pen and bee leg and absent in chitin and chitosan spectra, while the intense broad signal at 1100-1000 cm^{-1} as well as the band at 1202 cm^{-1} testify the presence of

a significant saccharide component. The presence of a shoulder at 1376 cm^{-1} and a small peak at 1316 cm^{-1} (see magnification in Fig. 9) are indicative of acetamide moieties pointing to a certain chitin content. However, the low intensity of these signals suggests that chitin was not located in the outermost layer of the tube surface, but more deeply, similar to the bee leg sample. On the other side, the strong relative intensity of the signal at 1100-1000 cm^{-1} suggests that further saccharide components other than chitin are present and/or chemical species other than saccharides contribute to the signal. The latter hypothesis is supported by the apparent absence of the peak at 895 cm^{-1}, which represents an IR marker quite common in carbohydrate FTIR spectra, such as in both chitosan and α-chitin spectra and is ascribable to the C-O-C stretching of glycosidic bonds, sensitive to crystallinity degree and H-bonding (Nelson 1964). Regardless of the role of this signal, which is absent also in squid pen and bee leg spectra, the intensity of the broad signal at 1100-1000 cm^{-1} in *R. recondita* spectrum remains too high to be explained with the sole saccharide contribution, suggesting a possible role by inorganic components such as silicon-containing minerals. This assumption is suggested by XPS analysis, a surface sensitive technique that gives elemental composition information on the 5-10 nm thick outermost layer of *R. recondita* tubes, which highlighted, near the carbon, oxygen and nitrogen macro-components the presence of expected hetero-elements like sodium, calcium, magnesium and chlorine ions (i.e. Na^{+} At% 1.9; Ca^{2+} At% 0.6; Mg^{2+} At% 0.43; and Cl^{-} At% 1.6), with silicon (At% 1.5) and aluminum (At% 1.0) oxides. Sulphur as sulfate (S At% 0.36) and iron oxide (At% 0.05, traces) were also detected. All XPS peaks associated to these elements are shown in Fig. 10.

XPS measurements detected aluminum, indicating that clay minerals (phyllosilicates) presumably from marine sediments could have been entrapped in the surface structures. Another signal clearly attributed to inorganic species is the sharp band at 875 cm^{-1} highlighting a calcium/magnesium carbonate content likely arising from bryozoan contamination. The presence of calcium/magnesium was confirmed by XPS analysis.

Finally, shoulders at 1736 cm^{-1} and 1718 cm^{-1} are strongly indicative of carbonyl groups such as esters or protonated carboxylic acids. The hypothesis of a lipid component responsible for C=O ester absorption is further supported by the intensity and band ratio of C-H stretching signals between 2800 cm^{-1} and 3000 cm^{-1}, which indicate the presence of aliphatic chains.

In conclusion, the ATR-FTIR analysis of *R. recondita* tubes showed that i) proteins represent the main component of *R. recondita* tube surfaces, ii) a saccharide component was definitely present but its chemical nature was not clear, since the bands were not well resolved, iii) some chitin IR markers were present, but were weak, indicating that chitin is not located on the outermost layer of the tubes, like the bee leg, iv) further polysaccharides, in addition to chitin, were likely present, v) inorganic species such as calcium carbonate and possibly phyllosilicates were present on the surface (as suggested also by XPS elemental analysis confirming the presence of Al, Si, Ca, Mg, Na, Cl, S, Fe), and vi) fatty acids from lipids were likely present.

Hoechst and Immunohistochemistry

Hoechst dye has the property to intercalate DNA, and to form a strongly fluorescent complex. We found no Hoechst fluorescence or cells in the tube matrix (not illustrated).

Immunohistochemistry experiments using anti-chitin primary antibody did not work on the *R. recondita* tubes, as a brown precipitate was also observed in control processed without the primary antibody (compare Figs. 11b and c with Fig. 11a showing an untreated tube).

This method is not suitable for the stolon material because its brown colour is similar to the precipitate given by the DAB reaction (Fig. 12). A positive reaction was observed for shrimp chitin. In these samples the control stayed whitish whereas the sample treated with anti-chitin primary antibody showed the brown precipitate, demonstrating a specific binding of the secondary antibody (Fig. 13).

Discussion

An OrthoFinder search of the *R. recondita* genome and transcriptomes did not find sequences similar to a keratin gene, effectively rejecting these molecules as candidates for the material composition of graptolite tubes. The hypothesis that *Rhabdopleura* tubes are keratin is based on the finding of fibres in the tubes (Dilly 1971). We support the critique that a molecular, or chemical analyses are needed to firmly establish the presence of keratin (Bairati 1972). Similarly, we did not find orthologues for cellulose or tunicin synthesis genes, rejecting the hypothesis that these molecules comprise graptolite tubes, confirmed also by the recent research of Inoue et al. (2019) that affirm tunicates are the only metazoans able to synthetize cellulose. Sewera (2011) used microscopy, histology and purification techniques to identify cellulose and tunicin but his results

were inconclusive. This result underlines the challenge of using microscopy and chemical analytical techniques to confidently identify fibrous structural proteins, and the power of gene sequences as a supplement to these methods. Conversely, gene sequence data is of little use to establish the presence of collagen in the tubes of *R. recondita*. The collagen protein is ubiquitous in the animal kingdom, so a search for collagen orthologs would give no information about the *Rhabdopleura* tube characterization. For this reason, we did not search for collagen in our *R. recondita* sequence gene databases.

Eight CSs gene sequences were recovered from our *R. recondita* databases including four from the genome, and four from the transcriptome. Chitin is a polysaccharide found in unicellular eukaryotes, fungi and most invertebrates including hydrozoans, arthropods, annelids, molluscs and bryozoans (Jeuniaux 1978; Zakrzewski et al. 2014). Chitin may be found in α, β and γ arrangements in crustaceans, squid pen and fungi or yeasts, respectively, according to the organization of the *N*-acetylglucosamine units that repeat to form long chains (Cuong et al. 2016). It is always associated with proteins, calcium carbonate or other compounds, which makes isolation complicated (Cuong et al. 2016). Chitin can be secreted and remain attached to the soma like in insects and crustaceans or be secreted and stay detached from the body as in hydrozoan thecae. This rarely happens for keratin which according our current knowledge cannot be detached from the soma, with few exceptions (Wang et al. 2016). Among deuterostomes, CSs gene sequences are available for *Branchiostoma floridae*, *C. intestinalis*, *Danio rerio* and *Xenopus tropicalis* (Zakrzewski et al. 2014), demonstrating that the genes are widespread in the deuterostomes. Our bioinformatics results are predictions, rather than a demonstration that chitin is a component of the tubes of *R. recondita*. For this, we used a chemical analytical method for characterizing the material composition of the tubes.

ATR-FTIR spectroscopic analysis revealed a protein component supporting the finding of Armstrong et al. (1984), and a fatty acid component. These in turn may be linked to the polysaccharide component as happens in many chitin-based matrices. Due to the exponential decay of the evanescent wave beyond the ATR prism interface, the IR beam probed mainly the outermost layer of the sample, producing spectra with a higher contribution of functional groups from the surface. The wavelength-dependent penetration depth, as arising from an average refraction index

of the sample equal to 1.39 and from specific characteristics of our ATR apparatus (i.e., diamond refraction index and incidence angle), spans from 0.4 μm at 4000 cm^{-1} to 2.2 μm at 750 cm^{-1}. These values represent a rough estimate of probed sample thickness and point out the increase of the spectral contribution by more internal layers at lower wavenumbers. These peculiar characteristics of ATR method should be always considered when ATR-FTIR spectra of chemically heterogeneous samples, such as whole living organisms, or parts of them, are considered (Giotta et al. 2011). Given the constraints of a spectrum that was not fully resolved, a definitive demonstration of chitin was not achieved. To achieve a well-resolved spectrum like that of our purified α-chitin sample, a consistent mass of tube material would need to be collected from what are sparse and near-to-microscopic tubes that project from a bryozoan matrix. Nevertheless, chitin cannot be excluded. Our tube results reflected our results from bee legs where chitin is surely present. The inorganic fraction from the XPS, including calcium carbonate and possibly phyllosilicates, Al, Si, Ca, Mg, Na, Cl, S, Fe were likely due to foreign material on the external layer of the tubes that originated from the marine environment.

Hoechst analysis confirmed the absence of nuclei in the *R. recondita* tube matrix, in agreement with authors who never observed cells in graptolites tubes (Dilly 1971, 1986; Urbanek and Mierzejewski 1984; Rigby 1994; Mierzejewski and Kulicki 2001). This finding supports that the tubes are an extracellular secretion from the cephalic shield of a zooid. Our anti-crab chitin antibody did not confirm the presence of chitin in the tubes. This negative result may be due to the nature of the polysaccharide chains that comprise a component of the tubes, or to the lack of specificity of the antibody which was developed against crab chitin, and so may not be expected to recognize graptolite chitin epitopes. Even if the sequence was identical to crab chitin, and they are not, the modifications of the final polysaccharide may be substantial compared with that of an arthropod.

The absence of gene sequence for the protein keratin or for a cellulose/tunicin synthesis enzyme from the genome and transcriptomes of *R. recondita* rejects the old hypotheses that the molecules are components of the tubes. Instead, we find sequences for eight chitin synthase genes hinting that the tubes of graptolites may be composed of a chitin-like polysaccharide. ATR-FTIR spectroscopy confirmed this by identifying a chitin-like polysaccharide, as well as additional polysaccharides,

internal to the tube surface. The outer surface contained proteins, fatty acids and a range of unanticipated molecules (calcium carbonate, and possibly phyllosilicates) and elements (Al, Si, Ca, Mg, Na, Cl, S, Fe) that may have originated from the environment. The composition of the graptolite tube is far more complex than previously hypothesized. It is a composite material, and characteristic of composite materials, the tubes are flexible not frangible, resistant to rips, and durable to decay (Beli et al. 2017). Their chemical composition, and the layering of cortical tissues interspersed with fibres is a recipe to a rich fossil record. This study closes the doors on old hypotheses and supports the chitin hypothesis. More importantly, it reveals that the molecular composition of graptolite tubes, one of the oldest and most abundant animal fossils that defines the Palaeozoic layers of the fossil record, is complicated. There are numerous lessons within for material scientists, who seek slender but resistant sheets for biomedical applications, chitin is the most abundant biopolymer on earth after cellulose, together with the deacetylated form, the chitosan, is characterized by low immunogenicity, biocompatibility, and biodegradability. These properties make the molecule suitable for a variety of applications in material and biomedical science, including wound healing, drug delivery, sponges and organic scaffolding (Jayakumar et al. 2010).

Rhabdopleura recondita tube composition is probably not significantly different from the composition of fossil graptolites. Extracellular matrix materials of fossil cnidarians, arthropods, molluscs, echinoderms and bryozoans are conserved through time (Miller 1991; Bottjer et al. 2006; Weaver et al. 2011; Landing et al. 2010). Moreover, the presence of 79 chitin synthase genes from four enteropneust families suggests that the tubes of the stem group acorn worms, believed to be homologous with graptolite tubes (Caron et al. 2013; Nanglu et al. 2016) may have been composed of chitin-like polysaccharides.

Genomic and proteomic databases are expanding at a rapid pace (Kahn 2011). In the near future we will have a more resolved and taxonomically diverse understanding of chitin synthase gene origin and evolution (see Zakrzewski et al 2014; Morozov and Likhoshway 2016). Future biochemical and mechanical studies are expected to reveal more about this extraordinarily versatile polymer family. As technology advances, other methodologies may provide a higher resolution of graptolite tube composition, including chitins associations with other molecules and elements.

References

Allman, G. J. (1869). On *Rhabdopleura*, a new form of Polyzoa, from deep-see dredging in Shetland. *The Quarterly Journal of Microscopical Science*, 9, 57–63.

Armstrong, W. G., Dilly, P. N., & Urbanek, A. (1984). Collagen in the pterobranch coenecium and the problem of graptolite affinities. *Lethaia*, 17, 145–152.

Bairati, A. (1972). Comparative Ultrastructure Of Ectoderm-Derived Filaments. *Italian Journal of Zoology*, 39, 283–308.

Beli, E., Piraino, S., & Cameron, C. B. (2017). Fossilization processes of graptolites: insights from the experimental decay of *Rhabdopleura* sp.(Pterobranchia). *Palaeontology*, 60, 389–400.

Beli, E., Aglieri, G., Strano, F., Maggioni, D., Telford, M. J., Piraino, S., & Cameron, C. B. (2018). The zoogeography of extant rhabdopleurid hemichordates (Pterobranchia: Graptolithina), with a new species from the Mediterranean Sea. *Invertebrate Systematics*, 32, 100–110.

Bottjer, D. J., Davidson, E. H., Peterson, K. J., & Cameron, R. A. (2006). Paleogenomics of echinoderms. *Science*, 314, 956–960.

Cameron, C. B. (2018). Treatise on Invertebrate Paleontology, Part V, second revision, chapter 2: Class Enteropneusta Gegenbaur, 1870: introduction, morphology, and systematic descriptions. *Treatise Online.*

Caron, J. B., Morris, S. C., & Cameron, C. B. (2013). Tubicolous enteropneusts from the Cambrian period. *Nature*, 495, 503–506.

Cuong, H. N., Minh, N. C., Van Hoa, N., & Trung, T. S. (2016). Preparation and characterization of high purity β-chitin from squid pens (*Loligo chenisis*). *International Journal of Biological Macromolecules*, 93, 442–447.

Dilly, P. N. (1971). Keratin-like fibres in the Hemichordate *Rhabdopleura compacta*. *Zeitschrift für Zellforschung und Mikroskopische Anatomie*, 117, 502–515.

Dilly, P. N. (1972). The structures of the tentacles of *Rhabdopleura compacta* (Hemichordata) with special reference to neurociliary control. *Zeitschrift für Zellforschung und mikroskopische Anatomie*, 129, 20–39.

Dilly, P. N. (1986). Modern pterobranchs: Observations on their behaviour and tube building. *Geological Society, London, Special Publication*, 20, 261–269.

Ehrlich, H. (2010). Chitin and collagen as universal and alternative templates in biomineralization. *International Geology Review*, 52, 7–8.

Emms, D. M., & Kelly, S. (2015). OrthoFinder: solving fundamental biases in whole genome comparisons dramatically improves orthogroup inference accuracy. *Genome Biology*, 16, 1–14.

Felsenstein, J. (1981). Evolutionary trees from DNA sequences: A maximum likelihood approach. *Journal of Molecular Evolution*, 17, 368–376.

Foucart, M. F., Bricteux-Grégoire, S., & Jeuniaux, C. (1965). Composition chimique du tube d'un pogonophore (*Siboglinum* sp.) et des formations squelettiques de deux pterobranches. *Sarsia*, 20, 35–41.

Garrone, R. (1998). *Evolution of metazoan collagens*. In *Molecular Evolution: Towards the Origin of Metazoa* (pp. 119–139). Springer, Berlin, Heidelberg.

Giotta, L., Mastrogiacomo, D., Italiano, F., Milano, F., Agostiano, A., Nagy, K., Valli, L., & Trotta, M. (2011). Reversible binding of metal ions onto bacterial layers revealed by protonation-induced ATR-FTIR difference spectroscopy. *Langmuir*, 27, 3762–3773.

Gullan, P. J., & Cranston, P. S. (2010). *The insects an outline of entomology*. John Wiley & Sons.

Hackman, R. H., & Goldberg, M. (1978). The non-covalent binding of two insect cuticular proteins by a chitin. *Insect Biochemistry*, 8, 353–357.

Halanych, K. M. (1993). Suspension feeding by the lophophore-like apparatus of the pterobranch hemichordate *Rhabdopleura normani*. *The Biological Bulletin*, 185, 417–427.

Inoue, J., Nakashima, K., & Satoh, N. (2019). ORTHOSCOPE analysis reveals the presence of the cellulose synthase gene in all tunicate genomes but not in other animal genomes. *Genes*, 10, 294.

Jang, M. K., Kong, B. G., Jeong, Y. I., Lee, C. H., & Nah, J. W. (2004). Physicochemical characterization of α-chitin, β-chitin, and γ-chitin separated from natural resources. *Journal of Polymer Science Part A: Polymer Chemistry*, 42, 3423–3432.

Jayakumar, R., Menon, D., Manzoor, K., Nair, S. V., & Tamura, H. (2010). Biomedical applications of chitin and chitosan based nanomaterials—A short review. *Carbohydrate polymers*, 82, 227–232.

Jeuniaux, C. (1978). Distribution and quantitative importance of chitin in animals. *Proceedings of the First International Conference on Chitin/Chitosan*, 6.

Jürgen, E., & Chiquet, M. (2011). *An overview of extracellular matrix structure and function*. In, *The extracellular matrix: an overview* (pp. 1–39). R. P. Mecham (Ed.) Springer, Berlin, Heidelberg.

Kahn, S. D. (2011). On the future of genomic data. *Science*, 331, 728–729.

Katoh, K., Misawa, K., Kuma, K., & Miyata, T. (2002). MAFFT: a novel method for rapid multiple sequence alignment based on fast Fourier transform. *Nucleic Acids Research*, 30, 3059–3066.

Kozłowski, R. (1948). Les Graptolithes et quelques nouveaux groupes d'animaux du Tremadoc de la Pologne. *Palaeontologia Polonica*, 3, 1–235.

Kozłowski, R. (1966). On the structure and relationships of graptolites. *Journal of Paleontology*, 40, 489–501.

Kraft, P. (1926). Ontogenetische Entwicklung und Biologic von *Diplograptus* und *Monograptus*. *Paläontologische Zeitschrift*, 7, 207–249.

Landing, E., English, A., & Keppie, J. D. (2010). Cambrian origin of all skeletalized metazoan phyla—Discovery of Earth's oldest bryozoans (Upper Cambrian, southern Mexico). *Geology*, 38, 547–550.

Lester, S. M. (1988). Ultrastructure of adult gonads and development and structure of the larva of *Rhabdopleura normani* (Hemichordata: Pterobranchia). *Acta Zoologica*, 69, 95–109.

Maletz, J., Lenz, A. C., & Bates, D. E. B. (2016). Morphology of the pterobranch tubarium. *Treatise Online*, 76, 1–63.

Maletz, J. (2017). *Graptolite paleobiology*. John Wiley & Sons.

Maletz, J., & Beli, E. (2018). Part V, Second Revision, Chapter 15: Subclass Graptolithina and *Incertae Sedis* Family Rhabdopleuridae: Introduction and Systematic Descriptions. *Treatise Online*, 101, 1–14.

Maletz, J., Mottequin, B., Olive, S., Gueriau, P., Pernègre, V., Prestianni, C., & Goolaerts, S. (2020). Devonian and Carboniferous dendroid graptolites from Belgium and their significance for the taxonomy of the Dendroidea. *Geobios*, 59, 47–59.

Mierzejewski, P., & Kulicki, C. (2001). Graptolite-like fibril pattern in the fusellar tissue of Palaeozoic rhabdopleurid pterobranchs. *Acta Palaeontologica Polonica*, 46, 349–366.

Mierzejewski, P., & Kulicki, C. (2003). Cortical fibrils and secondary deposits in periderm of the hemichordate *Rhabdopleura* [Graptolithoidea]. *Acta Palaeontologica Polonica*, 48, 99–111.

Miller, R. F. (1991). Chitin paleoecology. *Biochemical Systematics and Ecology*, 19, 401–411.

Mitchell, C. E., Melchin, M. J., Cameron, C. B., & Maletz, J. (2013). Phylogenetic analysis reveals that *Rhabdopleura* is an extant graptolite. *Lethaia*, 46, 34–56.

Morozov, A. A., & Likhoshway, Y. V. (2016). Evolutionary history of the chitin synthases of eukaryotes. *Glycobiology*, 26, 635–639.

Nakashima, K., Yamada, L., Satou, Y., Azuma, J. I., & Satoh, N. (2004). The evolutionary origin of animal cellulose synthase. *Development genes and evolution*, 214, 81–88.

Nanglu, K., Caron, J. B., Morris, S. C., & Cameron, C. B. (2016). Cambrian suspension-feeding tubicolous hemichordates. *BMC biology*, 14, 56.

Negri, I., Mavris, C., Di Prisco, G., Caprio, E., & Pellecchia, M. (2015). Honey bees (*Apis mellifera*, L.) as active samplers of airborne particulate matter. *PLoS ONE*, 10, 1–22.

Nelson, M. L. (1964). Relation of certain infrared bands to cellulose crystallinity and crystal latticed type. Part I. Spectra of lattice types I, II, III and of amorphous cellulose. *Journal of Applied Polymer Science* 8, 1311–1324.

Potter, P. E., Maynard, J. B., & Pryor,W.A. (1980). *Sedimentology of Shale: study guide and reference source*. Springer-Verlag.

Rigby, S. (1994). Erect tube growth in *Rhabdopleura compacta* (Hemichordata: Pterobranchia) from off Start Point, Devon. *Journal of Zoology*, 233, 449–455.

Rudall, K. M. (1955). Distribution of collagen and chitin. In Armstrong, W. G., P. N. Dilly, and A. Urbanek. 1984. Collagen in the pterobranch coenecium and the problem of graptolite affinities. *Lethaia*, 17, 145–152.

Sagane, Y., Zech, K., Bouquet, J. M., Schmid, M., Bal, U., & Thompson, E. M. (2010). Functional specialization of cellulose synthase genes of prokaryotic origin in chordate larvaceans. *Development*, 137, 1483–1492.

Sars, O. (1874). On *Rhabdopleura mirabilis* (M. Sars). *Journal of Cell Science*, 2, 23–44.

Sato, A. (2008). Seasonal reproductive activity in the pterobranch hemichordate *Rhabdopleura compacta*. *Journal of the Marine Biological Association of the United Kingdom*, 88, 1033–1041.

Sewera, L. J. 2011. Determining the Composition of the Dwelling Tubes of Antarctic Pterobranchs. Honors thesis. Paper 48. Illinois Wesleyan University.

Simão, F. A., Waterhouse, R. M., Ioannidis, P., Kriventseva, E. V., & Zdobnov, E. M. (2015). BUSCO: Assessing genome assembly and annotation completeness with single-copy orthologs. *Bioinformatics*, 31, 3210–3212.

Stamatakis, A. (2015). Using RAxML to Infer Phylogenies. *Current Protocols in Bioinformatics*, 51, 6–14.

Stebbing, A. R. D. (1970). Aspects of the reproduction and life cycle of *Rhabdopleura compacta* (Hemichordata). *Marine Biology*, 5, 205–212.

Strano, F., Micaroni, V., Beli, E., Mercurio, S., Scarì, G., Pennati, R., & Piraino, S. (2019). On the larva and the zooid of the pterobranch *Rhabdopleura recondita* Beli, Cameron and Piraino, 2018 (Hemichordata, Graptolithina). *Marine Biodiversity*, 49, 1657–1666.

Urbanek, A. (1976). The problem of graptolite affinities in the light of ultrastructural studies on peridermal derivatives in pterobranchs. *Acta Palaeontologica Polonica*, 21, 3–43.

Urbanek, A., & Mierzejewski, P. (1984). The ultrastructure of the Crustoidea and the evolution of graptolite skeletal tissues. *Lethaia*, 17, 73–91.

Wang, B., Yang, W., McKittrick, J., & Meyers, M. A. (2016). Keratin: Structure, mechanical properties, occurrence in biological organisms, and efforts at bioinspiration. *Progress in Materials Science*, 76, 229–318.

Weaver, P. G., Doguzhaeva, L. A., Lawver, D. R., Tacker, R. C., Ciampaglio, C. N., Crate, J. M., & Zheng, W. (2011). Characterization of organics consistent with β-chitin preserved in the Late Eocene cuttlefish *Mississaepia mississippiensis*. *PLoS One*, 6, e28195.

Wiman, C. (1901). Uber die Borkholmer Schicht in mittelbaltischen Silurgebiet. *Bulletin of the Geological Institution of the University of Upsala*. 5, 149–222.

Zakrzewski, A. C., Weigert, A., Helm, C., Adamski, M., Adamska, M., Bleidorn, C., Raible, F., & Hausen, H. (2014). Early divergence, broad distribution, and high diversity of animal chitin synthases. *Genome Biology and Evolution*, 6, 316–325.

Figures

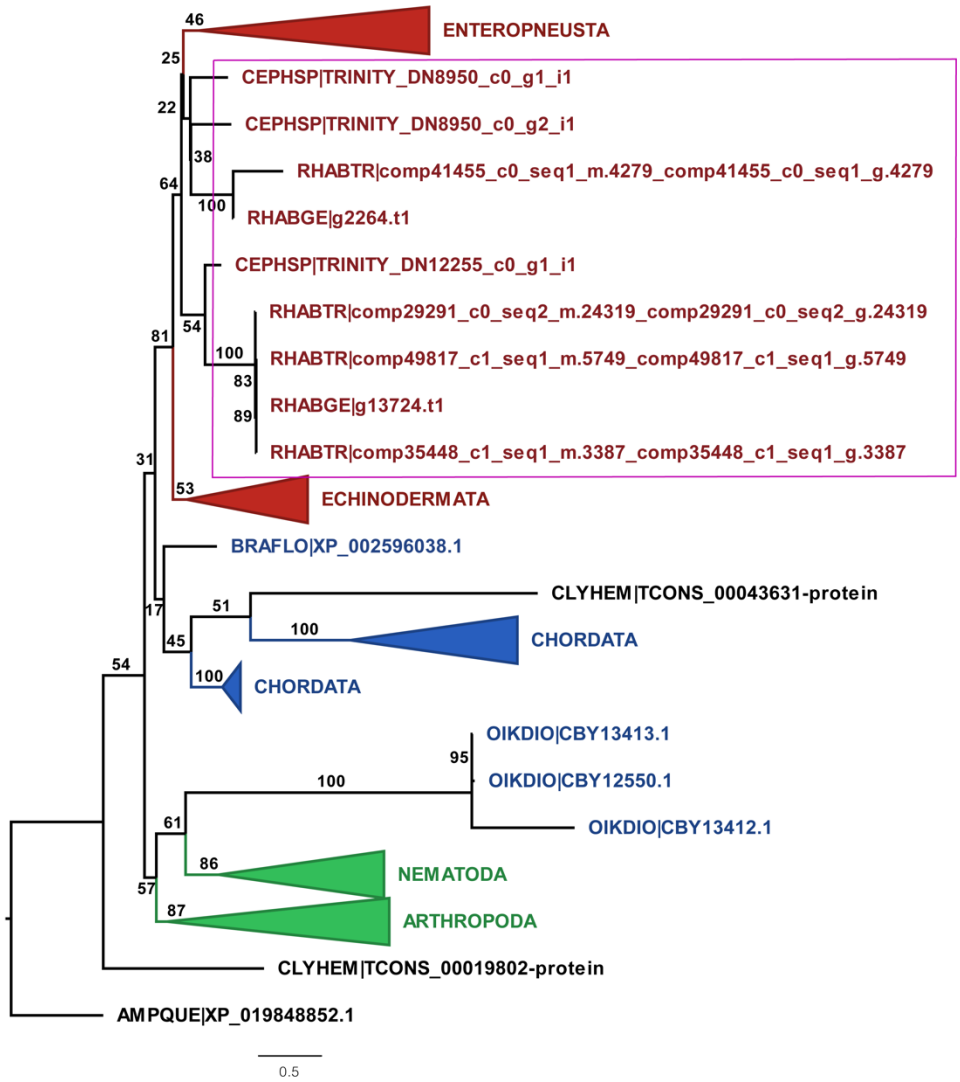

Fig. 1. OG0000859. Complete dataset. In red ambulacrarians. In the fuchsia box pterobranchs. Chordates (blue), arthropods and nematodes sequences (green). In black are the hydromedusae *Clytia hemisphaerica* and the sponge *Amphimedon queenslandica*. See the text for comments.

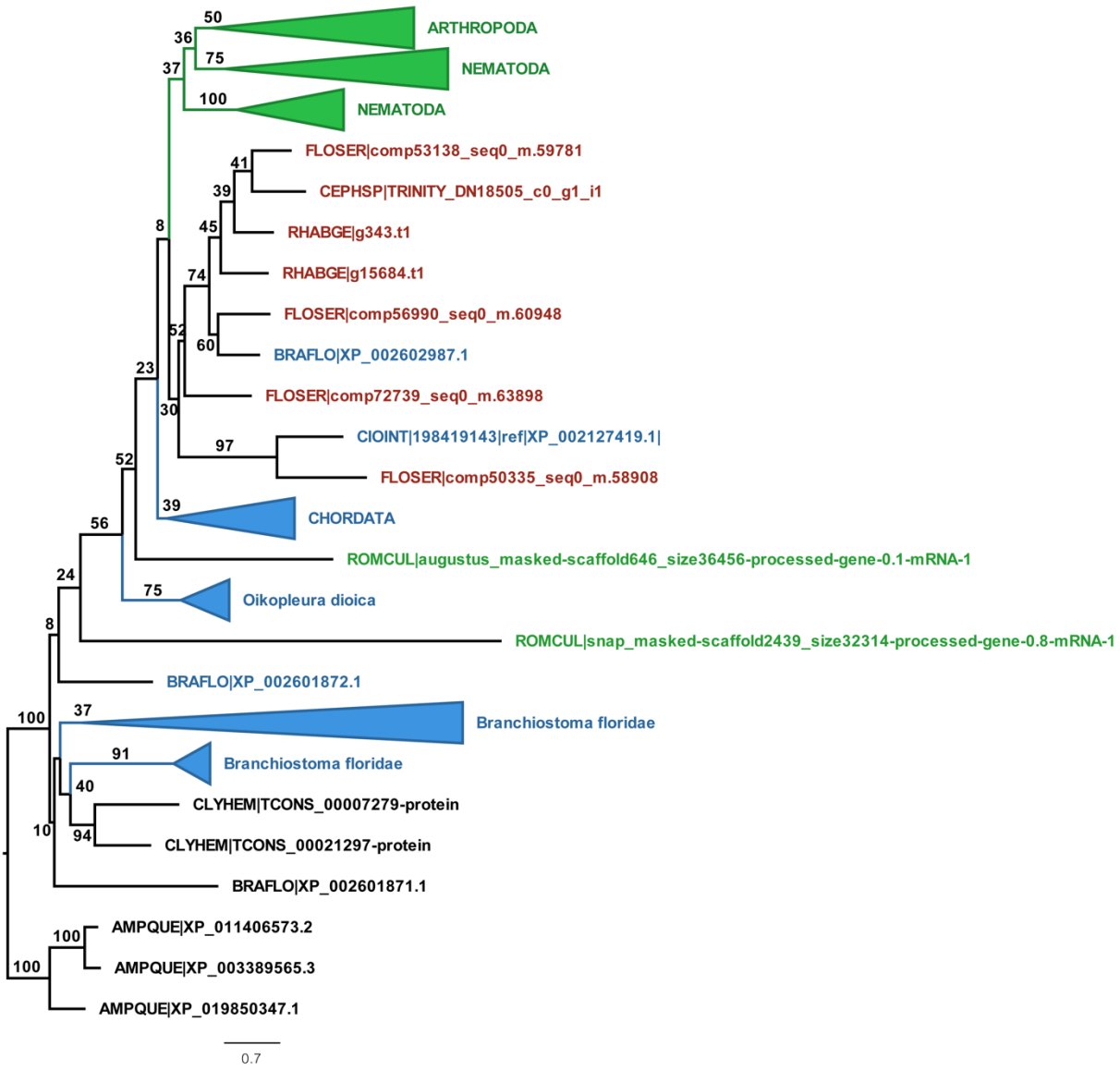

Fig. 2. OG0004142. Complete dataset. Coherent clustering of protostome (green), ambulacrarians (red) and chordates (blue). See the text for comments.

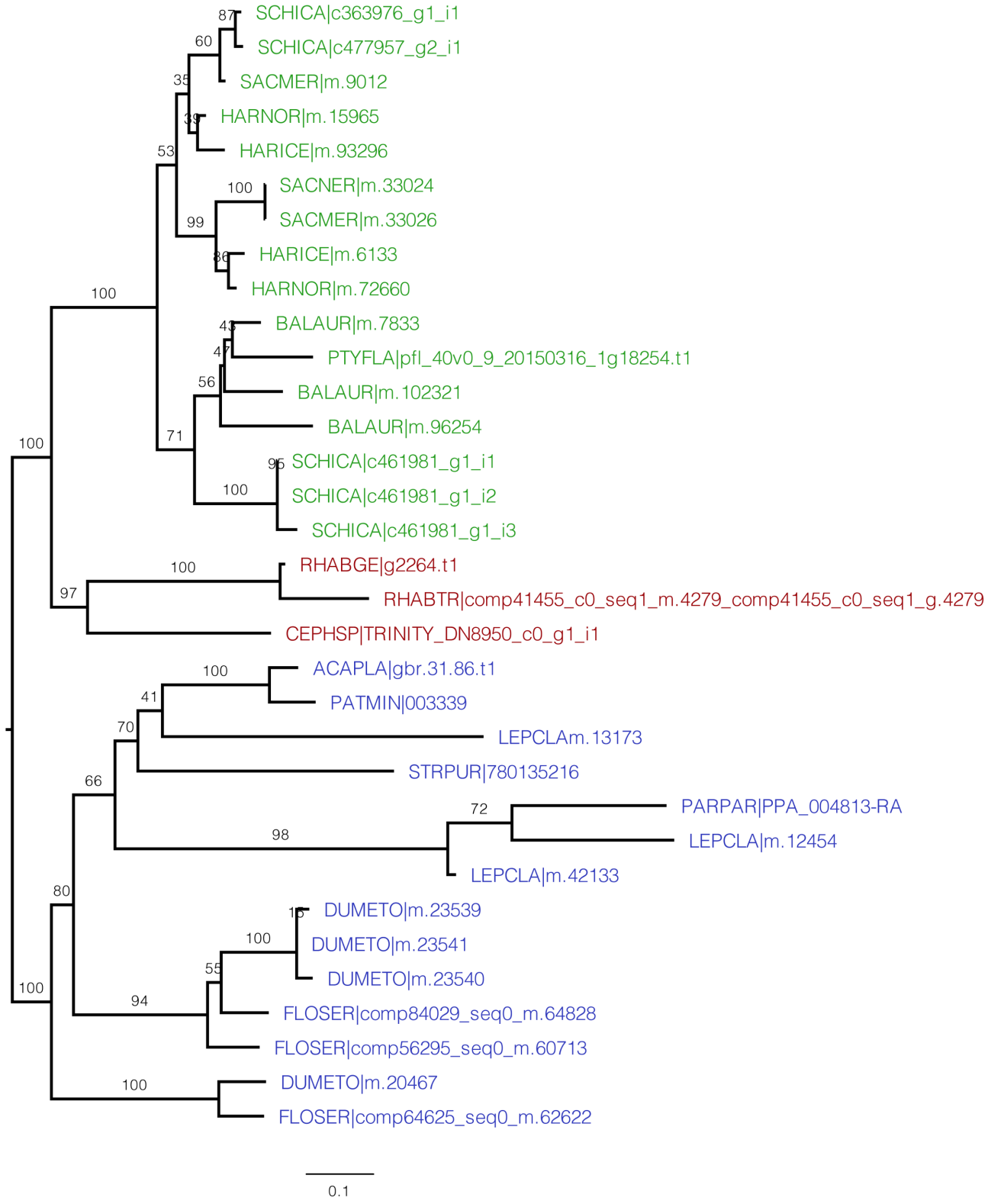

Fig. 3. OG0006824. Ambulacrarian dataset. Enteropneusts (green), pterobranchs (red) and echinoderms (blue). See the text for comments.

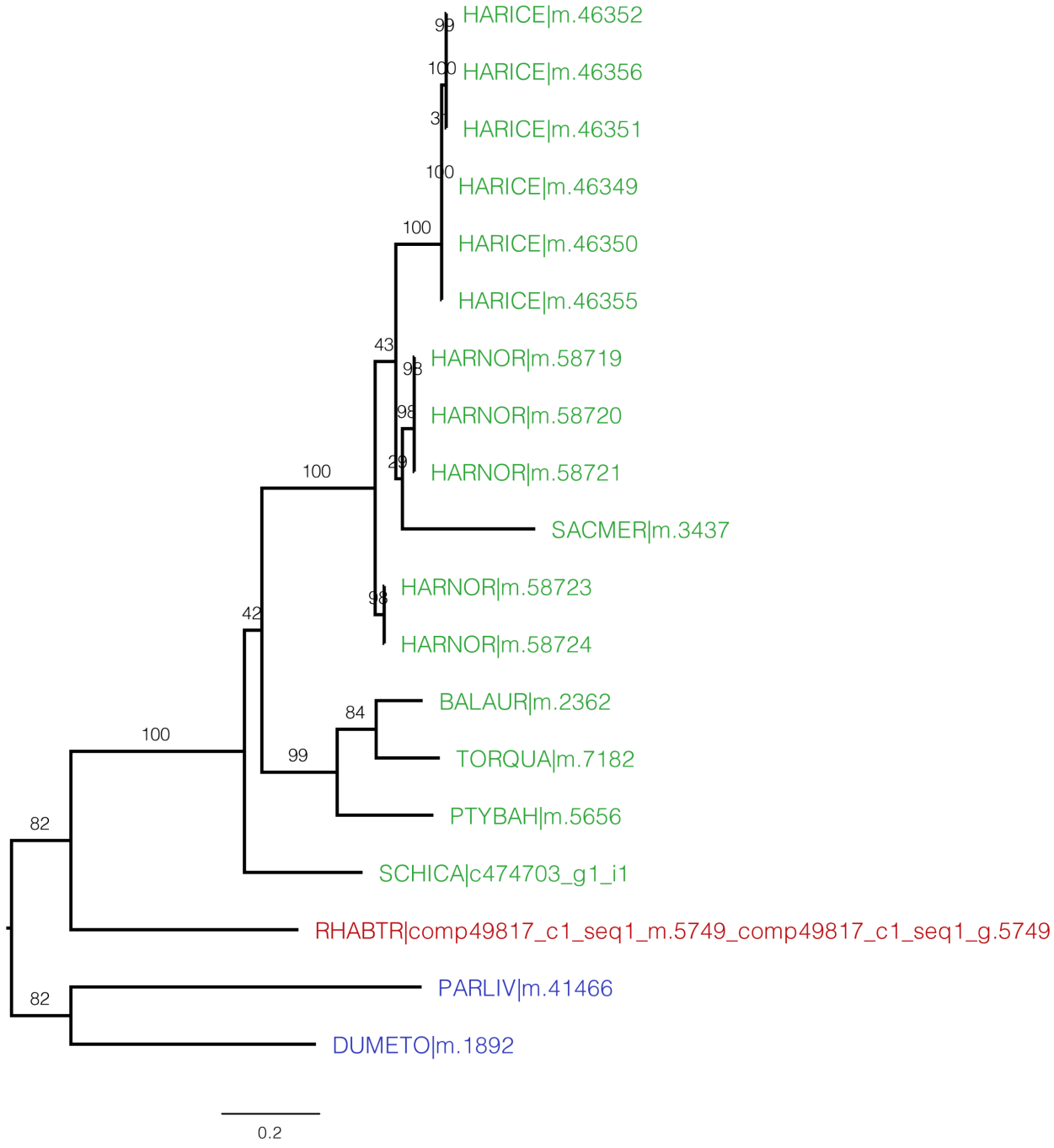

Fig. 4. OG0012451. Ambulacrarian dataset. Enteropneusts (green), pterobranchs (red) and echinoderms (blue). See the text for comments.

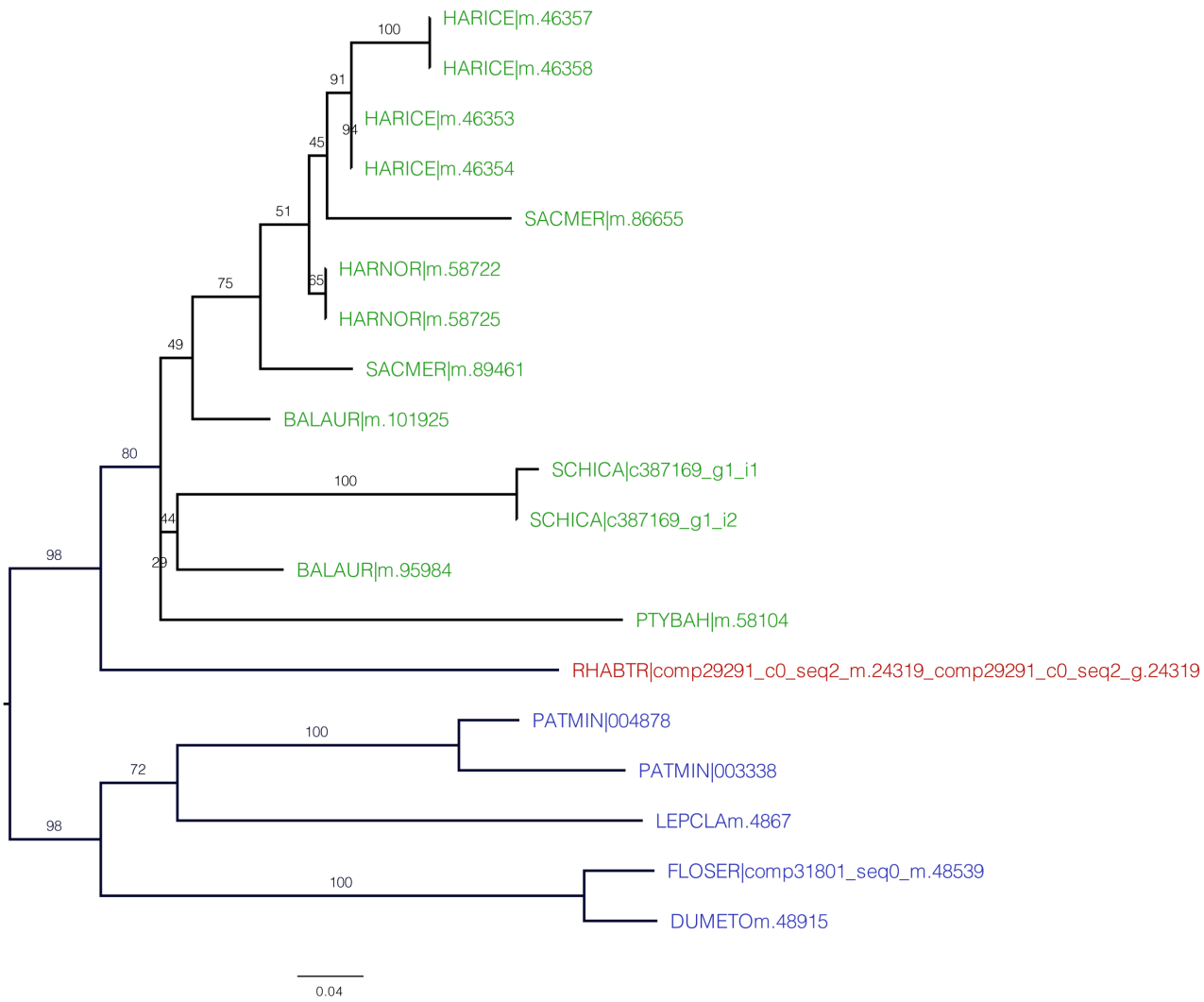

Fig. 5. OG0012607. Ambulacrarian dataset. Enteropneusts (green), pterobranchs (red) and echinoderms (blue). See the text for comments.

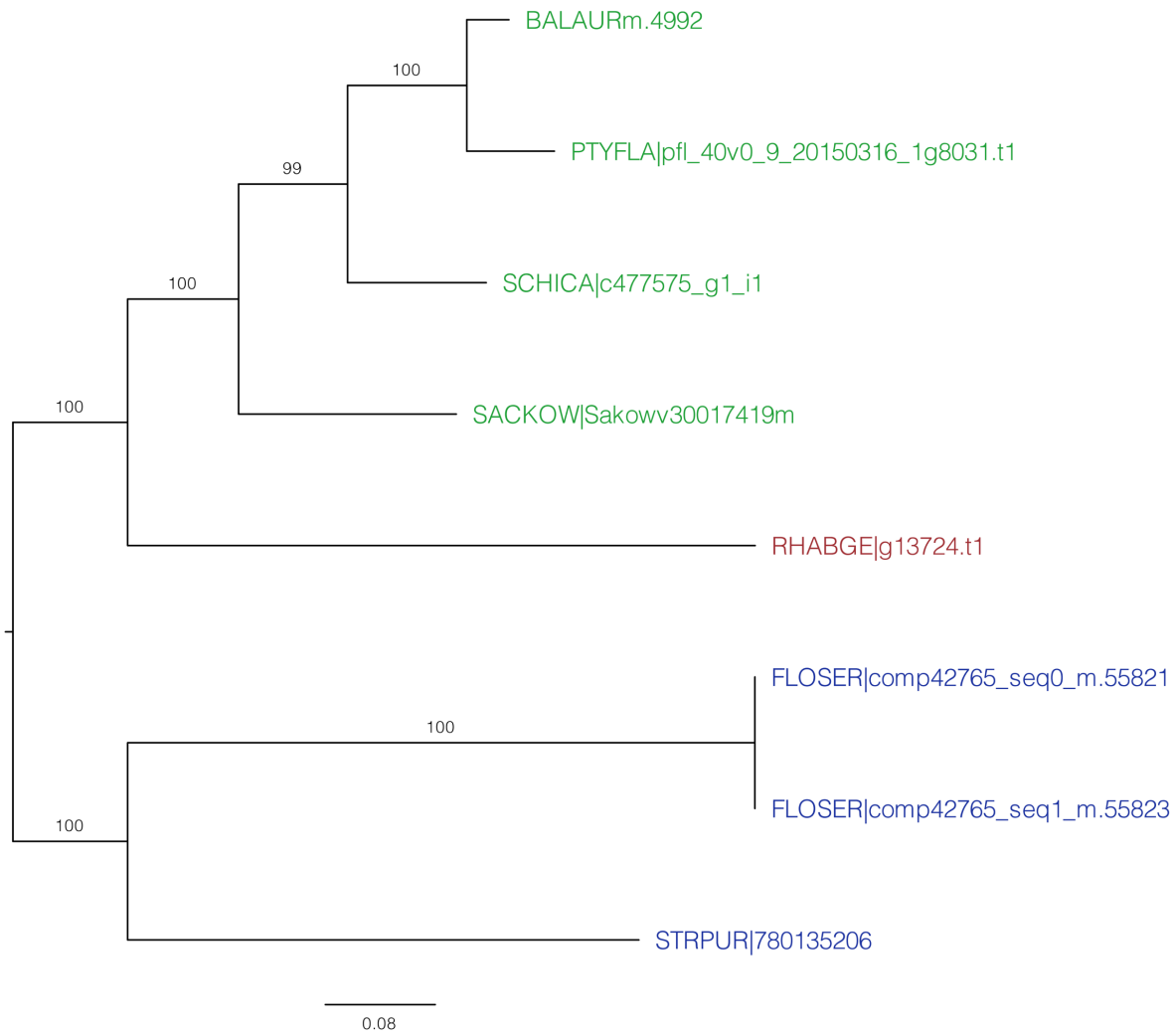

Fig. 6. GO0023337. Ambulacrarian dataset. Enteropneusts (green), pterobranchs (red) and echinoderms (blue). See the text for comments.

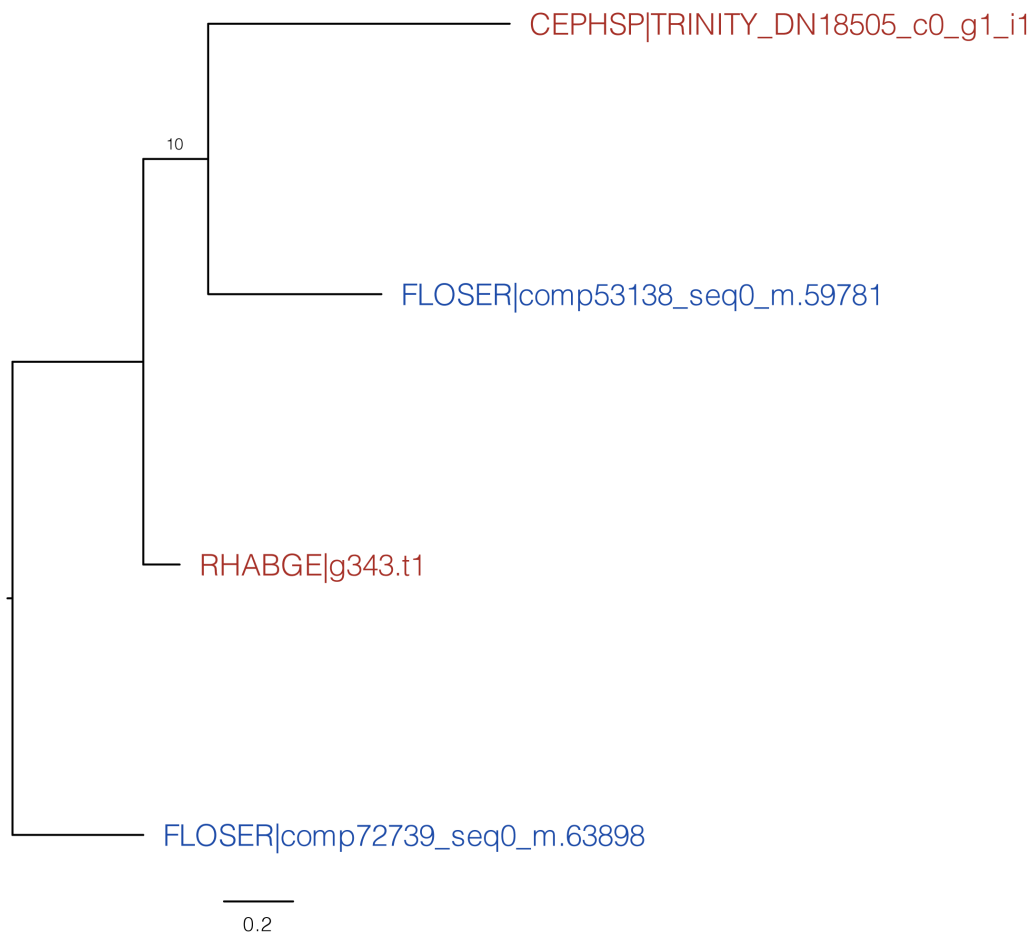

Fig. 7. OG0040366. Ambulacrarian dataset. Pterobranchs (red) and echinoderms (blue). See the text for comments.

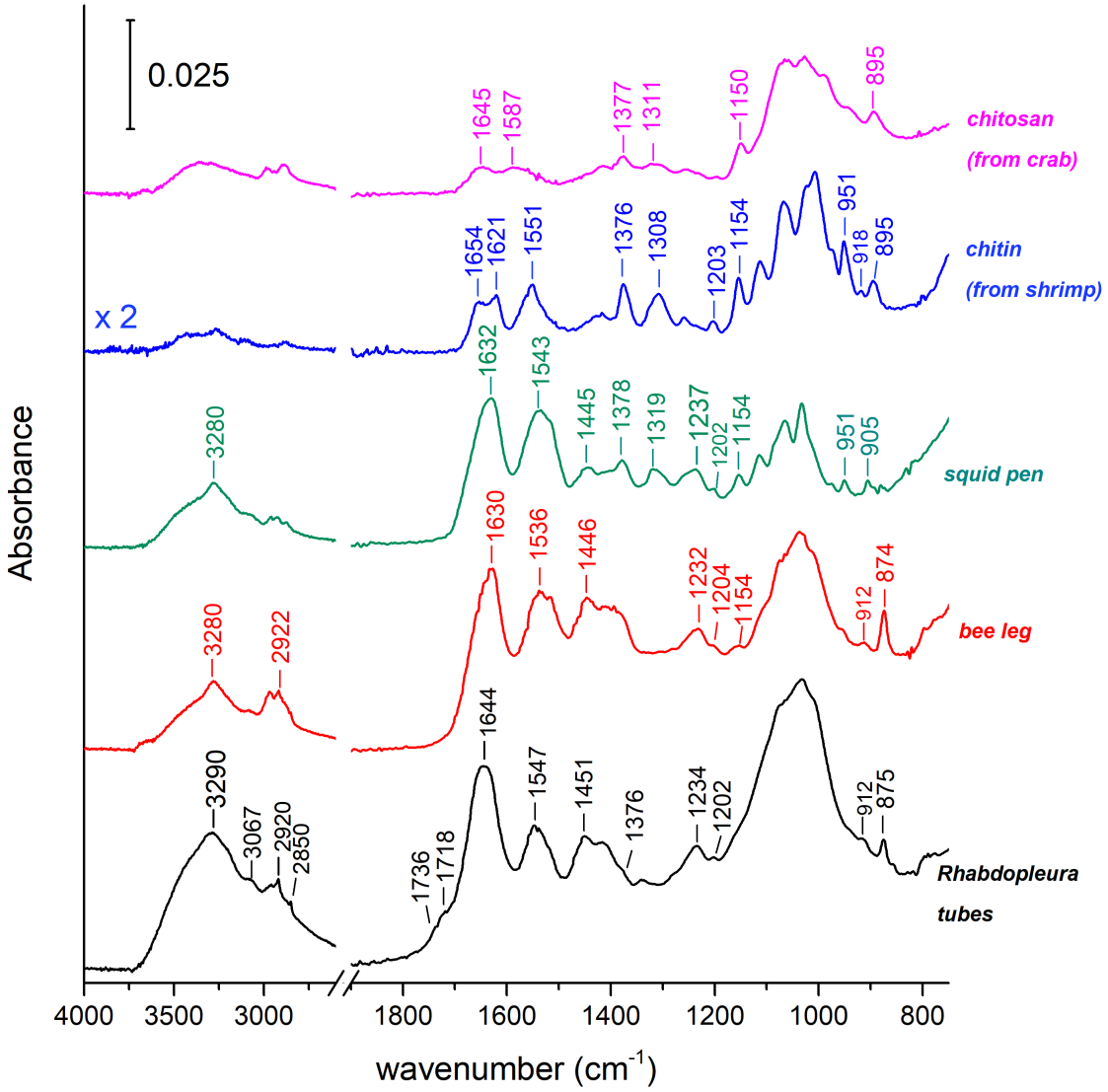

Fig. 8. ATR-FTIR spectra. Purple line, chitosan standard compound; blue line, chitin standard compound; green line, squid pen as a biological refence for β-chitin; red line, bee leg as a biological reference for α-chitin; black line, *R. recondita* tubes sample. See text for comments.

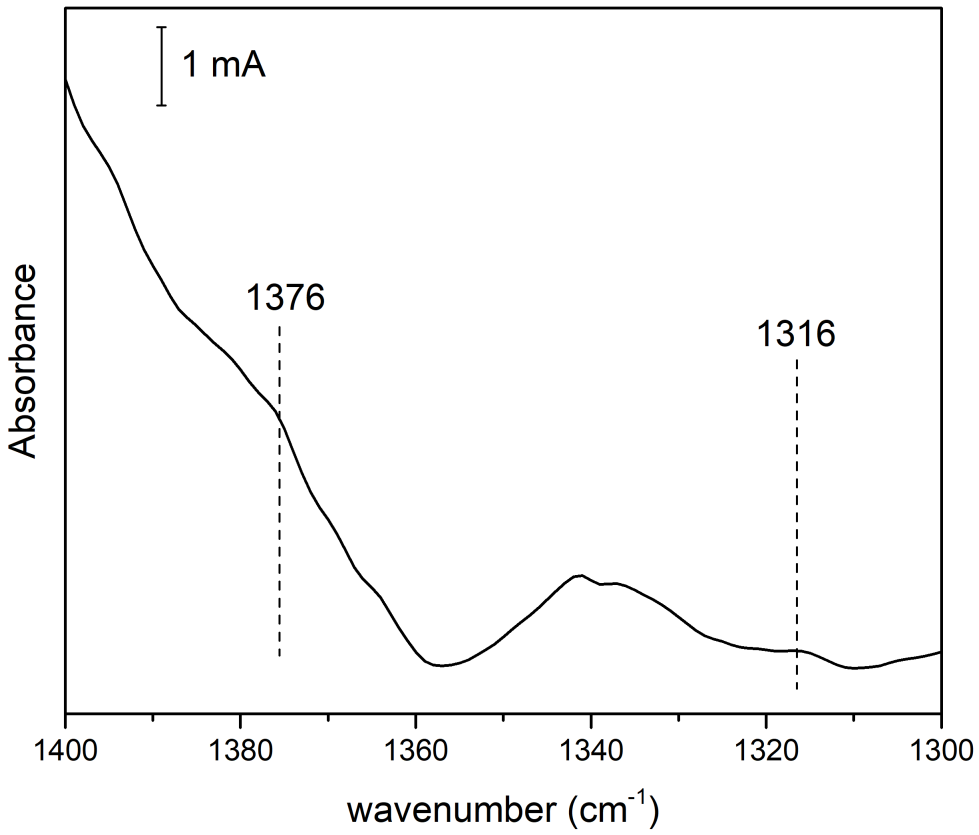

Fig. 9. Magnification signal of *R. recondita* spectrum from Fig. 8, in the range of absorbance of an acetamide moieties, indicating chitin.

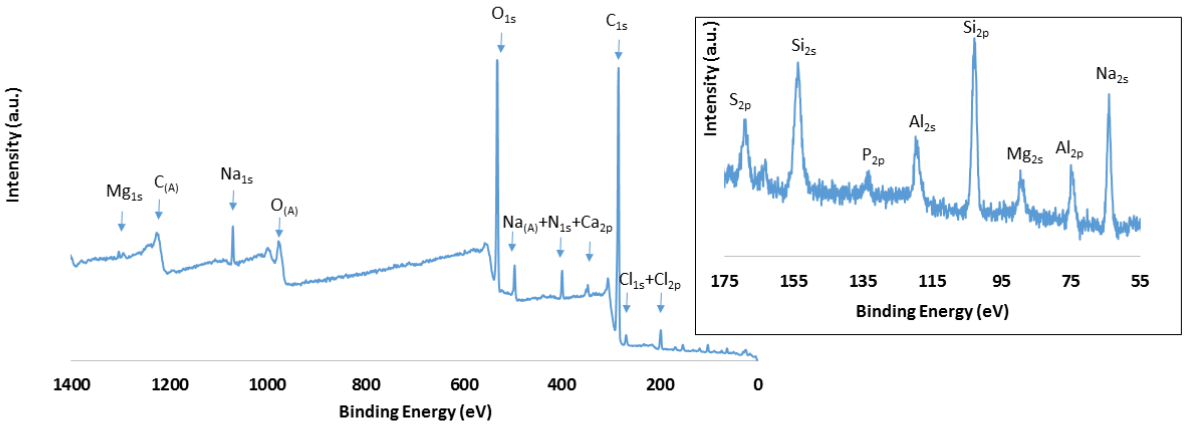

Fig. 10. Survey XPS spectra for samples of *R. recondita* tubes. Inset: XPS high-resolution region acquired between 55 eV and 175 eV. All peaks attributions refers to the NIST standard. reference database [NIST, X., Ray Photoelectron Spectroscopy Database: https://srdata. nist. gov/xps/Default. aspx.]

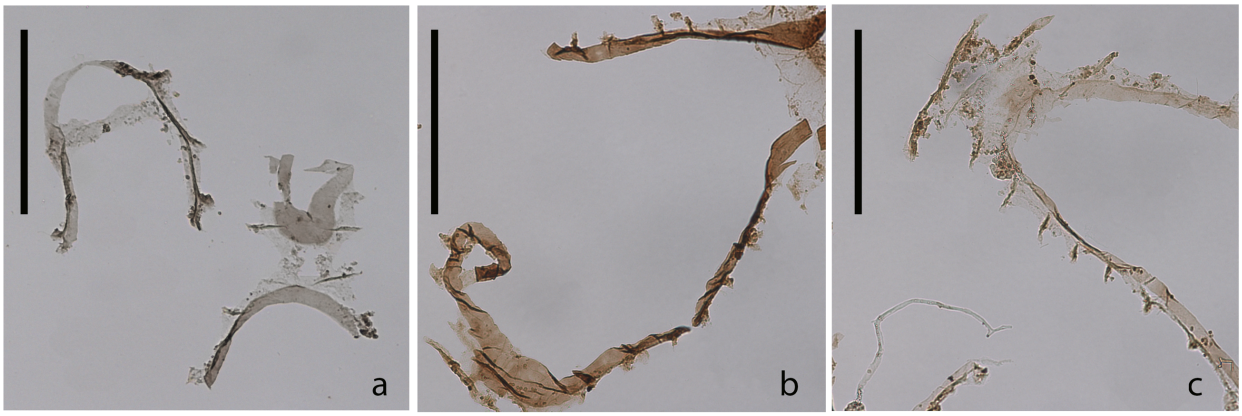

Fig. 11. *R. recondita* tube sections. a, before any treatment; b, Control; c, Experiment. The brownish tint observed both in control and experimental samples suggests that the labelling is not specific in the latter. Scale bars 50 µm for a, 100 µm form b,c.

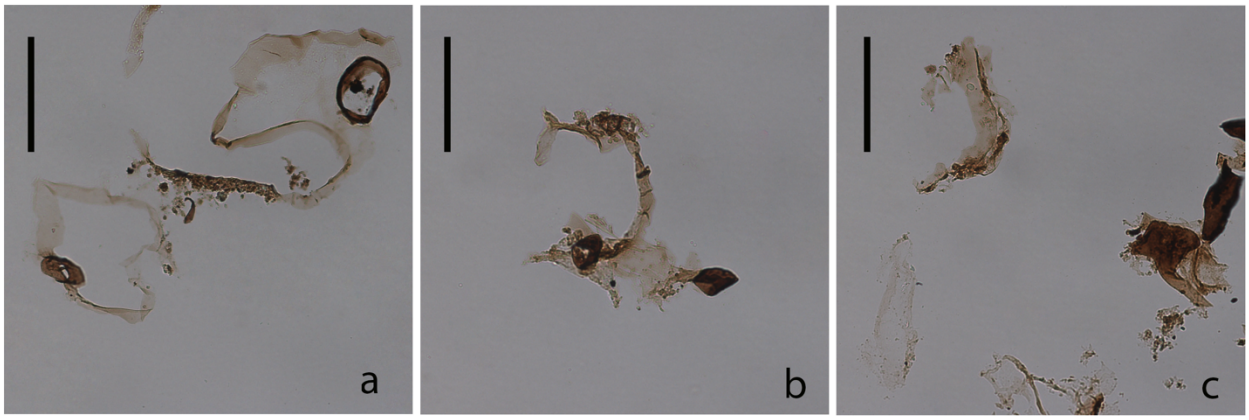

Fig. 12. *R. recondita* stolon sections. a, before any treatment; b, Control; c, Experiment. It was not possible to detect DAB reaction for the natural brownish colour of the stolon. Scale bar 100 µm.

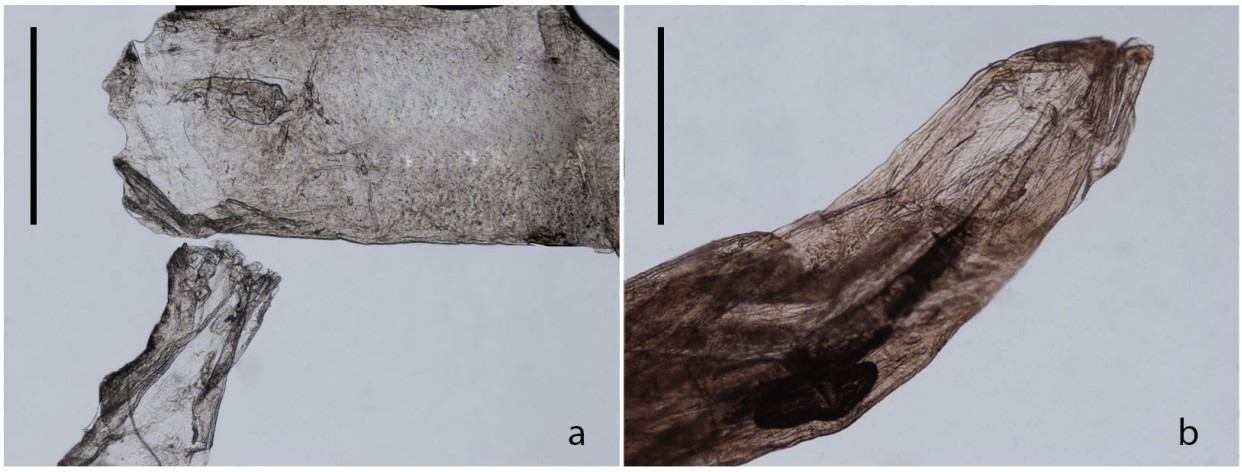

Fig. 13. Shrimp chitin. a, Control; b, Experiment. Contrarily to what has been observed for tube sections, the controls do not show a brownish tint suggesting a specific staining of chitin in b. Scale bar 0.5 mm.

Tables

Table 1. Dataset of genomes and transcriptomes used for OrthoFinder analysis. GT= genome or transcriptome.

Species	Phylum	Class	Abbreviation	GT	ambulacrarian
Acanthaster planci	Echinodermata	Asteroidea	ACAPLA	T	X
Amphimedon queenslandica	Porifera	Demospongiae	AMPQUE	G	
Ascaris suum	Nematoda	Chromadorea	ASCSUU	G	
Balanoglossus arantiacus	Hemichordata	Enteropneusta	BALAUR	T	X
Branchiostoma floridae	Chordata	Leptocardii	BRAFLO	G	
Caenorhabditis elegans	Nematoda	Secernentea	CAEELE	G	
Cephalodiscus planitectus	Hemichordata	Pterobranchia	CEPHSP	T	X
Ciona intestinalis	Chordata	Ascidiacea	CIONT	G	
Clytia hemisphaerica	Cnidaria	Hydrozoa	CLYHEM	G	
Danio rerio	Chordata	Actinopterygii	DANRER	G	
Daphnia pulex	Arthropoda	Branchiopoda	DAPPUL	G	
Drosophila melanogaster	Arthropoda	Insecta	DROMEL	G	
Dumetocrinus sp.	Echinodermata	Crinoidea	DUMETO	T	X
Florometra serratissima	Echinodermata	Crinoidea	FLOSER	T	X
Gallus gallus	Chordata	Aves	GALGAL	G	
Harrimaniidae sp. (Iceland)	Hemichordata	Enteropneusta	HARICE	T	X
Harrimaniidae sp. (Norway)	Hemichordata	Enteropneusta	HARNOR	T	X
Homo sapiens	Chordata	Mammalia	HOMSAP	G	
Leptosynapta clarki	Echinodermata	Holothuroidea	LEPCLA	T	X
Mus musculus	Chordata	Mammalia	MUSMUS	G	
Oikopleura dioica	Chordata	Appendicularia	OIKDIO	G	

Paracentrotus lividus	Echinodermata	Echinoidea	PALIV	T	X
Parastichopus parvimensis	Echinodermata	Holothuroidea	PPA	G	X
Parhyale hawaiensis	Arthropoda	Malacostraca	PARHAW	G	
Patiria miniata	Echinodermata	Asteroidea	PATMIN	G	X
Ptychodera bahamensis	Hemichordata	Enteropneusta	PTYBA	T	X
Ptychodera flava	Hemichordata	Enteropneusta	PTYFLA	G	X
Rhabdopleura recondita	Hemichordata	Pterobranchia	RHABGE	G	X
R. recondita	Hemichordata	Pterobranchia	RHABTR	T	X
R. annulata	Hemichordata	Pterobranchia		T	X
Romanomermis culcivorax	Nematoda	Enoplea	ROMCUL	G	
Saccoglossus kowalevskii	Hemichordata	Enteropneusta	SAKOWV	G	X
Saccoglossus mereschkowskii	Hemichordata	Enteropneusta	SACMER	T	X
Salpa thompsoni	Chordata	Thaliacea	SALTHO	T	
Schizocardium california	Hemichordata	Enteropneusta	SCHICA	T	X
Strigamia maritima	Arthropoda	Chilopoda	STRMAR	G	
Strongylocentrotus purpuratus	Echinodermata	Echinoidea	STRPUR	G	X
Torquaratoridae sp. Antarctica	Hemichordata	Enteropneusta	TORQUA	T	X
Tribolium castaneum	Arthropoda	Insecta	TRICAS	G	
Xenopus tropicalis	Chordata	Amphibia	XENTRO	G	

Chapter 6

Conclusions

Chapter one provided a brief overview of the Hemichordata, a taxon of exclusively marine animals, interesting for their phylogenetic proximity to echinoderms and chordates. The class Enteropneusta, or acorn worms, are thought to best represent the common ancestor of deuterostomes (Cameron et al. 2005). Pterobranchia are small colonial zooids that, with few exceptions, live at depth in polar seas. A relevant paleontological group, within the Pterobranchia, is represented by the Graptolithina which are mostly extinct and part of the fossil record. A phylogenetic nomenclature of the hemichordates, based on phylogeny, is the topic of Chapter two.

Chapter two of this thesis introduces the hemichordate clade. It is a contribution for *Phylonyms*, the volume that contains the description of clades based on *PhyloCode*. *PhyloCode* is the *International Code of Phylogenetic Nomenclature* and aims to integrate the "phylogenetics thinking" to the classic Linnaean "rank-based" nomenclature system. In the classical nomenclature system, the names describing a clade can change, generating ambiguity. The purpose of *PhyloCode* is to propose rules that univocally identify a clade, assigning a name that will not change over time. Clade names with this nomenclature code are redefined in terms of phylogenetic relationships rather than in terms of ranks. *PhyloCode* is currently developed to name clades rather than species, but in the future, rules for naming species could be proposed. Had we been permitted by the editors to make a major change to the contribution, after it was accepted for publication, it would have been in put *Rhabdopleura* within the graptolites, and Graptolithina within the class Pterobranchia (Mitchell et al 2013). This finding is equivalent to discovering the coelacanth because it allowed me to study the "living fossil" *Rhabdopleura recondita,* the subject of this thesis.

Chapter three is a comprehensive review of the Subclass Graptolithina and *incertae sedis* Family Rhabdopleuridae. It is chapter 15 of 29 in the Graptolite volume of the second edition of the iconic *Treatise of Invertebrate Paleontology*. As with all reviews, this chapter brings graptolite palaeontologists (and biologists!) up to date and sets the stage for future studies. *Rhabdopleura,* within the Graptolithina, represents the most primitive genus of graptolite and includes five species that survive to this day. It is the topic of this thesis. The discovery of *Rhabdopleura* in the

Mediterranean Sea, provided a unique opportunity to study this fascinating genus of animal because it is abundant and accessible by SCUBA diving (Beli et al. 2018).

Chapter four is the first to provide new data on *R. recondita*, and specifically its tubes. Here I make basic observations on larval settlement, metamorphosis, prosicula and tube secretion. I found that the larvae of *R. recondita*, without a substrate for settlement, are able to swim, begin the secretion of the prosicular dome and also start metamorphosis before secreting the dome. None of these larvae survived beyond the dome secretion. The one larva that survived the furthest did it in the presence of, and practically hidden inside of host bryozoan fragments. It settled, metamorphosed, secreted a dome, and the beginnings of an adult zooid tube, but it did not form a budding stolon. Its presence in the bowl seemed to have attracted other larvae that in turn settled and secreted a dome. This observation suggested that a larval settlement cue – the bryozoan substrate – and the presence of a successful larvae attracts conspecific larvae. Zooids also seem to have greater tube secretion success in the presence of bryozoan host fragments.

The isolated and naked zooids, attached to their stolon and to a small piece of calcium carbonate of the host, in which they were not able to hide, did not secreted new tubes or enlarged the colony. However, an exception was two zooids that were held together by a common stolon and partially cached inside a fragment of calcium carbonate. These two zooids each rebuilt an erect tube, the zooid which had the ability to move slightly deeper inside the zoarium, built a normal tube, whereas the second zooid, more exposed, built a distally flared tube to protect its soft body.
The total removal of the 23 erected tubes from a colony led to the reconstruction of only three new tubes. This result tells us that zooids are able to rebuild their tubes, in captive conditions, though in low number. Overall, we think that the development of *R. recondita* is profoundly adapted to a life inside the host. In this regard, it may differ from the other four *Rhabdopleura* species.

Of the fossil graptolites only the tubaria are captured in the sedimentary rocks. There is no way to know if there was reproductive isolation between populations of the same species, or genetic traits, leaving only the morphology of the tubaria for taxonomy. *Phenotypic plasticity* plays an important role in defining, among other things, the morphology of species exposed to different environments. In the aquatic world, flow velocity is among the most important selective forces that can shape a

species (Graus et al. 1977; Palumbi 1986; Marchinko 2003). In living organisms, we have the tools to understand whether two morphologies that differ due to plasticity are the same species whereas in the fossil record this is not possible. In the case of graptolites, we were able to test the plastic response of tube form in a living species of *Rhabdopleura*. Chapter four is the first experiment on the phenotypic plastic response of a *Rhabdopleura* to flow velocity. From this we can recover useful information to understand how a graptolite responded to flow velocity with a variation in the shape of the tubarium. We found no *phenotypic plasticity*, suggesting that *canalization* may be at play. Colonies of *Rhabdopleura recondita*, were deprived of their erect tubes, placed in flow channels at four different flow velocities. Our results that there is a slight tendency to form a greater number of tubes at intermediate velocities was not statistically supported. It also emerged that there is no significant difference between the four treatments with regards the length of the rebuilt tubes. To our surprise, there was a significant difference between the length of the original tubes versus the newly secreted tubes. Overall, we believe that the development of the *R. recondita* colonies in response to flow velocity is *canalized* - it does not change as the flow rate varies. However, we have to consider also other factors that may explain the low re-secretion and short tube length, the alternative reasons for these results may be i) the captivity conditions: the amount of food, the light, the time available to colonies for tubes resecretion, ii) conditions related to life cycle, like a seasonal or sporadic colony enlargement, or not enough zooids to rebuild all the dissected tubes. The boundary layer may also have played a role. The velocities directly next to the bryozoan matrix where the zooids reside may have been lower than those maintained in the mid-channel. This result is significant because it suggests that small differences that distinguish primitive, encrusting graptolite species may be real.

Chapter five addresses the composition of graptolite tubes. After sedimentation, fossil graptolites undergo diagenetic changes. They are subjected to high pressures, temperatures, and chemical transformation. This had made it very difficult to characterize with certainty the composition of the tubes. Our hypothesis in this study is that the composition of *R. recondita* tubes is similar or identical to those of fossil graptolites and to the tubes of Cambrian enteropneusts that were lost after the divergence from pterobranchs (Nanglu et al. 2016). These hypotheses are good because it is easier to maintain the composition of extracellular matrix structures than re-invent them anew. This is true for crustacean and mollusk calcium carbonate, echinoderm calcite, and vertebrate

apatite. Numerous attempts have been made to analyze the chemical structure of *Rhabdopleura* and fossil graptolites tubes, and four hypotheses have been advanced. They were, or are, composed of chitin, keratin, cellulose/tunicin, or collagen, but no results were definitive. We used a multidisciplinary approach based on genome sequencing and bioinformatics, immunohistochemistry and spectroscopy. The absence of sequence orthologues, or biochemical precursor sequence orthologues for keratin and cellulose rejects these two hypotheses. We found that the *Rhabdopleura* tube is made of a chitin-like polysaccharide, together with proteins, fatty acids, and unexpected elements that are probably integrated after the secretion of the tube.

Living pterobranchs are less studied than fossil graptolites. Few zoologists have had the opportunity to encounter these organisms (Barnes 1977) because they are rare and typically in deep polar seas. Our discovery of *R. recondita* in shallow waters provides an opportunity to study abundant and easily accessible colonies. This thesis provides new insights on their life history, notes on challenges to maintain zooids in captivity, a genomic informatics, spectroscopic and immunohistochemical analyses of the tubes. *Rhabdopleura recondita* is a new reference model for the study of a living pterobranch. Chapter two provides a description of Hemichordata in evolutionary, or phylogenetic context. It is one of the contributions for *Phylonyms*, a coding system that, I think, will be widely adopted by zoologists, botanists, protistologists, mycologists and microbacteriologists. Chapter three is an update of the family Rhabdopleuridae, published in the second edition of the *Treatise of Invertebrate Paleontology*, which will serve as a guide for years to come. Chapter four on tube secretion and form, includes an experiment designed to induce a phenotypic response in *R. recondita* exposure to different flow velocities. It is the first attempt to study a plastic response in a graptolite. It should be seen as a starting point to further studies on *Rhabdopleura* in aquaria. Nearly two years were spent doing mini experiments to increase survival in captivity and observe tubaria building behaviour. We found no plastic response to flow, instead we found *canalization*, and we concluded that this may be real, or due to captivity conditions, to *R. recondita* life cycle, or its unusual life habitat, inside of a bryozoan host. If the opportunity was to avail itself, parallel experiments should be run with other *Rhabdopleura* species. In particular, species with typical creeping tubes. Chapter five found that the tubes are composed of chitin and a surprising mix of fatty acids, and proteins. Further research is needed to characterize the non-chitin components of the tubes, and the relation of these components to each other and to the

microstructure of the tubes which make these structures tough but flexible and highly resistant to decay (Beli et al. 2017). The composition as it relates to the arrangement of cortical sheets, fibres, and age, are unknown. A transcriptome of the cephalic shield of *Rhabdopleura* would be a fruitful approach, and could be compared to the transcriptomic databases of other Ambulacraria. This would augment what we've learned from the genome by providing the location of gene expression as it relates to tube secretion. Another approach would be to apply a micro-purification protocol to better resolve with the spectroscopic analysis the presence of chitin in the *R. recondita* tubes, or collect a few tens of milligrams of tubes to subject to Nuclear Magnetic Resonance (NMR spectroscopy).

The systematics of graptolites, their development, tube secretion and chemical composition is a work in progress. This thesis is a significant contribution to graptolite biology and paleontology, and elevates, I hope, a greater appreciation of the prehistoric *Rhabdopleura*, inspiring future investigations into the last living species of Graptolithina.

References

Barnes, R. D. (1977). New record of a pterobranch hemichordate from the Western Hemisphere. *Bulletin of Marine Science*, 27, 340–343.

Beli, E., Piraino, S., & Cameron, C. B. (2017). Fossilization processes of graptolites: insights from the experimental decay of *Rhabdopleura* sp. (Pterobranchia). *Palaeontology*, 60, 389–400.

Beli, E., Aglieri, G., Strano, F., Maggioni, D., Telford, M. J., Piraino, S., & Cameron, C. B. (2018). The zoogeography of extant rhabdopleurid hemichordates (Pterobranchia: Graptolithina), with a new species from the Mediterranean Sea. *Invertebrate Systematics*, 32, 100–110.

Cameron, C. B. (2005). A phylogeny of the hemichordates based on morphological characters. *Canadian Journal of Zoology*, 83, 196–215.

Graus, R. R., Chamberlain Jr, J. A., & Boker, A. M. (1977). Structural modification of corals in relation to waves and currents: reef biota. In. Frost, S. H., Weiss, M. P., Saunders, J. B. (eds.) Reefs and related carbonates ecology and sedimentology. *American Association of Petroleum Geologists*, 135–153.

Marchinko, K. B. (2003). Dramatic phenotypic plasticity in barnacle legs (*Balanus glandula* Darwin): Magnitude, age dependence, and speed of response. *Evolution*, 57, 1281–1290.

Mitchell, C. E., Melchin, M. J., Cameron, C. B., & Maletz, J. (2013). Phylogenetic analysis reveals that *Rhabdopleura* is an extant graptolite. *Lethaia*, 46, 34–56.

Nanglu, K., Caron, J. B., Morris, S. C., & Cameron, C. B. (2016). Cambrian suspension-feeding tubicolous hemichordates. *BMC biology*, 14, 56.

Palumbi, S. R. (1986). How body plans limit acclimation: responses of a demosponge to wave force. *Ecology*, 67, 208–214.

Supplementary materials

OG0064236

>FLOSER|comp56990_seq0_m.60948

MYYLLGWILVGQQEGNEQLIEVKTHNSYVLALDGDIDFKPDAVQRLLDLMKRNRTVGAACGRIHPIGTGPL
VWYQKFEYATGHWFQKTAEHVLGCVLCSPGCFSLFRASALMDDNVMRKYATRSEKAEHYVQYDQGEDR
WLCT

>RHABGE|g15684.t1

MNSVLDENISLSNGRSDDKNKASSIIPEETSNDVNFVNSSTPKEVNRINSPNSVLLQDLESDDEQELKDTTEN
NDNSETFNSDVEEIEDNHPWDAPKVSPPRKPHEEKDVCLEGAKLTAKICSYIFFFSVVLITAVSSNLTMTTLT
NVDILTTESRNETILVGWTVEKMNRVIFIAGTLVIPEMMIFMLNTLKSLFGLKKSPDLSLIFKVCLLESLPAVG
LWLFVFRVMTNGHALVSIVLMESVCFVPALLSAFISIKEQKEPKQGKPRLCPIIFNSAAFMIQTTAIMAVVFT
NFYSGAAWEPVISVLLISVSWWENFANFEEGSSFPLTNLKLQIQKCRCKLYAYSLMMNRRRREQALEKEAR
DVEDNPDVATFGNSDSGDTLIYICATMWHETEQEMIQVLKSICRLDIHQYQLHVTANTTGQKRDDLYRFEA
HIFFDDSMEFDDDNNLVTNAFVKQLIQCVGIAVNAVRDDDDQVEVLPPTKYFLPYGGRLIWNLPCGNKLVA
HLKDKARIRHRKRWSQVMYMYYLLGYLLLQENRSRDGEDIEKLKENTYLLALDGDVDFQPSALQLLVDL
MKRHKKVGAACGRIHPIGSGPVVWYQKFEYAIGHWFQKTAEHVLGCVLCSPGCFSLFRASAIMDDNVMK
KYTTKASEPSHYVQYDQGEDRWLCTLMLQQGWRVEYCAASDALTYAPEEFKEFFNQRRRWTPSTMANIM
DLLQSGRETAKKNQSISNLYIFYQIALMISTILGPSTVVMMIAGAISFAFGLSDWGGFLASLIPAAFYLVICLTT
SSSTQLWIAQLLSIGYALITMGVIAALAGQIVGDGVLSPSALFFLVLIALFVFAAAIHPQEFTCLFAGCLYMLC
FPSGYLLLIIYSLCNLNVVSWGTREVKKKNKSKNDGSKKPKKNDTLKDNIMNFFKKSDVDFDGTFSCGCGA
LFRCALCLKSIDTNSGKYMSLQDAITFANQCGQSSSLTLKNGEVQVDKKSKLDTQNTDGAAPYEEKHEEED
LNYWVEEEELANSRLGVIDQEEILFWEYLSPPNSNNQSYTALNLEGKAPKINDRDVESSRQLTDDDVFEVD
NAIARRTRKESRRESKLRRLPSCPMFQPTDLPSANKTTAFPTQMIGIGGRPMSSARFPKSKSSIGCPRTSKSIRT
TDAENPIDEIDRHLKVNRMNPAPVPSPIYGDLESV

OG0071037

>PATMIN|026377

LAFPRKVKNKVYARSSFLGLGNLIGETTVTQRWERGEISNFKYLMALNTIAGRSYNDLMQYPVFPWILADY
DSEELRLDKFSTFRDLSKPMGAQTEARLQQFRKRYDEWEDPTAFSPSLAGSVGEFQGSFAIFF

>RHABSP|comp35448_c1_seq1_m.3387_comp35448_c1_seq1_g.3387

ARIMAEATRLTDNTSQSISGQKRNAQMEASTGLISSLMGEKTVTQRWERGEISNFQYLMYINTLAGRSYND
LMQYPVFPWVLADYESEELNLRDPSTFRDFSKPMGAQTEERLK